Investigating the Potential Role of SIRT1 in Glioblastoma Multiforme: A Comparison Between Glioma and Normal Astrocyte Cells in Culture

By

Susanna Brow

A thesis
submitted to the Victoria University of Wellington
in fulfilment of the requirements for the degree of
Masters in Biomedical Science

Victoria University of Wellington

2015

Abstract

Objective

Glioblastomas (GBMs) are the most prevalent primary brain tumours in adults and the outcome for this disease remains very poor. With treatment options limited, there is growing interest to find potential differences between normal and malignant molecular signaling pathways for this disease. SIRT1 is a histone deacetylase enzyme with key functions in cellular signaling responses including protecting DNA from damage and changing transcriptional events. SIRT1 can act as a switch to affect cellular senescence or anti-apoptotic responses, or alternatively affect autophagic and pro-apoptotic responses. The role of SIRT1 in GBM is unclear. This study aimed to investigate differences between glioma and normal astrocytes with respect to SIRT1.

Research design and methods

SIRT1 was analysed in murine normal and glioma astrocyte cell lines, and results compared to a normal human astrocyte cell line and a panel of human primary glioma cells taken from patients with GBM. Analysis of SIRT1 was assessed using Western blots and flow cytometry. Sub-cellular localisation was examined using Western blots and immunofluorescent microscopy. Activity for SIRT1 was assessed using acetylation of a key histone SIRT1 substrate, histone 4 lysine 16, and cell proliferation was measured using the MTT assay. Oxidative stress was induced using H_2O_2 and viability measured using propidium iodide exclusion and flow cytometry. To ascertain that activity was SIRT1 related, inhibition and activation of SIRT1 was done using nicotinamide and resveratrol, respectively.

Results

SIRT1 was mainly localised in the nucleus and to mitochondria of normal cells but was aberrantly distributed in the cytoplasm of glioma cells, which has not been reported before. This was consistent in both murine and human glioma models. Nicotinamide significantly inhibited cell proliferation more for glioma cells compared to normal, and resveratrol had the opposing effect. Nicotinamide rescued normal but not glioma cells from H_20_2-induced oxidative stress, and resveratrol had the opposing effect. Western blots revealed secondary protein bands for SIRT1

indicating possible smaller species of SIRT1, and results for nuclear/cytoplasmic extractions suggested FL-SIRT1 and the smaller species of SIRT1 have a dynamic pattern of localisation under oxidative stress, nicotinamide and resveratrol treatments.

Conclusions

These results indicated SIRT1 is involved in both cell proliferation and oxidative stress responses, with a differential activity between glioma and normal astrocyte cells. Aberrant localisation of SIRT1 to the cytoplasm in glioma cells is a significant finding that needs further exploration. The need for further studies to elucidate changes in localisation for SIRT1 under different conditions is highlighted, as is the possible role of truncated variants of SIRT1. This study suggests there may be some potential for SIRT1 inhibition in patients suffering from glioblastoma.

The art of knowing, is knowing what to ignore.

Rumi

Acknowledgements

The Rumi quote on the previous page may seem a strange choice given that this thesis is relatively long. It felt like an untameable beast at times. Every result threw up many more questions, and when you have a curious mind like I do, it can be a struggle to stop asking more, and to focus on a small aspect of the wondrous universe that is molecular biology. This study had so many changes in directions, had so many failed experiments, and it was a struggle for me to keep going. It was also a challenge for me to believe in myself. Then, there would be those few times in the lab when I saw an amazing result for the first time, or see the stunning internal world of a cell fluorescing under the microscope, and I felt so privileged to have been able to see into the secret life of SIRT1 for a brief moment, the ever-changing, ever moving molecule that I have come to love. So I kept going. I left out a whole lot, and I probably should have left out a whole lot more. I'm still a student in the art of knowing.

I am extremely thankful to the university for giving me assistance to complete. I got very stuck when writing this thesis. In particular, Shona de Sain and Patricia Stein on the VUW staff who have brought me to tears with kindness and support, thank you.

To Dr Sheena Gallocher, without your help I would never have even stepped into the lab or the university to begin with. Your work is truly God's service. Thank you.

I am very grateful to Dr Melanie McConnell, who took me on as her student for this research. She gave me so much freedom perhaps a little too much! However, doing this work has meant a lot to me in ways that she may never know, and without her accepting me as her student, this would not have happened.

Dr Bill Jordan has shown me support throughout this research, and in particular during the write-up, that I can only describe as magic. It would never have been completed without his care and help. Thank you so very much, Bill.

The Malaghan Institute of Medical Research, where I did my experimental work was very supportive. The use of the well-equipped labs and their attitude of generosity was much appreciated. The people in my group were instrumental to the work behind this dissertation, in particular Kate Broadley, a fantastic scientist

who would willingly help me with anything she could. Also James Baty, whose humour keeps everyone buoyant, Carole Grasso, An Tan, Prof. Mike Berridge, and Dr Patries Herst, plus the lovely bunch of people in Room Patagonia who supported me so much: Liz, Ching-Wen, Sara, and Colin. I'd also like to thank Api, Dianne and Janine for their kindness and care; I'll "pass it forward".

Other important people who have helped me include my ever-inspiring sister, Pip, and my son Barney who is a blessing and a treasure in my life. People know that they only need to mention Barney's name to cheer me up. I'd like to thank Poppa, my grandfather, for working so hard in his lifetime so that his descendants could follow their passions. Penny and David, Martin, Barbara, Pam, and my accomplished scientific friends, Shirley Martin, Sandra Anderson, Isabel Castro, Kim Young and Edward Abraham and my dependable, fun-loving, very accomplished friend Judge Christina – you all have inspired and supported me, thank you. Daniel, you are a constant reminder to believe in things beyond our understanding.

There have been some key people that have never stopped encouraging me after most others had given up. These people are so important in life, and I hope everyone is lucky enough to meet such people. Cornelia, Jess, Sally, thank you!

At home my young boarders have been just wonderful in this last leg of my journey. Xia has infected me with the practical "no nonsense bug", and Luke, my Godson, with his consideration and care – you are both 'godsends'! Renee, without you I would have been lost at the finish line.

Thank you to the Wellington Research Medical Foundation and Motor Neuron Disease Association of NZ for helping to fund this research.

Finally I'd like to acknowledge the patients who donated their tumours for this research. They have shown great courage and faith that glioblastoma will one day be treated effectively. I'd like to dedicate this thesis to them and to anyone else reading this who may be suffering from brain cancer or who has a loved one who has this cancer, or has died from this cancer. My wish is that this research gives some hope.

Contents

Figures

Tables

Abbreviations

AKT	Activated kinase
AMP	Adenosine monophosphate
DMNQ	2,3, dimethoxy-1,4 naphthoquinone
DMSO	Dimethyl Sulfoxide
EDTA	Ethylenediaminetetraacetic acid
FACS	Fluorescent-activated cell sorting
FBS	Fetal Bovine Serum
H4K16	Histone 4 lysine 16
H4K16-ac	Histone 4 lysine 16 acetylation
HAT	Histone acetyl transferases
HDAC	Histone deacetylase
HEPES	4-(2-hydroxyethyl)-1 piperazineethanesulfonic acid
mTOR	Mammalian target of rapamycin
MTT	3-(4,5-Dimethylthiazol-2-yl)-2,5-Diphenyltetrazolium Bromide
NAM	Nicotinamide
NFκB	Nuclear factor kappa B
PGC1α	Peroxisome proliferator-activated receptor gamma co-activator 1-alpha
PI	Propidium Iodide
PI3K	Phosphoinositide 3-kinase
IGF-1	Insulin-like growth factor 1
IGF-1R	Insulin-like growth factor 1 receptor
IRS-2	Insulin receptor substrate 2
RES	Resveratrol
RT	Room temperature
SDS	Sodium dodecyl sulfate
hSIRT1	Sirtuin 1 (human)
Sirt1	Sirtuin 1 (mouse)
SIRT1	Sirtuin 1 – used generically

Part 1: Introduction

1.1 Glioblastoma Multiforme (GBM)

Brain tumours originating from glial cells are termed gliomas. Around 70% of gliomas originate from astrocytes (astrocytoma) and most of the remaining gliomas originate from oligodendrocytes (oligodendroglioma), with a small percentage a mixture of origin from astrocytes, oligodendrocytes and ependymal cells (Lino et al 2010). The World Heath Organisation (WHO) classifies gliomas into grades I-IV. WHO Grade IV astrocytoma tumours are commonly known as glioblastoma multiforme (GBM) (Dunn et al 2012, Louis et al 2007).

Glioblastoma is the most common and most aggressive primary brain tumour (Louis et al 2007), and even though progress has been made with diagnosis and enhanced understanding of the disease through research, patients still have a very poor prognosis with median survival between 12–15 months (Dubrow et al 2013). Recurrence is expected even after treatment.

1.2 Treatment of GBM

Treatment for this disease remains largely unchanged in a decade, where surgery is followed by radiation and temozolomide treatment therapy (Dubrow et al 2013).

Much research into GBM to try to find better treatment options include identifying the cells from which recurrence occurs (“stem cells”) (Broadley et al 2011a) (Chen et al 2012a, Lim et al 2011), molecular and genetic markers (Dreyfuss et al 2009, Reynes et al 2011, Tafani et al 2011) (Liu et al 2006), immune therapy (Fadul et al 2011, Hunn et al 2015), and aberrant signaling pathways (Fassl et al 2012, Lino et al 2010) (Lino & Merlo 2011) (Krakstad & Chekenya 2010). Epigenetics, the study of the natural control over the genome from DNA modulation by enzymes is a relatively new area of interest to GBM research with much potential (Allen et al 2015, Clarke et al 2013, Rauscher 2005).

All cells have highly complex cell signaling network systems and epigenetic responses, which respond to the changing microenvironment. Cells are designed to switch on or off genes in response to environmental changes, or to change the activity of molecules that are always present. Cancer cells have aberrant signaling

systems that are believed to arise mostly from genetic mutations, but can also come about from the stress to the cell for example through tissue damage (Wu et al 2010).

1.3 Sirtuin Family of Histone Deacetylases

Around twenty years ago, the first enzyme in the sirtuin family of histone deacetylases was discovered in yeast, *Saccharomyces cerevisiae*, and was called Sir2 (Sinclair & Guarente 1997). It was found to extend lifespan by repressing genome instability, and thence its name Silent Information Regulator (Kaeberlein et al 1999). Further research uncovered a family of highly conserved sirtuin genes that are found from bacteria to mammals and much interest was generated due to the link sirtuins have to longevity in yeast, worms and flies (North & Verdin 2004) (Tissenbaum & Guarente 2001) (Haigis & Sinclair 2010) (Rogina & Helfand 2004).

In mammals seven sirtuins have been discovered, SIRT1-7, but research has failed to verify if any of them are specific regulators of aging, even though some research indicates a link with long-term survival and SIRT1 expression (Figarska et al 2013). All sirtuins have a highly conserved NAD+ binding domain, which characterises them to a different family of histone deacetylases (HDAC) from HDAC classes I, II and IV. Sirtuins have been classified as HDAC class III (Marmorstein 2001), and will be activated on nutrient deprivation or other stressors, such as heat shock and oxidative damage.

All sirtuins require NAD+ cleavage in their reactions linking their activity to the metabolic state of the cell (Landry et al 2000). While not much is known about the different functions of each sirtuin – there are key differences. Some of them have mono–ADP-ribosyltransferase function instead of or as well as deacetylase function, they locate to different subcellular locations, have differing terminal segments and different substrates, albeit with some overlap (Carafa et al 2012, Haigis & Guarente 2006).

1.4 Sirtuin 1 (SIRT1)

SIRT1 is the closest homologue to the prototype Sir2 in yeast, and is by far the most abundant and most studied member of the sirtuin family, to date. Unlike other sirtuins, it is functionally vital (Haigis & Sinclair 2010).

SIRT1 deacetylates histones to silence DNA transcription in times of stress, and to allow for chromatin stabilisation or DNA repair (Blander & Guarente 2004, Imai et al 2000). Histone acetylation is a reversible and highly dynamic modification process where histone acetyl transferases (HATs) and histone deacetylase enzymes (HDACs) alter chromatin structure thereby controlling transcription and assisting in DNA repair (Kurdistani & Grunstein 2003). A major substrate identified for SIRT1 is Histone 4 lysine 16 (H4K16). H4K16 is frequently acetylated – present in approximately 60% of total H4 in mammals – and represents a pattern of actively transcribed euchromatin distinct from other H4 lysine acetylation (Smith et al 2003) (Dion et al 2005) with a more specific role in cell cycle control compared to other histone acetylations (Megee et al 1995). SIRT1 deacetylates all four histones, but preferentially H4K16 where, in a co-ordinated process involving recruitment of other molecules, SIRT1 is directly involved in the formation of facultative heterochromatin, and indirectly in constitutive heterochromatin (Vaquero et al 2004, Vaquero et al 2007). Research has also shown that SIRT1 deacetylates H4K16 specifically in relation to other deacetylase enzymes (Imai et al 2000), and has a direct effect to silence tumour suppressor genes in breast and colon cancer cells where silencing of SIRT1 changes phenotypic aspects of these cancer cells (Pruitt et al 2006). Furthermore, hypoacetylation of H4K16 has been observed in a number of human cancers (Fraga et al 2005), and HDAC inhibitors have been investigated in the treatment of a number of cancers, including glioblastoma (Egler et al 2008).

Research has also revealed many substrates other than histones for SIRT1, a list that is still growing. The common thread for all SIRT1 activities is a response to stress in the cell to maintain cellular stability and homeostasis, or to switch the cell toward a death pathway through programmed cell death, apoptosis. In particular, SIRT1 is activated in response to metabolic and hypoxic or oxidative stress (Merksamer et al 2013, Salminen et al 2013, Yoon et al 2014). It also has influence on the immune and autophagic responses (Hou et al 2010, Lee et al 2008, Yang et al 2012, Yeung et al 2004, Yoshizaki et al 2009).

SIRT1 is found in the nucleus in most cell types at most times, but can be found in the cytoplasm under some conditions, in some cell types (Hisahara et al 2008, Sugino et al 2010, Tanno et al 2007). Research into localisation changes for SIRT1 is relatively new.

1.5 SIRT1 in metabolism and cell proliferation

SIRT1 activity is intrinsically linked to the metabolic state of the cell because NAD+, a key metabolite, is a coenzyme in the deacetylase function of SIRT1. SIRT1 is activated when levels of NAD+ are high, and inhibited when levels of NADH are high (Saunders & Verdin 2007). Research evidence supports the theory that nutrient availability regulates SIRT1 expression and activity (Chalkiadaki & Guarente 2012b) (Kanfi et al 2008) (Rodgers et al 2005).

SIRT1 deacetylates STAT3, FOXO1 and PGC1a to increase gluconeogenesis (Rodgers et al 2005) (Nie et al 2009), but SIRT1 can also down regulate expression of genes involved in gluconeogenesis under nutrient deprivation (Liu et al 2008) indicating SIRT1 activity is dependent on specific intracellular conditions.

Additionally, increased SIRT1 activity has been shown to increase mitochondrial content, increase energy expenditure and protect against metabolic disease (Lagouge et al 2006).

SIRT1 is implicated in cell proliferation. Most studies have involved cancer cells. For example down regulation of SIRT1 inhibits proliferation of breast cancer cells (Li et al 2012), and inhibition of SIRT1 blocks proliferation of chronic lymphocytic leukemia cells. Contrary to this, increased expression of SIRT1 after resveratrol treatment inhibits proliferation of osteoscarcoma and breast cancer cells (Li et al 2009) (Lin et al 2010).

Some studies looking at SIRT1's role in non transformed cells have been done. In endothelial cells, SIRT1 promotes proliferation through targeting liver kinase B1 (LKB1) (Zu et al 2010), and over-expression of SIRT1 increases muscle cell precursors proliferation (Rathbone et al 2009). However over-expression of SIRT1 using resveratrol suppressed proliferation in microglia (Li et al 2015).

1.6 SIRT1 in oxidative stress

There are many complex effects of intracellular reactive oxygen (ROS) species on SIRT1 activity and expression. Some well known actions of SIRT1 in oxidative stress environment are summarised in Figure 1.

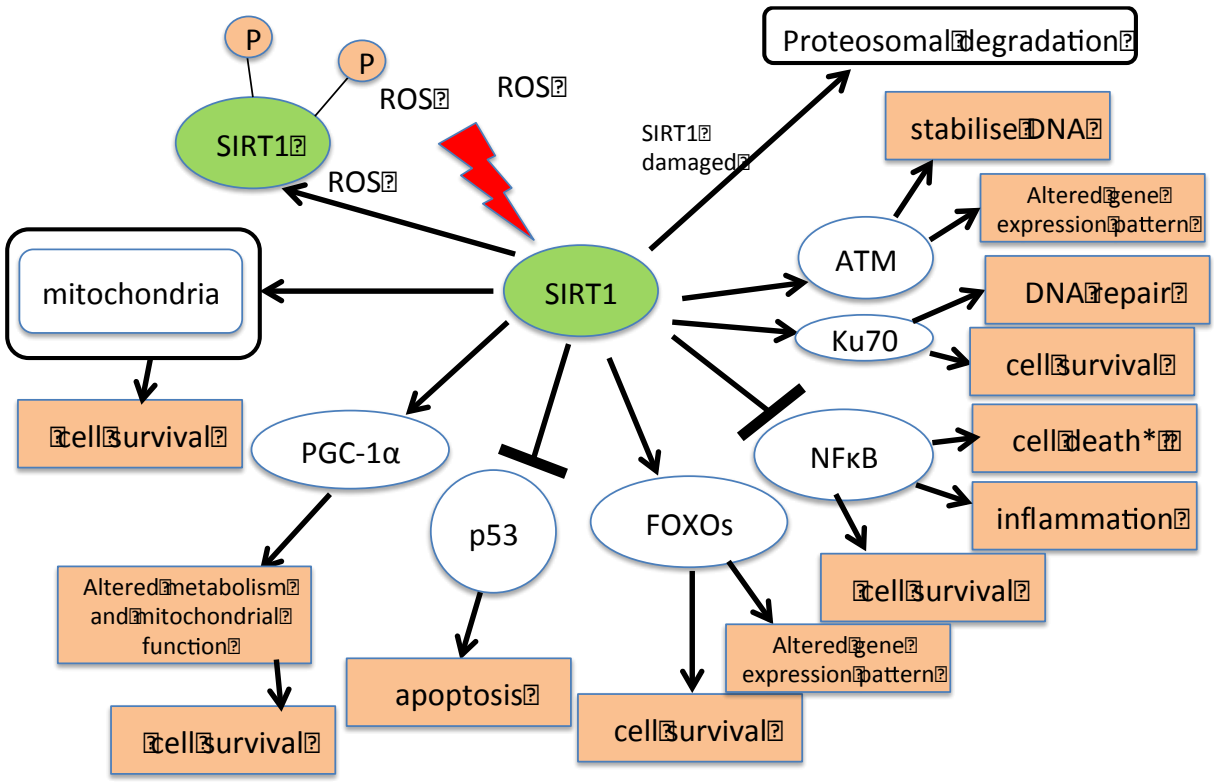

Figure 1. Simplified overview showing cellular substrates and pathways for SIRT1 under oxidative stress conditions

Blue circles represent substrates; orange rectangles show major outcomes for the action of SIRT1 deacetylation. Black arrows show where deacetylation activates the substrate, black T-lines show where deacetylation inhibits the substrate. Abbreviations: ROS = reactive oxygen species; ATM = ataxia telangiectasia mutated; Ku70= one part of the Ku heterodimer involved in DNA repair; NFκB = nuclear factor kappa B; FOXOs = forkhead box-O transcription factors; p53 = tumour suppressor transcription factor; PGC-1α = Peroxisome proliferator-activated receptor gamma co-activator 1-alpha; P = phosphate. Asterisk = cell death can occur on these pathways under specific conditions.*

The role of SIRT1 in conditions of oxidative stress is well studied. Central to SIRT1 role in protection of cells against oxidative stress is the anti-apoptotic response. DNA damage or oxidative stress activates SIRT1 deacetylation and attenuates p53 or Ku70 induced apoptosis (Cohen et al 2004, Kume et al 2006, Luo et al 2001). SIRT1 also deacetylates forkhead box-O transcription factors (FoxOs) –studied in a variety of cells – to resist oxidative stress by a number of mechanisms including increased antioxidant expression, promoting autophagy, diminishing pro-apoptotic

responses and increasing expression of DNA repair proteins (Wang et al 2015, Zhang et al 2015) (Hori et al 2013) (Brunet et al 2004) (Hariharan et al 2010).

Under some forms of oxidative stress, SIRT1 inhibits the NFκB transcriptional signalling pathway, by deacetylating the p65/RelA component of the NFκB complex (Yeung et al 2004) (Liu et al 2011). Depending on the cellular environment, inhibition of NFκB can lead to polar opposite outcomes. For example, it can lead to reducing inflammatory responses and promote anti-apoptotic gene expression (Salminen et al 2008) for cell survival, or it can lead to increased pro-apoptotic gene expression and cell death (Kucharczak et al 2003) (Salminen et al 2013).

SIRT1 expression under oxidative stress in endothelial cells was increased in a study where SIRT1, in part, induced cellular senescence (Ota et al 2008) and SIRT1 protein expression was increased in human renal cells exposed to H_20_2 (Hasegawa et al 2008). Oxidative stress can decrease SIRT1 expression in some brain cells (Wu et al 2006), and H_20_2 induced a decay of SIRT1 mRNA by the Human antigen mRNA binding protein (HuR) in response to check point kinase 2 (Chk2) (Abdelmohsen et al 2007). Furthermore, degradation or modification of SIRT1 is also reported under oxidative stress conditions (Caito et al 2010). Recent research shows that under inflammatory conditions, SIRT1 can be cleaved to reveal an enzymatically dysfunctional smaller protein which can relocate to mitochondria and block apoptosis (Oppenheimer et al 2012).

Specifically in astrocytes, anti-oxidant neuroprotective functions for SIRT1 have been identified by repression of inflammatory cytokines, increased expression of anti-oxidants, and deacetylation of FoxO4 transcription factor (Cheng et al 2014).

The cellular signaling pathways activated during oxidative stress are many and varied. Duration, level of exposure and different species of ROS will activate different responses in different cell types. Moreover, the signalling pathways that are activated or repressed will result in outcomes that affect each other in complex systems of cross-talk and feedback. SIRT1 is one of the key regulators involved in most, if not all of these pathways, and much is still unknown.

1.7 Control of SIRT1

SIRT1 activity is controlled by the metabolic state of cells, as it requires NAD+ a vital metabolite for its enzymatic function (Borra et al 2004). Its own reaction product, nicotinamide (NAM) inhibits SIRT1 in a self-regulatory feedback loop (Bitterman et al 2002).

Due to the non-competitive inhibiton of NAM and potent effect, it is used extensively to inhibit SIRT1 in experiments *in vitro* and *in vivo* (see Figure 2). However, its use is not specific. NAM inhibits other sirtuins, in particular SIRT2 (Giammona et al 2009), and it also inhibits Poly (ADP ribose) polymerase (PARP) involved in DNA repair (Avalos et al 2005, Clark et al 1971). NAM also has other anti-inflammatory and antioxidative effects (Lappas & Permezel 2011).

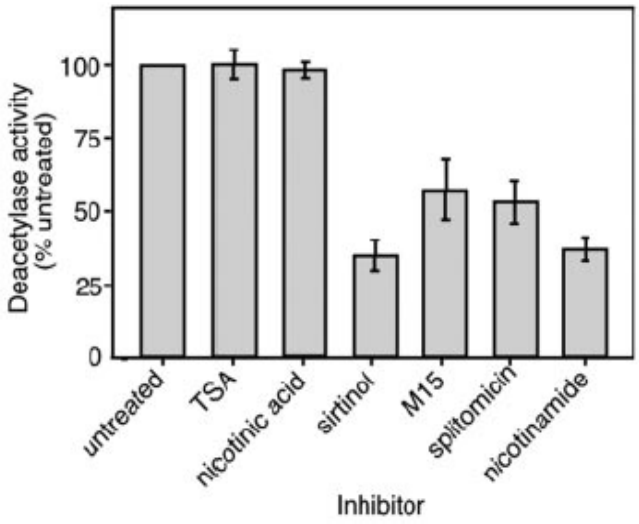

Figure 2. Efficacy of nicotinamide to inhibit SIRT1 activity

Bar graph from an experiment by Bitterman et al, showing the efficacy of NAM inhibition in comparison to synthetic inhibitors sirtinol, splitomicin and M15. TSA is total serum albumin and is used as a control. From (Bitterman et al 2002).

Additionally, SIRT1 is under transcriptional and translational control. The transcription factor E2F1 can induce SIRT1 expression, while deacetylation of E2F1 by SIRT1 can inhibit its activity (Wang et al 2006). The tumour suppressor transcription factor p53 also binds the SIRT1 promoter to decrease transcription where SIRT1 also deacetylates and decreases activity of p53, and can attenuate p53 transcription in feedback loops (Lynch et al 2010) (Lou et al 2015) (Luo et al 2001). SIRT1 is reported to also bind to its own promoter to suppress its own transcription (Han et al 2010).

Changes in SIRT1 protein expression can be controlled in several ways. The micro RNA, MiR-34a, binds mRNA for SIRT1, to decrease its translation and expression. Additionally, increased MiR-34a will increase stabilization of p53, and p53 expression can bind SIRT1 promoter to suppress transcription or bind the MiR-34a gene increasing transcription of that gene (Raver-Shapira et al 2007). The SIRT1 transcript can be stabilised by mRNA binding protein HuR, which is disrupted by oxidiative stress in HeLa cells (Abdelmohsen et al 2007).

Activate Regulator of SIRT1 (AROS) activates SIRT1, while Necdin and Deleted in Breast Cancer 1 (DBC1) inhibits SIRT1 by binding SIRT1 protein directly (Kim et al 2007), (Hasegawa & Yoshikawa 2008, Kim et al 2008). Peroxisome proliferator-activated receptor- γ (PPAR γ) which inhibits cellular proliferation, can bind SIRT1 directly to suppress its activity or bind to the SIRT1 promoter to suppress transcription (Han et al 2010). Resveratrol, a natural compound found abundantly in the skins and seeds of grapes, activates SIRT1 when ingested and is used widely in experimentation to activate SIRT1 (Howitz et al 2003)} (Sulaiman et al 2010). However, it also has other actions within the cell that are not specific to SIRT1.

In addition to transcriptional control, posttranslational changes to SIRT1 including phosphorylation, ubiquitination, and SUMOylation affect SIRT1 activity. There are several recognised phosphorylation sites on SIRT1 (Sasaki et al 2008) (Lau et al 2014). Increased ROS conditions activate c-Jun kinase 1 (JNK1) which phosphorylates SIRT1 and activates it in the nucleus to specific target substrates (Nasrin et al 2009). However, persistent JNK1 activation in the liver led to ubiquitination and degradation of SIRT1 (Gao et al 2011) showing that cell types or micro-environmental changes are important to SIRT1 responses. SUMOylation of SIRT1 by SENP1 lessens deacetylase activity under stress conditions resulting in a lessening of SIRT1s anti-apoptotic response (Yang et al 2007). It may be that multiple PTMs on SIRT1 at any one time alters its function according to the microenvironment.

SIRT1 can change subcellular localisation which also regulates its activity. Depending on cell type, state of stress or stage of development, SIRT1 can be found in the cytoplasm or nucleus to affect cellular responses for example apoptotic responses in response to oxidative stress or differentiation signals (Jin et al 2007) (Sugino et al 2010) (Hisahara et al 2008).

1.8 SIRT1 splice variants and cleavage products

Only in the last ten years of research, cleavage and splice variants of SIRT1 have been revealed.

There is little research into the activity of SIRT1 cleavage products. The C and N terminals of SIRT1 protein have different functional elements (Pan et al 2012), which would be disrupted after cleavage.

Elevated levels of tumour necrosis factor alpha (TNFα) induces SIRT1 to cleave in chondrocytes and draining lymph node cells altering its function (Dvir-Ginzberg et al 2011) (Gardner et al 2015) and high fat diet induces cleavage of SIRT1 in adipose tissue contributing to metabolic dysfunction (Chalkiadaki & Guarente 2012a). Altered gene expression was observed after SIRT1 cleavage (Dvir-Ginzberg et al 2011). Cleaved SIRT1 75kDa fragment blocked apoptosis in osteoarthritic chondrocytes (Oppenheimer et al 2012), and cleaved SIRT1 moved to the cytoplasm from the nucleus in apoptotic HeLa cells (Ohsawa & Miura 2006). Cleavage of SIRT1 in endothelial progenitor cells mediated premature senescence (Chen et al 2012b).

The first splice variant of SIRT1, SIRT1-Δ8, was reported five years ago in a range of human tissue indicating evolutionary conservation (Lynch et al 2010). SIRT1-Δ8 showed altered function including association with p53. Interestingly, p53 controlled the expression of this variant isoform of SIRT1. A second splice variant of SIRT1, SIRT1-Δ2/9 was also found even more recently- also in a range of human tissue(Shah et al 2012). This variant also associated with p53 opposing the function of full-length SIRT1 indicating a role of SIRT1 in malignancy (Shah et al 2012).

1.9 SIRT1 and cancer

It remains unclear whether SIRT1 is a tumour suppressor or promoter. Much research into this area is being carried out recently due to the likelihood for a SIRT1 role in initiation and progression of cancer mainly due to its function to stabilise chromatin in times of DNA stress (Lee et al 1999, Martin et al 1999), but also due to SIRT1 involvement in apoptosis, autophagy and senescence (Broadley et al 2011a, Huang et al 2014, Luo et al 2001). Additionally, SIRT1 is involved in stress resistant pathways therefore it may be involved with maintaining cancer cells

under stress within the tumours and promoting drug treatment resistance. SIRT1 plays a role in pathways central to cancer etiologies including glycolysis and differentiation (Tiberi et al 2012) (Ghosh et al 2010, Mantel et al 2008), and it binds to or deacetylates many molecules that are closely linked to cancer.

However, research shows SIRT1 can be either promoting or suppressing cancer, for example, recent studies have shown a correlation with SIRT1 expression and poor disease prognosis in breast cancer (Cao et al 2015) and a high level of SIRT1 is seen as a negative prognosticator for pancreatic cancer (Stenzinger et al 2013); yet no correlation with SIRT1 expression is found in hepatocellular carcinoma or cholangiocarcinoma progression (Al-Bahrani et al 2015). SIRT1 expression is elevated in some cancers compared to the normal tissue, for example in acute myloid leukemia, primary colon cancer and non-melanoma skin cancers (Bradbury et al 2005) (Stuenkel et al 2007) (Hida et al 2007); yet SIRT1 expression is reported to be decreased in other cancers compared to normal tissues for example in bladder (Sanchez-Carbayo et al 2006), and ovarian cancers (Hendrix et al 2006).

Moreover, SIRT1 expression data from different studies of the same cancer don't always agree – in one prostate cancer study SIRT1 expression is elevated (Huffman et al 2007) and in another it is reduced (Lapointe et al 2004). SIRT1 appeared benign in hepatocarcinoma progression in one study (Al-Bahrani et al 2015) while other studies have shown that inhibiting SIRT1 and cortactin in prostate cells attenuated migration and metastasis (Nakane et al 2012) and transgenic overexpression of SIRT1 in mice with PTEN deficiency promotes thyroid carcinogenesis (Herranz et al 2013). It may be that SIRT1 has different roles at different stages of cancer.

It is also unclear whether increased SIRT1 expression occurs before onset or as a consequence of malignancy. Examples include the overexpression of nicotinamide phosphoribosyltransferase (NAMPT) in prostate cancer which may increase SIRT1 expression and activity (Wang et al 2011), and a study of lung cancer found SIRT1 activity increased in airway epithelium of smokers but not in non-smokers, yet SIRT1 activity was significantly decreased in lung adenocarcinoma (Beane et al 2012). This last example indicates a protective role of SIRT1 in lung cancer, and is reflected in another more recent study where repression of SIRT1 transcription contributes to lung cancer metastasis (Sun et al 2013).

1.10 SIRT1 in glioblastoma

There is not much SIRT1 research in association with GBM, but in the last few years more research has looked into SIRT1 because treatment options for GBM have highlighted the need to target survival and apoptotic pathways (Krakstad & Chekenya 2010), which is central to the role of SIRT1.

SIRT1 knockdown in glioma cell lines found inhibited growth and proliferation, and increased apoptosis strongly indicating a role of SIRT1 in progression of GBM, through the PTEN/PI3K/AKT signaling pathway (Qu et al 2012). FOXM transcription factor, reported to be a central regulator of glioma cell proliferation and tumour progression, was found to positively regulate SIRT1 expression in another study using glioma cell lines, suggesting SIRT1 plays a role in glioma tumour progression (Zhu et al 2014).

SIRT1 is likely to play a role in GBM due to its importance in growth signaling (Lu et al 2013) in particular through activated PI3K/AKT signaling which is commonly abherently over-activated in GBM (Narayan et al 2013). This pathway involves five or six transcription factors all of which are substrates for SIRT1 deacetylation (Sundaresan et al 2011) (Ikenoue et al 2008). However, although SIRT1 contributes to the activation of AKT signaling in some circumstances (Pillai et al 2014), it can also ameliorate the effects of hyperactive signaling along this pathway (Salminen et al 2008), highlighting the need to elucidate the role of SIRT1 in GBM.

Aerobic glycolysis, an alternative metabolic pathway, is often seen in cancer cells and is apparent in glioblastoma (Oudard et al 1996) (Zhou et al 2011). Additionally, glycolysis appears to support invasion in glioblastoma (Beckner et al 2005). However, there is some research to show that “stem cells”, the cells that regenerate tumours after treatment in glioblastoma, are not driven by glycolysis (Vlashi et al 2011). The role of SIRT1 in glycolysis is not determined.

Radio-chemoresistant glioblastoma cell clones adapted metabolically to reduced glucose dependence had increased cellular NAD+ and SIRT1 expression (Ye et al 2013), further indicating that SIRT1 may be involved in tumourigenesis in GBM. However another study found SIRT1 activation was in part responsible for the effective treatment of temozolomide’s anti-tumour effects on glioma cell lines (Jiang et al 2012).

Conflicting evidence for SIRT1 in cancer highlights the likely different activities of SIRT1 after different treatments, and probably for different stages or areas of the tumour. In fact it was found that glioblastoma cells categorised by the World Health Organisation (WHO) grade I-III have increased SIRT1 compared to normal brain tissue, however WHO grade IV had comparatively decreased SIRT1 (Annabi et al 2012).

1.11 Aims of this research

Glioblastoma treatment options have remained limited for many years, with prognosis for patients very poor. Glioma cells remain resistant to treatment, and recurrence of the disease is usual. SIRT1 is a key regulator of stress response in cells, and intimately involved in metabolism, development, and the autophagic and apoptotic responses, while research into the role of SIRT1 in glioblastoma is very limited, it is likely to have a role in this disease. The aim of this research is to investigate the differences between glioma and normal astrocyte cells in a mouse culture model and primary human glioma compared to normal human astrocytes to look for differences in SIRT1 – in expression, activity, and under oxidative stress. The cell lines chosen for this research were the immortalised murine cell lines GL261, a glioma model cell line, which was compared to the immortalised normal murine astrocyte cell line, C8D1A. In the human model, cell lines established from cells taken during resection of tumours in patients with GBM WHO Grade IV, and results from these cells were compared to SVGp12, an immortalised human astrocyte cell line.

Astrocytes are the most abundant cells in the central nervous system (Cheng et al 2014) and are important in oxidative and cytotoxic stress conditions (Bresgen et al 2006). Moreover, glioblastoma derives from astrocytes which is why astrocytes are the normal comparison cell used in this study.

The focus has been threefold:

1. Comparison of basal expression levels of SIRT1, localisation, and its deacetylation activity on histone 4 (H4K16) between
    a. Murine cell lines of glioma (GL261) compared to normal astrocytes (C8D1A) and;

b. Human primary glioma cells taken from patient tumours compared to the normal astrocyte cell line taken from embryonic origin (SVG p12)

2. Investigating the role SIRT1 may have in proliferation for the same cells as stated above, and

3. Investigating the role SIRT1 may have under oxidative stress in the same cells as stated above.

For the purposes of this thesis, SVG p12 cells are referred to as SVG, hSIRT1 is used when referring to human cells, Sirt1 for mouse cells, and SIRT1 when discussing the enzyme generically.

Part 2: Materials and Methods

2.1 Cell culture

2.1.1 Cell lines

Murine cell line C8D1A, the human cell lines SVGp12 and the human glioblastoma cell line LN18 were obtained from the American Type Culture Collection, (Rockville, MD, USA), http://www.atcc.org/. HeLa cells were a kind gift from An Tan, Malaghan Institute of Medical Research The murine glioma cell line, GL261, was obtained from DTTD Tumour Repository, National Cancer Institute (National Institute of Health, USA).

Human primary cells were from glioblastoma tumour tissue obtained under informed consent and isolated as described by Broadley et al (Broadley et al 2011b), approved by Central Regional Ethics Committee, Ministry of Health from patients, CEN/09/06/037, 2009. Patients were all diagnosed with glioblastoma (GBM WHO Grade IV), both male and female, aged 34–77 years. Available patient data is presented in Table 1.

Table 1. Patient data for human primary glioma cell lines

Human primary glioma cell line	Age at resection (years)	Gender	Survival (months)
705	34	F	34
902	38	M	26
1005	42	M	16
813	47	M	34
903	47	F	-
906	57	F	8
804	61	M	10
804	61	M	10
711	62	M	13
905	64	F	17
713	65	M	33
816	65	M	23.5
803	67	F	5
708	70	M	10
907	77	F	12.5
801			10
815			26
817		M	16
1011			12

2.1.2 **Cell culture hardware**

Cells were grown in T25 and T75 flasks, 150 mm tissue culture dishes and 6-, 12- and 96-well plates supplied by Falcon (BD Biosciences, San Jose, CA). Serological pipettes were from by BD Biosciences. Pipette tips (Axygen, Union City, CA) were sterilised by autoclaving at 121°C for 20 min.

2.1.3 **Cell culture media**

Human primary glioma and SVG cells were grown in RPMI-1640 (Invitrogen, Carlsbad, CA) supplemented by 10% heat inactivated foetal bovine serum (Sigma Aldrich, St Louis, MO), 100 Units/mL penicillin, 100 µg/mL streptomycin (supplied as a combined supplement by Gibco (Invitrogen). Murine cell line C8D1A was grown in DMEM with 10% heat inactivated FBS (Sigma Aldrich) and GL261 were grown in both 10% and 20% FBS separately. Both murine cell lines were supplemented by penicillin/streptomycin in the same way as for the human cell cultures.

2.1.4 **Cell culture**

All cells used in this study grew as adherent cultures.

Cells were passaged between 70–90% confluency, with passage number not exceeding 25. To passage cultures, cells were rinsed with phosphate buffered saline (PBS) (Invitrogen) incubated at 37°C with trypsin-EDTA (0.05%, Invitrogen) for 3–10 min, followed by resuspension of a reduced number of cells in media – unless more culture dishes were needed – where cells were plated back out into several culture dishes. All cultures were grown in HERAcell incubators (Thermo Scientific, Waltham, MA) at 37°C, in humidified air with 5% CO_2. Handling of cells for culture and treatment was performed under sterile conditions in a Class II Biological Containment Hood (Herasafe, Heraeus, Germany). Cell counting was performed using trypan blue with a Neubauer heamocytometer (Weber Scientific, Hamilton, NJ). Regular checks were made to ensure cultures were mycoplasma free using e-Myco mycoplasma PCR detection kit (iNtRon Biotech, Korea). All cells were harvested in the log phase of growth.

2.1.5 **Storage of cells**

For long-term storage, cells were stored in cryotubes (Greiner Bio-one, Belgium) with 10% v/v dimethylsulfoxide (Sigma Aldrich)/media in the vapour phase of liquid nitrogen. Cells were slowly cooled using a controlled rate cooler to -80°C then transferred to liquid nitrogen. To recover cells from liquid nitrogen, cells were thawed in a 36°C waterbath, transferred to pre-warmed media for one day, and then the media was replaced.

2.1.6 **Cell harvesting**

To harvest cells, media was removed, cells were rinsed with PBS and trypsin-EDTA (0.05%) was applied. Cells were incubated with trypsin-EDTA for a few minutes until cells lost their adhesion to the plate, then media was added to reduce the concentration of trypsin-EDTA, followed by centrifugation at 736 g for 5 min, then rinsed and resuspended in PBS and centrifuged again as before.

2.2 **Protein extraction and western blotting**

2.2.1 **2.2.1 Whole cell extraction**

For whole cell extraction, at least $1x10^6$ cells were rinsed with PBS, released from culture dishes with trypsin-EDTA, and washed twice with PBS. Centrifuge and microcentrifuge speeds and times for the washing steps were 736 g for 5 min, and 1,073 g for 4 min respectively. PBS was removed by pipette and 20-70 µL Lysis Buffer (see Section 2.3.1) and Protease Inhibitor – either Roche Diagnostics 7x (Basel, Switzerland Product no.04693159001), or Halt Protease inhibitor Cocktail 100x (Thermo Scientific Product No. 78410) was added to the pellet and pipetted up and down for at least 20 times. Following incubation in Lysis Buffer for 1 h on ice, the lysate was centrifuged at 11,337 g for 5 min and the supernatant carefully removed with a pipette and transferred to a clean microfuge tube.

The protein yield was measured using a Bradford DC protein Assay Kit (Bio-Rad, Hercules, CA) with absorbances measured at 750 nm (Versamax MicroPlate reader, Molecular Devices Pty Ltd, with SOFTmax PRO 4.0 software) against a standard curve generated from bovine serum albumin (BSA). Lysates were suspended in 2x or 6x sample loading buffer depending on how much quantity was extracted before heating to 90°C or 35°C for 5 min and then stored at -80°C. The different

temperatures were used as it was found 90°C affected the quality of SIRT1 protein. Unless stipulated in Figure legends, the temperature used was 35°C.

2.2.2 **Histone extraction**

At least $2x10^6$ cells were washed with ice cold PBS, released from the culture dish by trypsin-EDTA and washed with PBS. PBS was pipetted off the cell pellet followed by resuspension of cells in 1mL ice-cold Histone Extraction Buffer (Section 2.3.2) and centrifuged at 2000 g for 15 min. The buffer was removed and the pellets were washed four times by resuspending in Histone Extraction Buffer and centrifugation. The washed pellet containing nuclei was resuspended in 100 µL Tris-EDTA solution (0.01 M Tris-HCl, 0.13 M EDTA, pH 7.4), with addition of 1.1 µL/100 µL H_2SO_4 (BDH Aristar ® Plus, BDH Chemicals, Radnor, PA) followed by vortexing and incubation for 3 h at 4°C. Supernatant was collected after a 15 minute centrifugation at 11,337 g followed by addition of 1 mL acetone and incubation at 4°C overnight. Precipitated material was collected by centrifugation at 11,337 g for 15 min, and washed once in 1 mL acetone. Acetone was completely removed and the powder was air dried for 5 min, then resuspended in 20-50 µl TE buffer (0.028 M Tris, 0.037 M EDTA, pH 6.9). Protein was measured as described in Section 2.2.1, then 2x or 6x loading buffer was added before heating at 95°C for 5 min and storage at -20°C.

2.2.3 **Nuclear and cytoplasmic extracts**

Nuclei- and cytoplasm-enriched fractions were isolated using two methods. Both fractions were expected to be partial purifications, contaminated by other organelles. Measurements for purity were included.

Method one

After Andrews and Faller, 1991 Premade buffers A and B were stored at 4°C (Section 2.3.6). Protease Inhibitor 7x (Roche Diagnostics) or 100x (Thermo-Fisher), and Triton X-100 (for Buffer B) were added on the day of extraction. At least 3 x 10^6 cells were washed once with ice cold PBS, and then harvested by the standard method (Section 2.1.6). Between 0.2-1 mL Buffer A (for 1-8 x 10^6 cells) was added to the cell pellet and pipetted up and down gently, and left at room temperature (RT) for 10 min. A cytosolic fraction was collected as the supernatant after centrifugation at 11,337 g at 4°C for 6 min, and kept on ice before protein

quantification and storage. Between 50-300 µL (1-8 x 10^6 cells) Buffer B was then added to the remaining pellet, and resuspended thoroughly by pipette, followed by vortexing for 10 sec. The pellet was continuously rotated at 4°C for 20 min. The nuclear fraction was collected in the supernatant after centrifugation at 11,337 g at 4°C for 10 min.

Method two

NE-PER® Nuclear and Cytoplasmic Extraction Kit (Pierce, Thermo-Scientific)

The manufacturer's instructions were followed. Briefly, at least 2 x 10^6 cells harvested using trypsin-EDTA were washed twice with PBS and after centrifugation at 736 g for 5 min, PBS was removed carefully, and for each 40 µL packed cells, 200 µL ice-cold CER I solution was used to resuspend the pellet, followed by vortexing and incubation on ice for 15 min. Next, 11 µL ice-cold CER II was added followed by vortexing and incubation on ice for 1 min. Then, vortexing followed by centriguation at 16,000 x g the supernatant (cytoplasmic fraction) was removed and stored on ice. The pellet was rinsed in PBS twice, then resuspended in ice-cold 100 µL NER, vortexed and held on ice for 10 min. This was repeated four times, followed by centrifugation at 16,000 x g for 15 min to obtain the nuclear fraction in the supernatant. Where fixation of cells was used before extraction, cells were fixed in 1% v/v formaldehyde in the culture dish at RT for 10 min and 0.125 M glycine was then added and left for 5 min, followed by washing with PBS two times.

2.2.4 **SDS electrophoresis**

Ten percent acrylamide SDS gels were used for electrophoresis of non-histone proteins, 15% acrylamide SDS gels were used for electrophoresis of histones. Each gel was made with a 4% resolving gel. The reagents and solutions were:

10% SDS acrylamide running gel

0.454 M Tris pH 8.8

0.347 M SDS

10.5% acrylamide solution (N,N'methyl acrylamide) electrophoresis reagent, (BioRad)

2.2 mM ammonium persulphate

0.05% v/v TEMED (BioRad)

15% SDS acrylamide running gel

0.454 M Tris pH 8.8,

0.347 M SDS,

15% acrylamide solution

2.2 mM ammonium persulphate

0.05% v/v TEMED

Resolving gel

0.125 M Tris pH 6.9

6.9 mM SDS

3.9% acrylamide solution

2.2 mM ammonium persulphate

0.1% TEMED

Gels were mounted into a Bio-Rad Mini-PROTEAN Tetra Cell gel box, and cold Running Buffer (Section 2.3.4) was added to the chamber. Between 25-100 µg whole cell lysate, 2-5 µg histone, and 10-15 µg nuclear and cytoplasmic fractions were loaded into each well. Unless stated in figure legends, equal amounts of protein was loaded into each well for the same blot. Precision Plus Protein™ All Blue standard (Bio-Rad) or PageRuler™ Prestained Protein Ladder (Thermo

Scientific) were used for molecular weight markers. Electrophoresis was at 190 V for 1 h.

2.2.5 **Western blot transfer**

After gel electrophoresis, the protein was transferred to polyvinylidene difluoride (PVDF) (BioRad) using a BioRad Criterion™ Blotter gel box. PVDF membrane was hydrated with 100% methanol and then equilibrated in freshly made chilled Transfer Buffer (Section 2.3.5) for 5–10 min. Gels were equilibrated in cold Transfer Buffer also, and then the gels were covered with PVDF, placed between sponges and filter paper which had been fully pre-soaked in Transfer Buffer, and sandwiched tightly in a cassette. The transfer was for 2 h at 300 mA. PVDF membranes were dried and stored at RT, or used immediately for antibody probing.

2.2.6 **Antibody probing**

After transfer, PVDF membranes were rehydrated and blocked for 1 h by rocking at RT in either 3% w/v non-fat milk (Anchor, New Zealand) dissolved in PBS.

Following blocking, membranes were rocked for 1.5 h at RT, or overnight at 4ºC in a milk/PBS solution containing the primary antibody (Table 2). The membrane was then washed three times in PBS, and left to soak in PBS for five min, after which the membrane was rocked in a milk/PBS or BSA/PBS solution containing secondary antibody conjugated to horseradish peroxidase (Table 3) for 1.5 h at RT. Following the secondary antibody probe, membranes were washed three times with PBS and left to soak in PBS with 0.02% Tween 20 for 5 min, and rinsed three more times with PBS.

Table 2. Primary antibodies used in Western blotting

Antibody	Source and type	Concentration used
Anti-SIRT1 H(300) SC 15404	Santa Cruz Biotechnology (Dallas, TX) Rabbit, polyclonal IgG	0.2-0.4 μg/mL
Anti-SIRT1 [SIRII] ab 50517	Abcam® (Cambridge, UK) Sapphire Biosciences, Mouse, monoclonal C terminal aa 722-737	0.575 μg/mL
Anti-β-actin A5441	Sigma-Aldrich Mouse monoclonal	1:100,000
Anti-Lamin A/C orb18081	Biorbyt (Cambridge, UK) Rabbit polyclonal	1 μg/mL
α-tubulin SAB4500087	Sigma-Aldrich Mouse monoclonal	1:5000
Anti-acetyl-Histone H4 (Lys 16) 07-329	Merck Millipore (Billerica, MA) Rabbit polyclonal	0.75 μg/mL

Table 3. Secondary antibodies used in Western blotting

Antibody	Source and type	Concentration used
Goat Anti-rabbit HRP Sc 2004	Santa Cruz Biotechnology IgG	0.25 μg/mL
Goat Anti-mouse HRP Sc 2005	Santa Cruz Biotechnology IgG	0.25 μg/mL

2.2.7 **Amido Black staining, Stripping Buffer, and chemiluminescence**

Amido Black solution

Amido Black staining (0.1 g/mL Naphthol Blue Black, 7.5% v/v glacial acetic acid, 20% v/v methanol) of PVDF membranes was used as a protein loading measure during histone acetylation analysis. Membranes were rocked with Amido Black solution for 2 min, rinsed in ethanol and left to dry before scanning to make an image.

Chemiluminescence

Enhanced Chemiluminscence (ECL) Western Blotting Substrate (Pierce, Thermo Scientific) was used to detect horseradish peroxidase activity, which corresponds to quantity of antibody bound to the membrane and therefore protein levels in the lysate. Where there were low levels of protein, Western Lightning Ultra (Perkin Elmer, Waltham, MA) was used.

Stripping Buffer

When stripping of membranes was required, membranes were rocked at RT in stripping buffer (Restore™Western Blot Stripping Buffer) (Thermo Scientific) for 10–15 min.

2.2.8 Western blot imaging

Scanned images from film developed using a Kodak X-OMAT 1000 film processor, or a GelLogic 4000 Pro imaging system (with Carestream software) were analysed using Image J software (Schneider et al 2012). To adjust for loading differences, a housekeeping protein, β-actin, was used for whole cell extracts and lamin B or lamin A/C and α-tubulin were used for nuclear/cytoplasmic extracts, respectively. Image J ‘gel analysis’ was used to measure the area under the curve generated from the electronic measurement of band density. Where measurements across different gels were made, one sample was used for the reference point. This sample was used across the gels and adjusted to 1, and other bands from samples were expressed as a fraction of this (Figure 3).

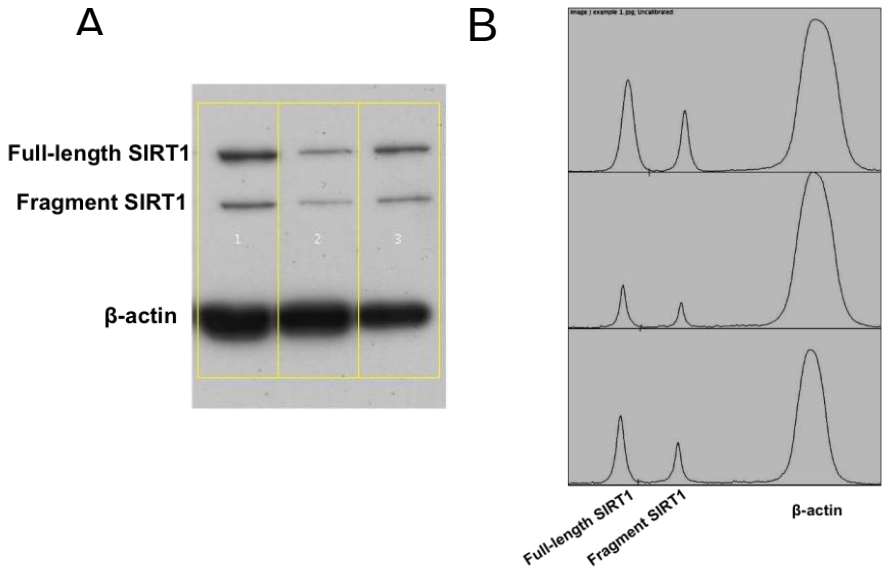

	Full-Length SIRT1	Full-Length SIRT1 adjusted	β-actin	β-actin adjusted	Relative difference
1	3785	1	2842	1	1
2	1173	0.31	2800	0.99	0.32
3	2257	0.60	1900	0.67	0.89

Figure 3. Example of analysis of protein bands using Image J analysis

(A) Electronic image from HRP- generated fluorescence using a membrane immunoblotted with SIRT1 and β-actin. (B) Image J gel plots of bands shown in A. (C) Tabulated measurement of area under the curves in B, measured in Image J. All measurements used in analysis were adjusted to take into consideration of loading differences.

2.3 Buffers

2.3.1 Lysis Buffer

0.14 M NaCl

0.05 M Tris

1% v/v Triton X-100

0.1% w/v SDS

pH 8.5

7x Protease Inhibitor (Product No. 78430) (Thermo-Fisher Scientific)

2.3.2 **Histone Extraction Buffer**

0.01 M Tris

0.023 M $MgSO_4.6H_2O$

0.25 M sucrose

0.05% v/v Triton X-100

2.3.3 **Sample Loading Buffers (Laemmli Buffers)**

SDS Sample Buffer 2x

0.124 M Tris-Cl pH 6.8

20% v/v glycerol

4% w/v SDS

0.2% v/v 2-mercapthoethanol

0.05% w/v bromophenol blue

SDS Sample Buffer 6x

0.375 M Tris-Cl pH 6.8

60% v/v glycerol

12% w/v SDS

9.3% w/v dithiothreitol (DTT)

0.06% w/v bromophenol blue

2.3.4 **2.3.4 SDS gel electrophoresis Running Buffer**

0.025 M Tris

0.192 M glycine

0.0173 M SDS

pH 8.3

2.3.5 **Western blot Transfer Buffer**

0.025 M Tris

0.192 M glycine

10% v/v methanol

2.3.6 **Nuclear cytoplasmic Extraction Buffers**

Buffer A

10 mM HEPES (pH 7.9)

10 mM KCL (Scharlab, Spain)

0.1 mM EDTA

7x protease inhibitor (Roche Diagnostics)

Buffer B

20 mM HEPES (pH 7.9)

0.4 M NaCl

1 mM EDTA

10% v/v glycerol

2.3.7 **Flow Cytometry (FACS) Buffer**

HBSS buffer (Gibco)

2% v/v heat-inactivated FBS

2.4 Immunofluorescent staining

2.4.1 Fixation and staining

Cells were seeded on sterile Lab-Tek 8-well chamber slides at a density of 6-8,000 cells per well, with 300 µL media, and left for 48 h before treatment or fixation.

Fixation of cells was preceded by removal of media followed by two gentle washes with warmed PBS, and then drained well. Freshly made paraformaldehyde (PFA) (see Section 2.4.3) was applied to cover the cells, and left at RT for 10 min. Cells were washed twice with PBS, followed by permeabilisation using PBS with 0.2% Triton X-100 (Sigma-Aldrich) for 3 min at RT. Cells were then rinsed four times over 5 min with PBS, and incubated for 1 h with primary antibody buffered in 3% w/v bovine serum albumin in PBS solution, with enough liquid to cover the cells. After incubation with the primary antibody, cells were washed with PBS two times, and once with PBS/0.02% Triton X-100 over five min. Cells were then incubated with fluorescent-labelled secondary antibodies in 3% w/v BSA in PBS at RT, in the dark, for 40 min, followed by two rinses with PBS and one rinse with PBS/Triton X-100 over 5 min. Isotype or secondary-only controls were included (Tables 4–5).

Table 4. Primary antibodies for immunofluorescent staining

Antibody	**Source and Type**	**Concentration Used**
Goat anti-Sirtuin 1 EB10826	Everest Biotech (Ramona, CA) Aa 577-590	10 μg/mL
Anti-SIRT1 [SIRII] ab 50517	Abcam® Sapphire Biosciences, Mouse monoclonal, IgG aa 722-737	4.6 μg/mL
Anti-SIRT1 H(300) SC 15405	Santa Cruz Biotechnology Rabbit polyclonal, IgG Aa 448-747	4 μg/mL

Table 5. Secondary antibodies for immunofluorescent staining

Antibody	Source and type	Concentration used
Goat anti-rabbit Alexa Fluor® 488 A11608	Invitrogen IgG	10 μg/mL
Goat anti-mouse Alexa Fluor® 488 A11001	Invitrogen IgG	10 μg/mL
Goat anti-rabbit Alexa Fluor® 647 A21244	Invitrogen IgG	10 μg/mL
Goat anti-mouse Alexa Fluor® 647 A21235	Invitrogen IgG	10 μg/mL
Rabbit anti-goat CF488A	Biotium (San Francisco, CA) IgG	10 μg/mL

2.4.2 **Microscopy**

Microscopy was carried out using an Olympus BX51 immunofluorescence microscope (Olympus Optical Co. Ltd, Tokyo, Japan,) with an Olympus DP70 camera and Olympus LS Research software.

2.4.3 **Paraformaldehyde solution**

4% w/v paraformaldehyde

1x PBS

The above reagents were added to a conical flask with a few drops of 5 M NaOH, vortexed and fully dissolved in a water bath at 55-65°C for 30 min or until clear. The solution was left to adjust to RT before using.

2.5 **Mitochondrial staining**

MitoTracker ® Green FM (Invitrogen) was dissolved in anhydrous dimethyl sulfoxide to a concentration of 1 mM. A solution of 150 nM MitoTracker ® Green FM in media was applied to cells and left for 1.5 h at 37°C.

2.6 Intracellular staining and measurement by flow cytometry

To measure levels of SIRT1 by flow cytometry, intracellular staining was performed. Approximately $1x10^6$ cells were harvested as described in Section 2.1.6. Cells were transferred to a round-bottom 96-well plate and rinsed once in PBS (200 µL per well), followed by centrifugation at 2080 x g for 2 min. To remove fluid from wells after centrifugation, plates were flicked once and fluid was removed by inversion of the plate. Cells were resuspended in the viability dye, LIVE/DEAD® Fixable Blue (Invitrogen), using a dilution of 1:500 in PBS (50 µL per well), and incubated on ice in the dark for 20 min. Cells were centrifuged and rinsed twice with PBS. Fixation and permeabilisation was carried out using BD Cytofix/Cytoperm™(BD Biosciences). All antibodies were diluted in Perm/Wash Buffer. SIRT1 primary antibody, Sc15404 (see Table 2, Section 2.2.6), was used at a concentration of 0.4 µg/mL and incubated on ice, in the dark, for 20 min, followed by two washes with Perm/Wash Buffer. The secondary antibody, goat anti-rabbit (Alexafluor ® 647, A21244) (Table 5, Section 2.4.1), was used at a concentration of 5 ng/mL and incubated on ice, in the dark, for 30 min, followed by two washes using 1x Perm/Wash.

Cells were suspended in a FACS buffer (Section 2.3.7) acquired using a BD LSR-II and FACSDiva software. Between 5,000–10,000 cells were collected. Data were analysed using FlowJo 9.5.2 software (Tree Star). Background fluorescence, compensation and non-specific binding were controlled for using the isotype control anti-dansyl rabbit IgG antibody (A-6398, Invitrogen).

2.7 MTT Assay

In this assay, the yellow tetrazole, MTT (3-(4,5-dimethylthiazol-2-yl)-2,5–diphenyltetrazolium bromide), is reduced to a purple formazan in living cells. The formazan is insoluble, and therefore an SDS Lysis Buffer (10% w/v sodium dodecyl sulphate (SDS), 45% v/v N-N-dimethylformamide, adjusted to pH 4.7 using glacial acetic acid) is used to dissolve these crystals so that an absorbance reading can be made. The reduction of MTT depends on the presence of active reductase enzymes so the results reflect metabolic activity of the cells (Berridge & Tan 1993).

Cells were seeded at 5000 cells per well in 100 µL of media, in 96-well plates. After 24 h, cells were treated with fresh media with appropriate concentrations of treatment chemicals prepared in media en masse. The media was also replaced for untreated control cells. Control wells with media alone, or media with treatment alone, were included. At 48 h after seeding (day one of treatment) and 96 h (day 3), MTT was added at 2.5 mg/mL suspended in HBSS buffer (Gibco). After 2 h 100 µL SDS Lysis Buffer was added to every well. When the wells had no bubbles, absorbances were measured at 570 nM using a FLUOstar OPTIMA Microplate Reader (BMG LABTECH, Ortenberg, Germany). Control absorbance values for media with or without treatment were subtracted from values for the equivalent wells with cells.

2.8 Oxidative stress

2.8.1 Hydrogen peroxide

The concentration of the stock hydrogen peroxide (AnalaR grade, BDH/Merck, Poole, England) was determined by spectrophotometry at 240 nm using a molar extinction coefficient of 43.6 $M^{-1}cm^{-1}$. Cells were seeded and left for 24 h before treatment. For treatment, media was removed and replaced with fresh media with H_2O_2 at the desired concentration, and this remained until cells were harvested. Concentrations of H_2O_2 used for each cell line were determined by establishing viability titration curves and propidium iodide exclusion assay (Section 2.10). Untreated control cells were always measured at the same time as treated cells.

2.9 Inhibition and activation

2.9.1 Inhibitor

Nicotinamide (NAM) (Sigma Aldrich) at concentrations of 1 and 10 mM was used as an inhibitor for SIRT1. After leaving cells for 24 h after seeding, the desired concentration of NAM was added to cultures and remained until cells were harvested.

2.9.2 **Activator**

Resveratrol (RES) (Sigma Aldrich) at concentrations of 10, 25 and 50 μM was used as an activator for SIRT1. Working stock of RES was dissolved in 100% ethanol and stored for up to 6 weeks. After leaving cells for 24 h after seeding, the desired concentration of RES was added to cultures, which remained until cells were harvested.

2.10 Measurement of cell death

To measure cell death, a propidium iodide (PI) (BD Biosciences) exclusion assay was used. Cells were grown for 24 h before treatment, and harvested when they were in exponential growth (untreated cells 60-85% confluence). All cells were collected and subjected to the standard wash (Section 2.1.6). A concentration of 0.5 μg/mL PI suspended in FACS Buffer (Section 2.3.7) was added to the cell pellets and, after 15 min incubation, PI exclusion was measured by flow cytometry. Between 5,000–10,000 cells were analysed using BD FACSCalibur (BD Biosciences), and CellQuest Pro software (BD Biosciences). Data were analyzed using FlowJo 9.2 software (Tree Star, Ashland, OR).

2.11 Statistical Analysis

All statistical analysis was performed using Prism Graphpad version 5.0 and 6.0 software (CA, USA). *P* values were generated using linear regression, one-way ANOVA with Tukey or Sidak's multiple comparison post test, unpaired Student *t*-test and values of $P < 0.05$ were considered significant.

Part 3: Results – Basal Levels

Exploring the potential role of SIRT1 in untreated glioma and normal astrocyte cells

It has not been established if SIRT1 acts as a tumour promoter or tumour suppressor in glioblastoma. In this study, C8D1A and GL261 murine astrocyte cell lines were used as a model for glioblastoma. GL261 cells lines are a transformed cell line used as a model for glioblastoma, as it closely resembles the pattern of human glioblastoma when implanted in the brain of a mouse (Newcomb 2009), while C8D1A cells are used as the normal murine astrocyte comparison cell line. In the human model, SVG – a normal human astrocyte cell line was used as a comparison to primary glioma cells obtained from patient tumours.

To begin investigating the role of SIRT1 in glioblastoma, basal levels of SIRT1 were measured by Western blotting.

3.1 SIRT1 levels in murine and human glioma and normal astrocyte cells

3.1.1 Levels of Sirt1 in untreated murine C8D1A and GL261 cell lines

To begin the comparison of Sirt1 in normal astrocytes versus glioma cells, basal levels of Sirt1 were measured using Western blotting, for untreated C8D1A and GL261. To investigate the levels of hSIRT1 in human primary glioblastoma cells, whole cell lysis followed by SDS PAGE and Western blotting for Sirt1 was performed.

Immunoblotting using a C-terminus monoclonal antibody revealed a trend for greater Full-Length Sirt1 (FL-Sirt1) in GL261 compared to C8D1A (Figure 4), but the difference was not significant for six independent experiments ($p > 0.05$). A rabbit polyclonal antibody used for Western blotting but designed to recognise human SIRT1 was used while optimising experimental procedures. This experiment, performed once, showed FL-Sirt1 but also some second protein bands running at about 75 kDa, which may or may not be Sirt1 variants (Figure 4 C).

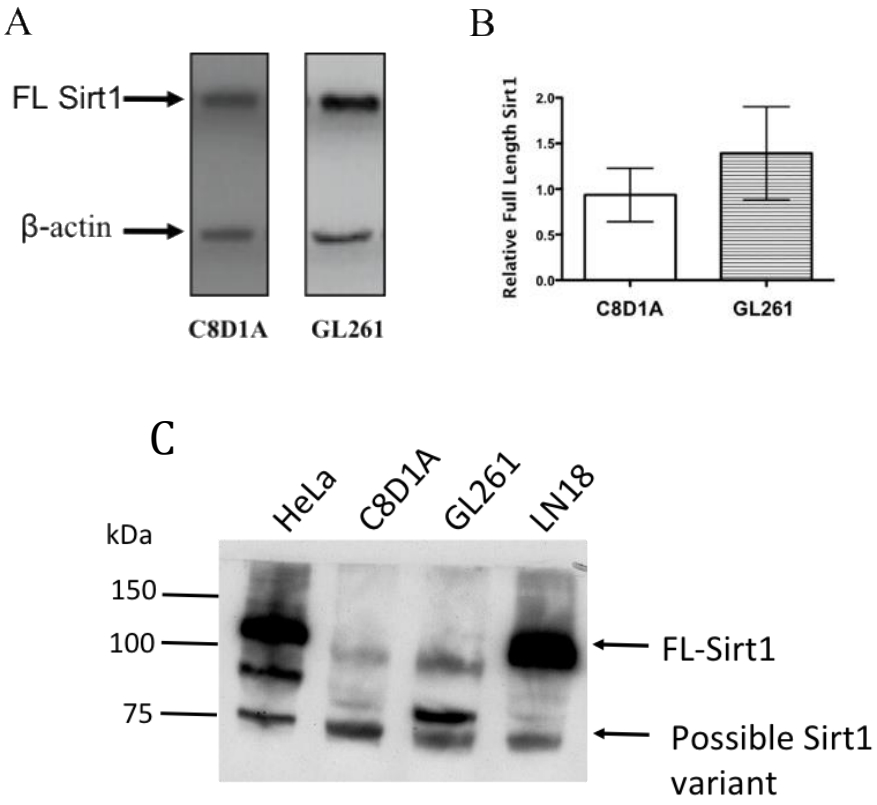

Figure 4. Sirt1 levels were not significantly different between C8D1A and GL261 cell lines

Representative Western blot images from untreated C8D1A and GL261 cells in exponential growth phase at approximately 70% confluence. (A) Western blot image for Sirt1. The monoclonal antibody Ab50517 recognising C-terminus amino acids 722-737 of mouse Sirt1 was used, with β-actin as a loading control. FL-Sirt1 was 120 kDa in these cells; (B) Relative abundances of FL-Sirt1 in C8D1A and GL261 cells. Measurements were ratios of FL-Sirt1 to β-actin, n=6 for each cell line, (p > 0.05 Student's t-test, error bars representing SEM). Measurements taken from immunoblots using Image J analysis with adjustment for actin were done using the antibody specified above; (C) Immunblot image taken using antibody designed to recognise human hSIRT1, sc15404 recognising C-terminus amino acids 448-747 was used. HeLa is a human epithelial adenocarcinoma cell line and LN18 is a human glioma cell line.

3.1.2 **hSIRT1 levels in human primary glioblastoma cells and SVG, a human astrocyte cell line**

To investigate the levels of hSIRT1 in human primary glioblastoma cells, whole cell lysis followed by SDS PAGE and Western blotting for hSIRT1 was performed. The antibody used was a polyclonal hSIRT1 antibody that recognised the C-terminus region (aa 448-747). We compared levels of hSIRT1 in astrocyte cell line, SVG, to primary cells taken from glioblastoma tumours and adjusted to β-actin on quantification using Image J software.

Primary glioblastoma cell cultures were established from tumours taken from patients as described by Broadley *et al*, (Broadley et al 2011b). Some clinical data was available for these patients, which are described in the methods section. Primary cells from the tumours were used at as early a passage as possible in an attempt to avoid cells transforming in culture. Some primary cells grew more quickly than others, and some stopped growing and appeared to enter senescence during the course of the experiments, hence not all experiments have data from the same panel of primary cells.

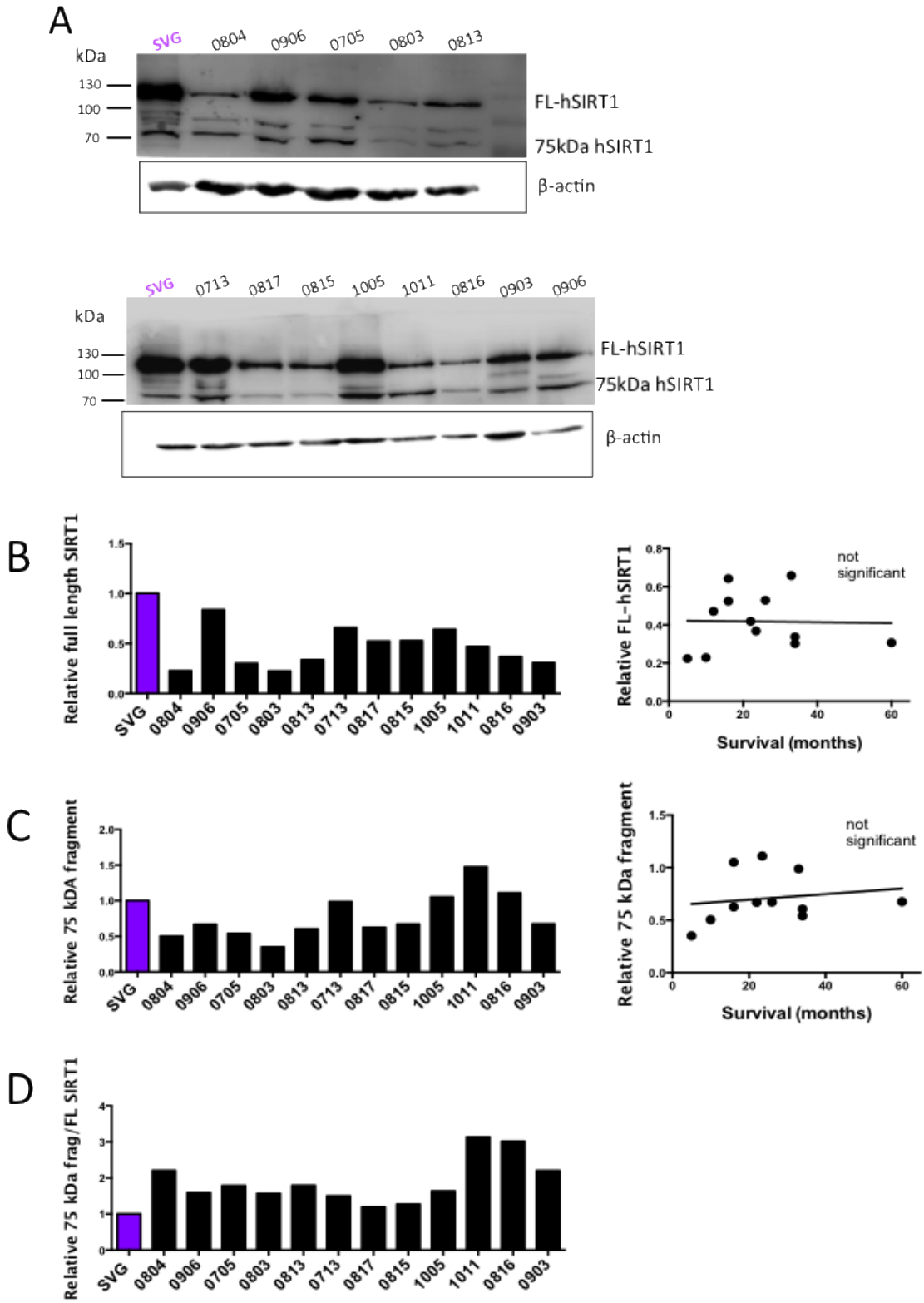

Figure 5. Comparison of FL-hSIRT1 and hSIRT1 smaller species in human glioma and normal SVG astrocyte cell line and the relationship to patient survival

SVG cell line and 12 primary glioma cell cultures were grown to 70% confluency before extraction and western blotting for hSIRT1 was performed. (A) Western blot image for SVG and human primary gliomas after probing for hSIRT1 and β-actin (B) Histogram showing relative levels of FL-hSIRT1 after adjusting to β-actin loading control levels, SVG set to one, and correlation plot showing glioma primary cell line hSIRT1 levels against patient survival; (C) as in B, but for the hSIRT1 fragment at about 75 kDa; (D) as in B but for the ratio of hSIRT1 75 kDa fragment over FL-hSIRT1.Note B, C and D have different y-axes for ease of visual comparison. Linear regression analysis was performed using Prism 6 software. Data used from a single Western blot experiment.

Results showed a prominent band at around 120 kDa, which is full-length hSIRT1 (FL-hSIRT1). This was present in all primary glioma cells in varied amounts, and in SVG (Figure 5 A). The second most prominent band ran at about 75 kDa, which was present in all the primary cells tested and in SVG. There was also a third band present in many, but not all of the primary cells, at 90 kDa. However, in the SVG cell line, there were more than two bands consistently present, while the primary glioma cells had only two or three bands (120, 90, and 75 kDa).

Without using sequencing or mass spectrometry, it is not possible to identify the smaller bands, but based on the recent literature it is likely that at least some of them are hSIRT1 variants (Chalkiadaki & Guarente 2012a, Chen et al 2012b, Dvir-Ginzberg et al 2011, Shah et al 2012). However, a hSIRT1 variant running at 75 kDa on Western Blot has been listed on the NCBI BioSystems database and is an accepted isoform of hSIRT named SirT1 75 kDa fragment. Thus, in this study, the band seen at approximately 75 kDa was thought to be this isoform, and has been labelled 75 kDa SIRT1 in the results.

Overall, these results suggest there was less FL-hSIRT1 in all the human primary cell lines measured in this assay compared to SVG (Figure 5 B). However, a third of the primary cell glioma cell lines had increased 75 kDa hSIRT1 compared to SVG (Figure 5 C), and interestingly, when the ratio of the 75 kDa fragment against FL-hSIRT1 was measured, all the primary glioma cells exceeded that of the normal cell line (Figure 5 D). To gain more understanding for the role of hSIRT1 in GBM, linear regression using survival data and FL-SIRT1 and 75kDa hSIRT1 was assessed (Figure 5 B and C). No significance was found in these analyses. Repeated measurements of hSIRT1 from more patient samples would be more informative.

Of note, 0903 has a different hSIRT1 Western blot profile to the other primary cells extracted, with a second band at around 90 kDa, as in the normal SVG profile. Curiously, only this patient survived long-term, at least 60 months with no sign of disease recurrence.

3.1.3 **Intracellular staining verifies SIRT1 levels in glioma primary cells is less than in SVG astrocytes**

To further examine the difference in hSIRT1 levels in glioma cells compared to normal cells, SVG and a panel of glioma primary cells were fixed and permeabilised, stained with hSIRT1 or an isotype control, and a secondary antibody, Alexafluor 647. Cells were analysed by flow cytometry, after gating out doublets and dead cells using LIVE/DEAD Fixable Blue, to determine cellular hSIRT1 levels, using a different method to extraction and Western blotting.

These results agreed with the Western blot data, where levels of hSIRT1 were mostly decreased in primary cells compared to the normal astrocyte cell line, SVG. While overall levels of hSIRT1 were decreased (Figure 6 B), intracellular staining data showed higher levels of hSIRT1 in glioma cells than in the results from Western blotting. This is most likely because the intracellular staining does not differentiate between different hSIRT1 isoforms, Alternatively it could be due to differential sensitivities of the techniques. There was a positive trend for increased survival and greater levels of hSIRT1 (Figure 6 C), but this did not reach significance.

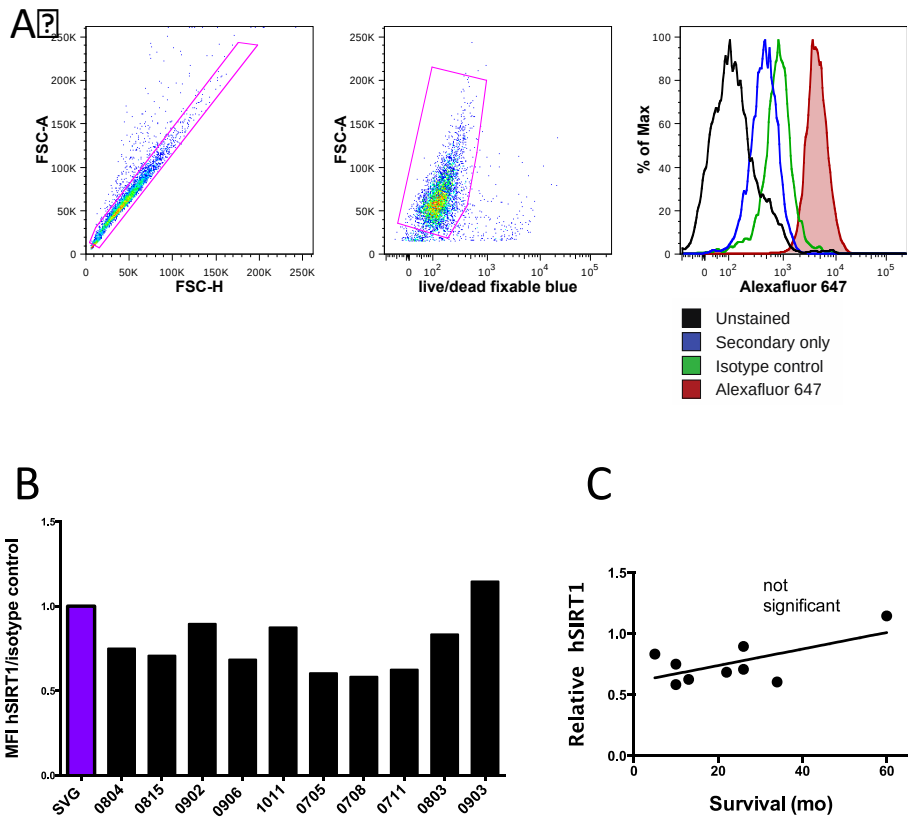

Figure 6. Intracellular staining analysis of hSIRT1 protein levels in SVG normal astrocyte cell line and primary glioma cells

Primary glioblastoma and normal astrocyte SVG cells were cultured to reach 70% confluency, then fixed, permeabilised and stained with hSIRT1 or an isotype control, and secondary antibody, Alexafluor 647. Levels of hSIRT1 were measured by flow cytometry. (A) Flow cytometry gating strategy – gating out doublets and dead cells, and histogram showing how isotype and secondary only controls show higher fluorescent intensity compared to unstained cells; (B) histogram showing relative MFI of hSIRT1/isotype control in 10 human primary GBM cell lines and SVG normal astrocytes; (C) Plot to show linear regression of GBM primary cells in relation to patient survival. n=1, using triplicate flow cytometry measurements from the same experiment.

3.2 Acetylation for H4K16 showing SIRT1 activity in normal and glioma cells

H4K16-ac was measured to assess SIRT1 activity on this nuclear substrate. Hypoacetylation is seen as a hallmark in a panel of cancer cell lines including lung, neuroblastoma, testis, prostrate, osteosarcoma, lymphoma, breast and colon with specific H4K16-ac loss occurring early on and accumulating during the tumourigenic process (Fraga et al 2005). As previously mentioned, H4K16 is a well-known substrate for SIRT1, and relatively specific for SIRT1 in relation to other deacetylase enzymes (Imai et al 2000). SIRT1 deacetylation of this substrate is linked to breast and colon cancer because it silences tumour suppressor genes (Pruitt et al 2006) and acetylation of this residue on H4 is associated with cell cycle

control more specifically than other residues on histone 4 (Megee et al 1995). Together, these reasons make H4K16 a good substrate to measure in this study looking at differences between normal and glioma cells.

The activity of SIRT1 is not necessarily directly related to levels of protein seen on Western blots, because SIRT1 activity can be influenced by other modifications, such as phosphorylation, binding to other proteins, and localisation. Results for H4K16-ac is one of many substrates for SIRT1.

Histone extraction and Western blotting for H4K16-ac were performed on murine C8D1A and GL261, then followed by a comparison between H4K16-ac on human SVG normal astrocytes and a panel of primary glioblastoma cells. Decreased acetylation on H4K16 indicates *more* SIRT1 activity as it is a deacetylase enzyme.

3.2.1 **Acetylation of H4K16 in C8D1A and GL261 cell lines**

To determine Sirt1 activity in murine cell lines, histones were extracted from control untreated C8D1A and GL261 cells and probed for H4K16-ac.

The results showed a greater acetylation for GL261 on H4K16 compared to C8D1A, which did not reach significance (Figure 7). Hyperacetylation was unexpected because hypoacetylation at this residue is common in other cancers (Fraga et al 2005).

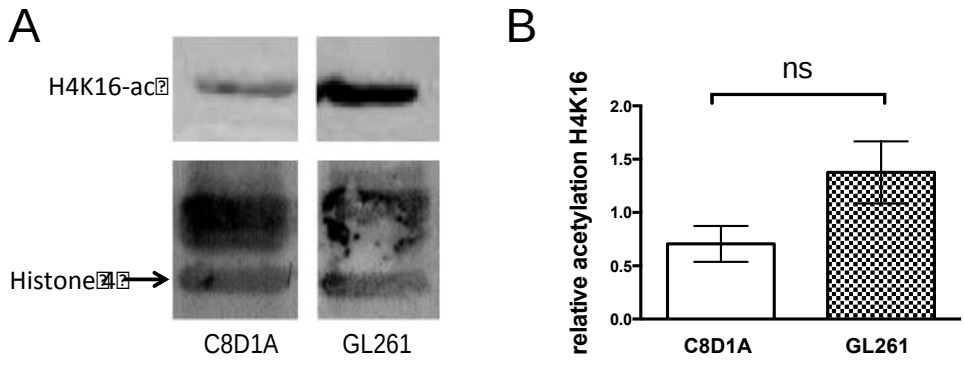

Figure 7. H4K16 acetylation in GL261 and C8D1A cells

(A) Representative Western blot images of 2.5 µg protein histone extracts from C8D1A and GL261 cells in exponential growth phase at approximately 70% confluence. Top panel shows the acetylation of H4K16; bottom panel shows the H4 loading control achieved using amido black staining showing H4 at expected location (indicated by arrow). (B) Analysis of H4K16-ac relative to loading control. n=7 C8D1A; n=8 GL261. The difference was not significant (ns) p > 0.05, Student's t-test.

3.2.2 **Histone 4 lysine 16-acetylation is variable in primary glioblastoma cells**

The results showed half of the primary glioblastoma cell lines extracted had reduced H4K16-ac compared to SVG, with the other half having greater acetylation compared to SVG (Figure 8 A and B), showing a variation in H4K16-ac states between patients. Statistics showed no significant correlation between survival and H4K16-ac, using linear regression analysis (Figure 8 C). Finally, repeat extractions for H4K16-ac were made to investigate variation for acetylation status in primary cell cultures for each patient. This showed that there was not a great variation in acetylation status between extractions of the same cells – with one or two exceptions (Figure 8 E). SVG was not included in this repeat analysis, however, so averages were not used for regression analysis.

A linear regression analysis was also made between FL-hSIRT1 expression levels and H4K16-ac, to see if there was a relationship between these two variables. While there was no statistical correlation found in this analysis, unexpectedly a trend for greater acetylation levels (that is, *less* SIRT1 activity) with increased hSIRT1 levels was observed (Figure 8 D). Either the hSIRT1 is deacetylating another nuclear substrate, or perhaps FL-hSIRT is not predominantly localised in the nucleus in primary glioblastoma cells, as seen with murine glioma cells.

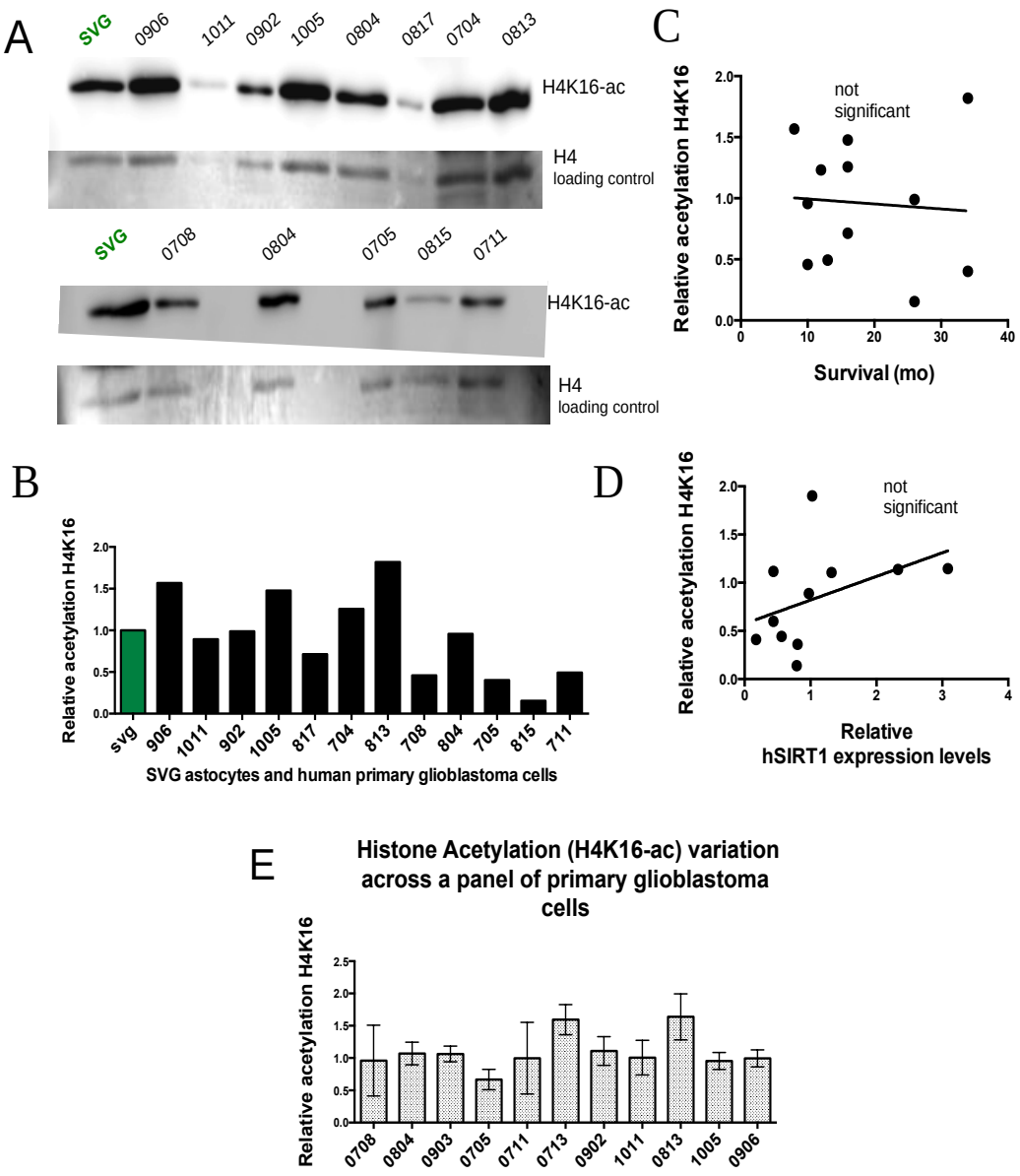

Figure 8. H4K16-ac in human primary glioblastoma cells

Cells were grown for one day, and then histone extraction was performed, followed by Western blotting for H4K16-ac. These results are from two separate extractions each time using SVG cells extracted at the same time as a control measure – adjusted to one (A) Images from Western blot of SVG and 12 human primary glioma cells from two extractions; (B) Histogram showing results of Western blot for H4K16-ac as in A, after adjustment for amido black loading control, and setting SVG to one, using Image J software; (C) Linear regression plot for H4K16-ac in the primary glioblastoma cells in A, against survival in months for patients; (D) Linear regression plot for relative H4K16-ac against relative FL-hSIRT1 levels in primary glioblastoma cells, n=1; (E) Histogram showing variation in relative H4K16-ac across a panel of glioblastoma cells. These were not measured against a standard SVG, but against each other, after adjustment to loading control. Repeats are as follows: 0708:2, 0804:5, 0903:2, 0705:3, 0711:2, 0713:2, 0902:2, 1011:3, 0813:5, 1005:4, 0906:5. Bar represents mean with standard error of the mean.

3.2.3 **FBS concentrations in media affect histone acetylation in GL261 cultured cells but not FL-Sirt1 levels**

A recent publication showed there was aberrant Sirt1 localisation in cancer cells versus normal cells, due to increased protein stability in the cytoplasm, and was regulated by P13K/IGF-IR signaling (Byles et al 2010).

In this research, C8D1A cells were routinely cultured in DMEM with 10% FBS, while GL261 cells were grown in 20% FBS (as recommended by suppliers). It was therefore questioned whether the altered histone acetylation was due to the higher levels of growth factors when 20% FBS was used. Changes in serum levels of FBS are known to alter insulin related cell signaling pathways (Berenguer et al 2010). To investigate this, GL261 cells were grown in 10% FBS supplemented media for five passages, and then immunoblotted for Sirt1 and H4K16-ac. Comparison was made with C8D1A and GL261 cells grown in 10% and 20% FBS.

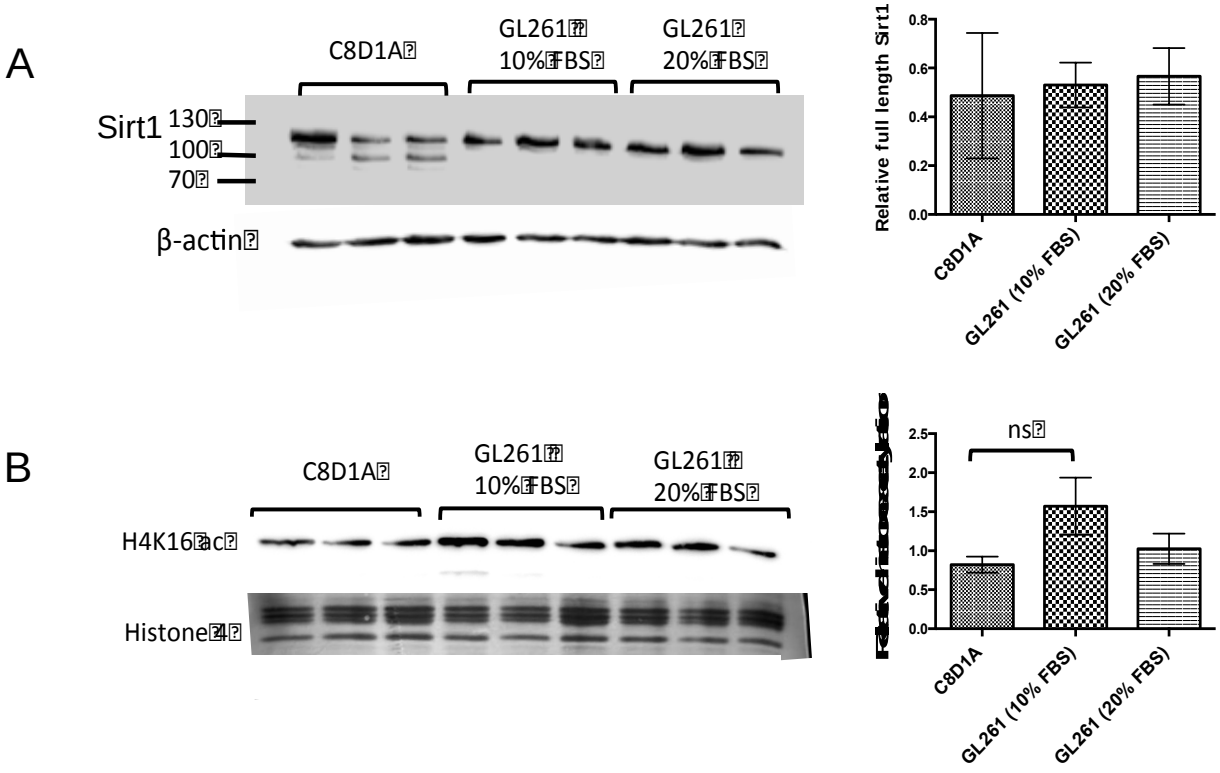

Figure 9. Neither FL-Sirt1 expression levels nor activity showed any significant change when FBS levels were altered

(A) Immunoblot for Sirt1 with histogram showing quantification; (B) immunoblot and control amido black images for H4K16-ac and H4 in C8D1A cells, and GL261 cells grown in 10% or 20% FBS, and histogram showing quantification. The loading controls were β-actin for Sirt1, and amido black staining of the H4 region for H4K16-ac. Lysate was heated to 90°C. One-way ANOVA analysis was carried out on the images, ns= not significant $p > 0.05$. Error bars represent mean ± s.d for the three independent experiments.

These results showed no statistical significance between the Sirt1 or H4K16-ac levels for GL261 grown in 20% FBS compared to C8D1A and GL261 grown in 10% FBS. While there was no significance in the results, there was a tendency for greater levels of H4K16ac in GL261 cells grown in 10% FBS compared to the same cells grown in 20% FBS, or C8D1A cells grown in 10% FBS. This needs further research, but if further repeats showed a significant difference in Sirt1 activity on H4K16, it would indicate that increased FBS levels would also increase Sirt1 activity on this substrate. There were extra bands seen for some of the C8D1A Sirt1, which was thought to be related to the lysate being heated to 90°C. Temperatures were kept lower in other expermiments. This was no evidence to suggest this was related to FBS levels.

3.3 Subcellular localisation for SIRT1 – immunofluorescent microscopy

Deacetylation of H4K16 requires nuclear localisation; a possible explanation for different acetylation states on H4K16 could be explained by different localisation. Therefore, localisation of SIRT1 was next investigated. Control untreated cells were fixed in 4% paraformaldehyde solution and permeabilised with 0.2% Triton X-100, both in PBS, followed by immunofluorescent staining for SIRT1 (Section 2.4)

3.3.1 Sirt1 is aberrantly localised to the cytoplasm in GL261 cells

As expected, Sirt1 was predominantly localised to the nucleus in C8D1A normal astrocyte cells, however Sirt1 was seen localised to the cytoplasm and nucleus in GL261 cells strongly contrasting to the pattern seen in C8D1A (Figure 10). This general observation was seen consistently, however both cell lines showed variation in the localisation of Sirt1, suggesting Sirt1 is mobile in both these cell lines, and depending on the environment or conditions, Sirt1 localisation can change. For example, when cells were bunched together, Sirt1 would appear much more cytoplasmic in the normal cell line, C8D1A, than in single cells spaced apart from each other.

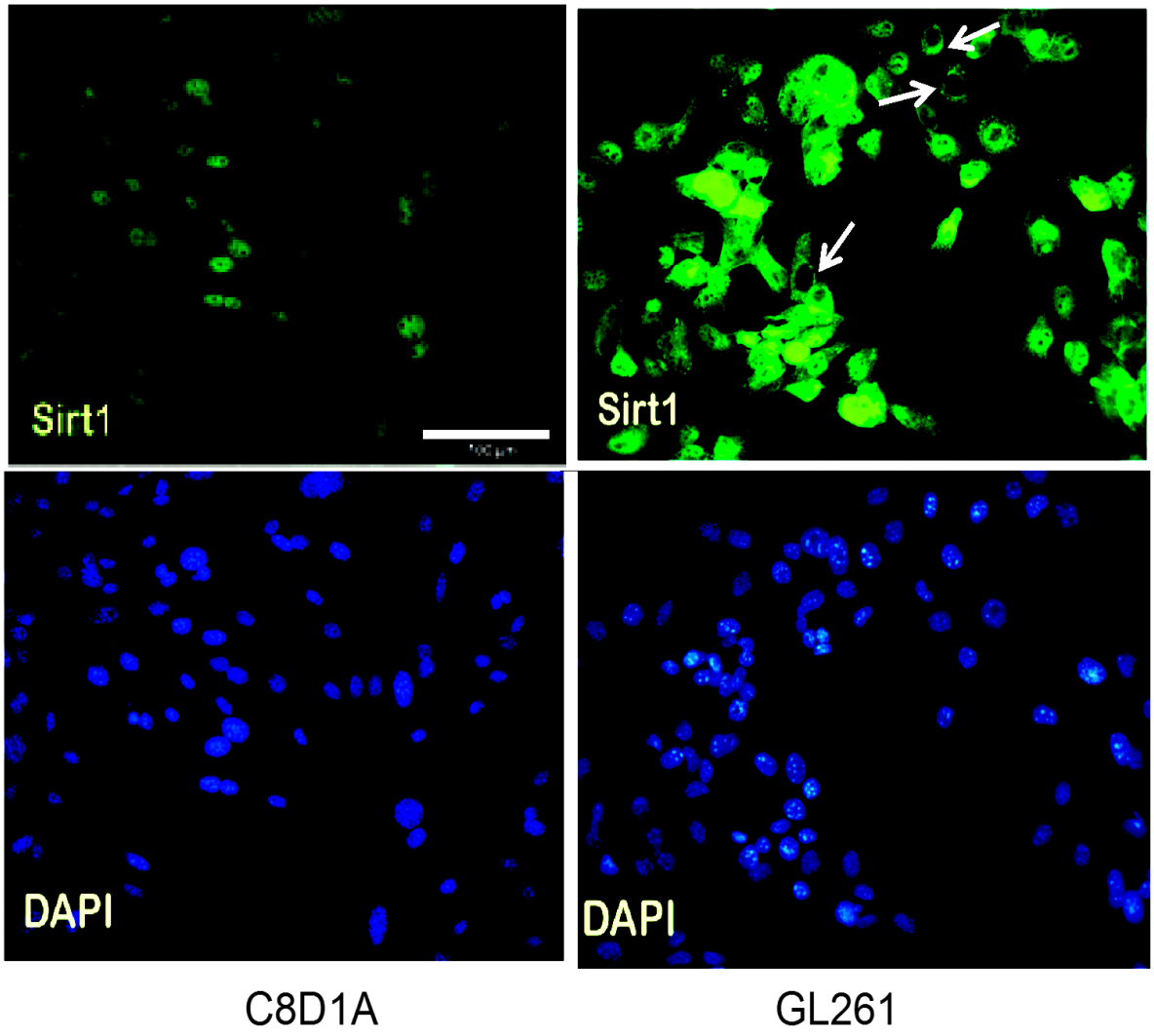

Figure 10. Aberrant cytoplasmic localisation of Sirt1 in GL261 cells

C8D1A and GL261 cells were grown on coverslips for two days before fixation of cells with paraformaldehyde, incubation with mouse monoclonal anti-Sirt1 (Ab50517) then secondary antibody rabbit anti-mouse IgG H&L (Alexa Fluor® 488). Top panel shows Sirt1 (green); bottom panel DAPI staining of nuclei (blue). Scale bar is 100 μm, and is relevant for all images. Arrows show examples where Sirt1 was absent in the nucleus of GL261 cells.

Aberrant cytoplasmic localisation of Sirt1 has been reported in cancer cells compared to normal tissue from breast, prostate and lung cells (Byles et al 2010) but it has not been reported in glioma cells.

3.3.2 hSIRT1 is aberrantly localised to the cytoplasm in human glioblastoma cells compared to the SVG normal astrocyte cell line

In the mouse model of glioblastoma, aberrant Sirt1 cytoplasmic localisation in cancer cells was found. In the human primary GBM cells, more FL-hSIRT1 tended to show more H4K16-ac, a key substrate in the nucleus for hSIRT1, indicating a possible cytoplasmic localisation for hSIRT1 in these cells also. To investigate

intracellular localisation of hSIRT1 in human primary glioblastoma cells compared to SVG normal astrocytes, paraformaldehyde fixation followed by intracellular immunofluorescent staining for hSIRT1 was performed for SVG and a panel of primary GBM cells.

Fluorescent microscopy revealed that in SVG cells, hSIRT1 was found mostly in the nuclei, with a small amount in the cytoplasm in clearly defined areas (Figure 11 top panel). hSIRT1 in glioblastoma primary cells was also seen in nuclei but with a greater amount seen in the cytoplasm compared to SVG, and was more diffuse compared to cytoplasmic hSIRT1 in SVG (Figure 11 panels below first panel).

Each primary glioblastoma has an apparent different level of cytoplasmic hSIRT1 relative to nucleic hSIRT1. On analysis of immunofluorescent photographs, however, the pattern of cytoplasmic SIRT1 was diffuse, with some exceptions, notably 0814 (see Figure 11 B). While SVG cytoplasmic hSIRT1, even though it was minimal, was more defined to filamentous structures not far away from the nucleus compared to more diffuse cytoplasmic hSIRT1 seen in primary glioma cells (Figure 11 B). As confocal microscopy was not available, hSIRT1 localisation could not be quantified.

Figure 11. hSIRT1 is found aberrantly in cytoplasm of primary glioblastoma cells compared to SVG normal astrocytes

(Facing page)
SVG astrocyte cell line and a panel of glioma primary cells were grown on 8-chamber well slides for two days, then fixed with paraformaldehyde and incubated with SIRT1 antibody, Alexafluor 488 (green fluorescent) secondary antibody, and DAPI for nuclei staining. Microscopy with a camera attached was used to visualise results and to take electronic images for analysis. (A) Images of hSIRT1 (green) and nuclei (blue) in SVG and five primary glioma cell lines. Scale bar: 100 µm; (B) Enlarged pictures, or larger scale images showing SVG with predominantly nucleic with some cytoplasmic hSIRT1 with filamentous structures, and primary glioblastoma cells with more diffuse cytoplasmic SIRT1 (0713, 0907, 0906). Except for 0814 DAPI is excluded in these larger images to show more clearly differences in hSIRT1 between SVG and primary glioma cells. Scale bars shown for individual photos.

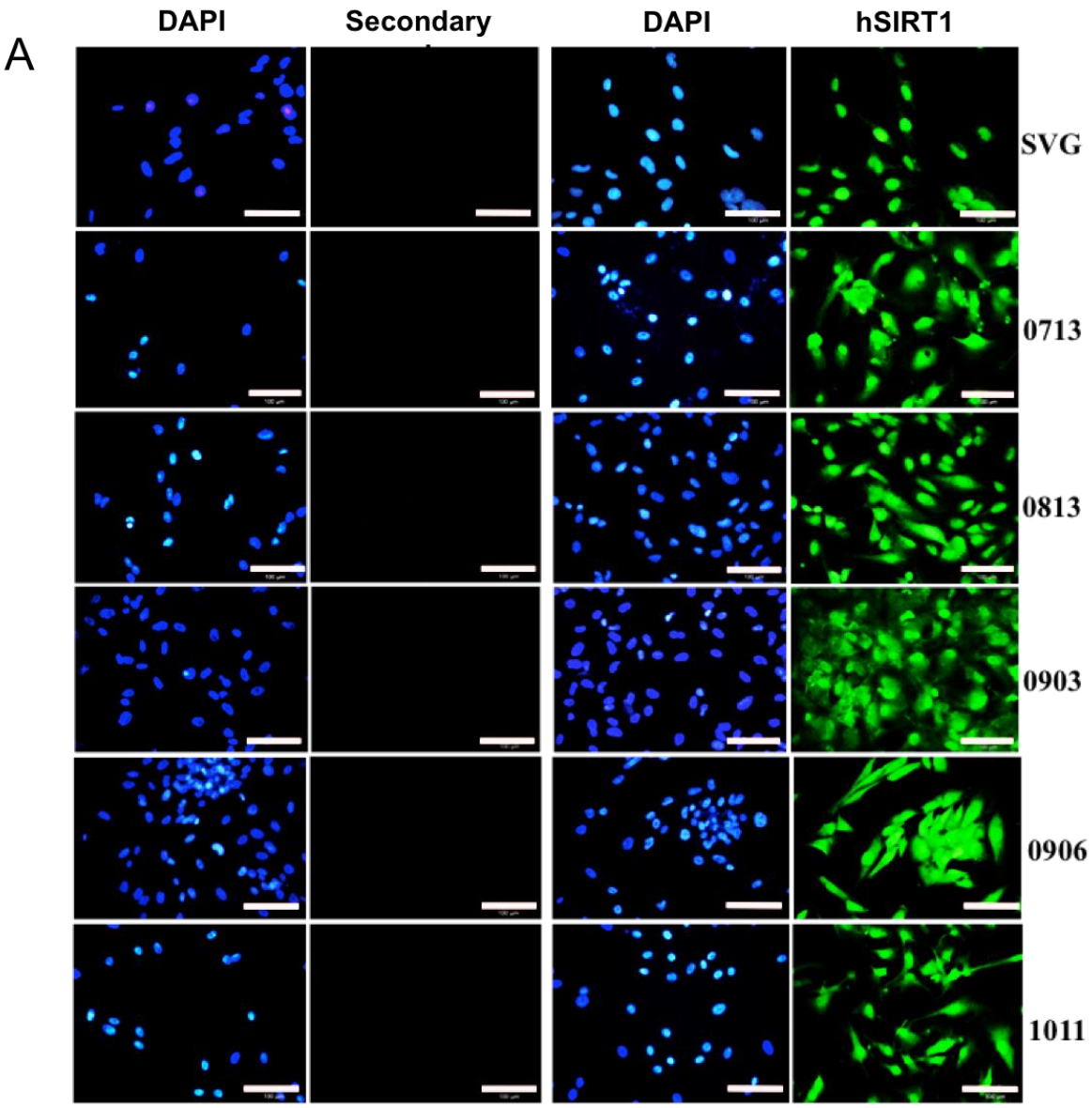
A
DAPI
Secondary
DAPI
hSIRT1
SVG
0713
0813
0903
0906
1011

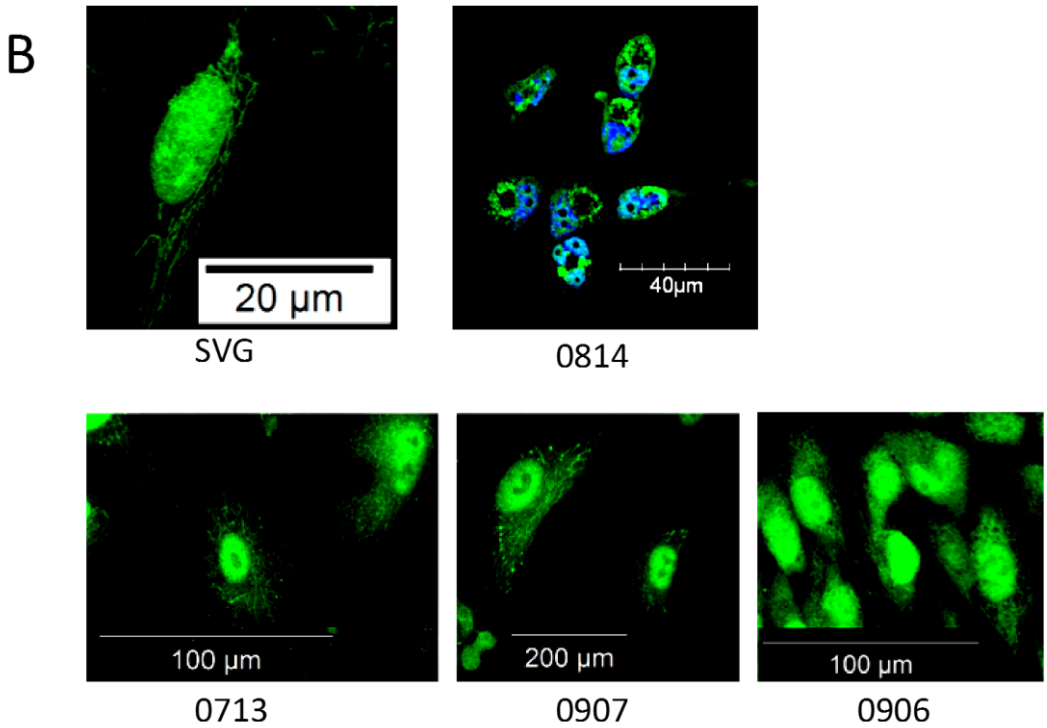
B
20 µm
SVG
40µm
0814
100 µm
0713
200 µm
0907
100 µm
0906

3.4 Subcellular localisation for SIRT1 – Western blotting

Next, verification for the aberrant localisation by Western blotting of nuclear and cytoplasmic fractions for glioma and normal astrocytes was sought. Nuclear and cytoplasmic extracts were prepared by homogenisation and centrifugation. A variety of methods were used.

3.4.1 Western blot nuclear/cytoplasmic fractionation using NE-PER Extraction

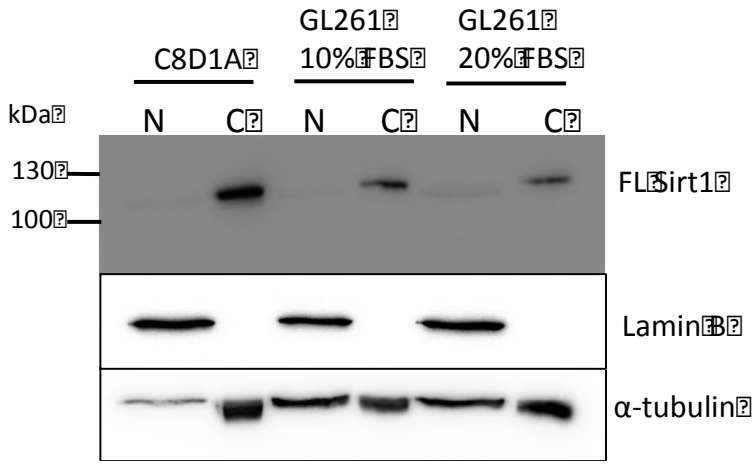

Figure 12. Nuclear/Cytoplasmic fractionation and immunoblotting of C8D1A and GL261 cell lines.

Top panel: immunoblot for Sirt1 using mouse monoclonal antibody ab50517. Middle panel shows immunoblot for the nuclear protein lamin B, and bottom panel shows immunoblot for α-tubulin, a cytoplasmic marker, n=1.

Using this fractionation process, Sirt1 was observed predominantly in the cytoplasm of all extracts, with very little in the nuclear fraction (Figure 12), unlike the distribution observed using immunofluorescent staining using the same antibody which showed predominantly nuclear Sirt1 in C8D1A cells and a significant proportion of nuclear Sirt1 in GL261 cells. Although lamin B was detected only in the nuclear fraction, as expected, the nuclear extracts also contained α-tubulin indicting contamination by this cytoskeletal protein. This result could be partly explained by cross-contamination of the subcellular fractions, as cytoplasmic fractions could have nuclear content, showing a false high level of Sirt1 in the cytoplasm. However, the relative absence of Sirt1 in the nuclear preparation was puzzling.

3.4.2 **Nuclear/Cytoplasmic fractionation and Western blotting of C8D1A and GL261 cells after fixation**

To attempt to retain Sirt1 in the nucleus during subcellular fractionation, cells were fixed in formaldehyde prior to fractionation.

Fixation of cells followed by extraction using NE-PER Thermo-Scientific nuclear and cytoplasmic reagents was performed followed by Western blotting. Results showed a sub-cellular distribution of Sirt1 agreeing with results using microscopy with immunofluorescent staining, where there was greater levels of cytoplasmic Sirt1 in GL261 cells compared to C8D1A cells (Figure 13 A, B and C). For GL261 cells grown in either 10% or 20% FBS, there was no difference in nuclear/cytoplasmic ratios, but an overall increase in Sirt1 expression was seen in cells grown in increased FBS. This was unexpected, as other studies show increased SIRT1 expression in a variety of cells with nuturient or serum deprivation (Alcendor et al 2007, Kanfi et al 2008), suggesting unusual activity for Sirt1 in glioma cells compared to other cells. Crosslinking the cytoskeleton together made it difficult to use lamin or tubulin as controls, so other proteins would be required to confirm the fractionation purity levels. Further experiments are required for validation. However, these results, taken together with those using IF and microscopy, indicated that the localisation of Sirt1 is more cytoplasmic in the glioma murine cell line, GL261 compared to the normal astrocyte comparison cell line, C8D1A. There appeared to be no effect of FBS level on cytoplasmic to nuclear Sirt1 ratio. Both the crosslinking experiment shown here, and the acetylation of H4K16 in 3.2.3 indicated that nuclear Sirt1 was not altered with different FBS.

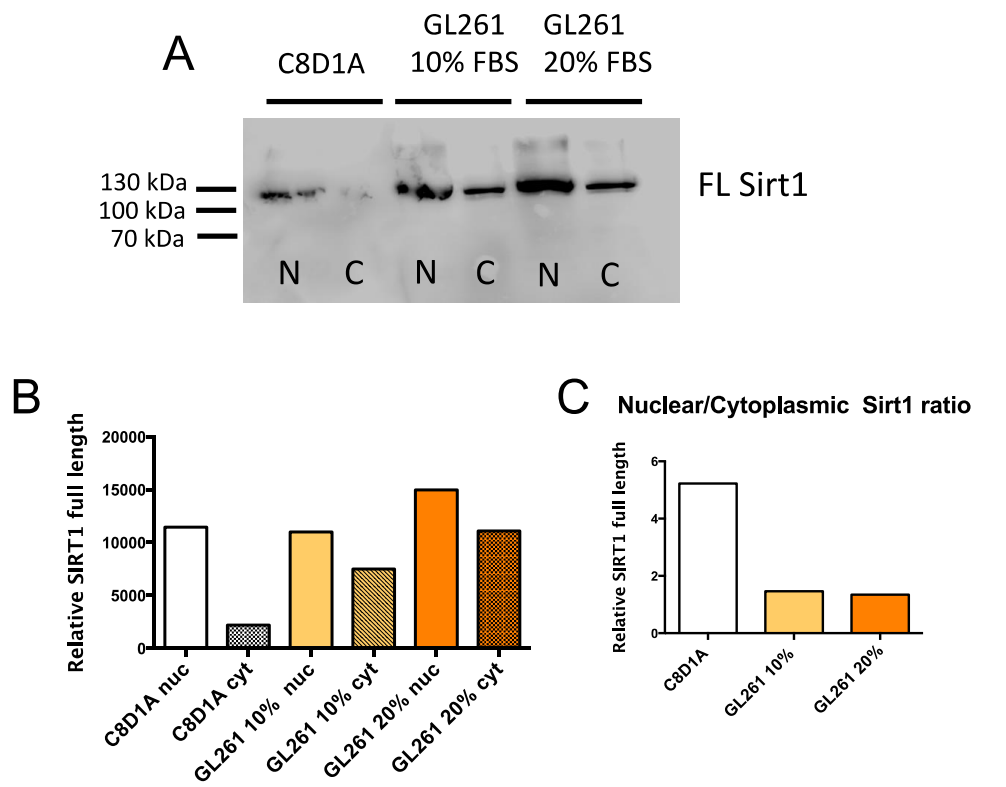

Figure 13. Nuclear/cytoplasmic extraction of C8D1A and GL261 cells after fixation

C8D1A cells and GL261 cells were grown for one day and nuclear/cytoplasmic extraction was performed after crosslinking proteins with formaldehyde as described in methods section. GL261 cells were grown in media supplemented with 10% or 20% FBS. At least five passages of growth in either culture was established before extraction. (A) Western blot image of nuclear and cytoplasmic fractions of cells. Note less C8D1A was available to load, due to poor extraction yield for these cells, and there is no loading control; (B) histogram showing relative Sirt1 levels for each compartment. C8D1A levels were doubled to adjust for a known deficit in loading due to a poor extraction yield of C8D1A fractions; (C) histogram-showing relative amounts in the nucleus relative to the cytoplasm. Abbreviations: N = nuclear extraction, C = cytoplasmic extraction. n=1

3.4.3 Extraction of Cytoplasm and Nuclear Fractions of SVG astrocyte cells

To confirm hSIRT1 localisation differences between nucleus and cytoplasm, nuclear/cytoplasmic extractions were carried out. Using only SVG cells initially, nuclear and cytoplasmic fractions were isolated using extractions using Buffers A and B as described in methods section and described in Andrews and Faller (Andrews & Faller 1991). Western blotting was then performed.

Results using this process showed that the extractions for different compartments were reasonably pure, and yet there was more cytoplasmic hSIRT1 compared to nuclear hSIRT1 (Figure 14 B). This did not correspond to the immunofluorescent

photographs that were obtained earlier (Figure 14 A), and was the same inconsistency as was seen with the murine cells after extraction.

An alternative method using an extraction kit purchased from Thermo Scientific was then used (NE-PER). Results from extraction using this kit resulted in a cleaner compartmental extraction, cytoplasmic hSIRT1 was still predominant, and nucleic hSIRT1 was minimal (figure 14 C). This could have been due to poor nucleic yield, or nucleic hSIRT1 being lost during the extraction process either by degradation or movement out of the nucleus. These results were similar to the nuclear/cytoplasmic extractions for the murine cells.

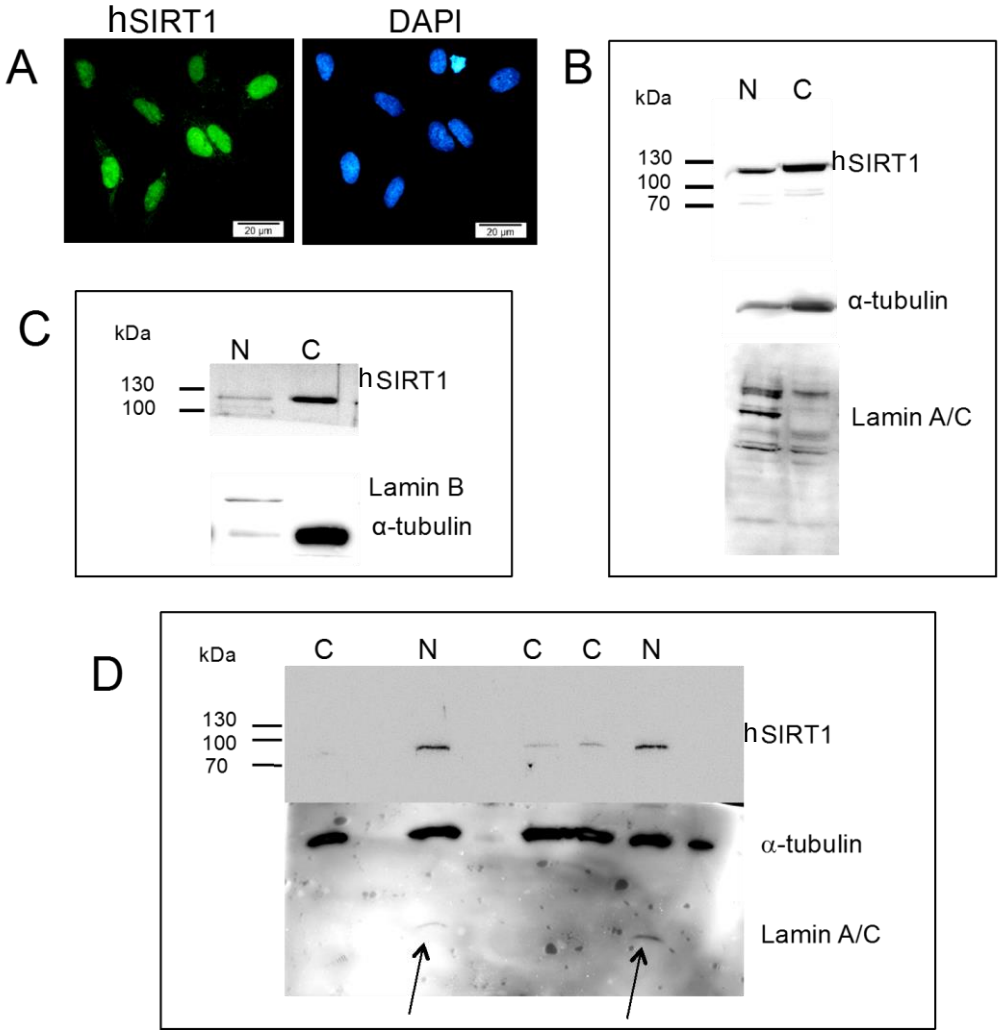

Figure 14. Nuclear/cytoplasmic extraction for untreated SVG cells – using different processes

(A) Intracellular immunouorescent staining for SVG cells showing SIRT1 (green) and DAPI, staining nuclei (blue); (B) Nuclear/cytoplasmic extraction using buffers A and B made in the lab. Cells were grown for one day to approximately 70% confluency before extraction was performed. Alpha-tubulin and lamin A/C were used to check for purity of cytoplasm and nucleic extraction respectively; (C) As for B, but using NE-PER extraction kit; (D) As for B, but using a mild fixative agent, before using the NE-PER extraction kit. Arrows point to a smaller labile form of lamin A that is only found within the nucleus. Abbreviations: N = nuclear extraction, C = cytoplasmic extraction.

Finally, a third extraction technique using mild crosslinking fixative used before using the commercial nuclear/cytoplasmic extraction kit, as for the murine cells in Section 3.4.2. Results showed that hSIRT1 was predominantly nuclear, with a small portion in the cytoplasm (Figure 14 D). Measuring purity of compartmental extraction was difficult due to crosslinking and α-tubulin was seen in both compartments. However a small isoform of lamin A/C known to be more labile and nucleic only, was seen in the nuclear lysate only (Figure 14 D arrows), indicating separation of compartments may have been successful. However, the size of hSIRT1 seen in the extraction was smaller than in the other extractions. The reason for this was not understood, and highlighted the difficulty in studying a molecule responding to cellular stress and which may localise differently depending on micro-environmental conditions.

Given that the results for the extraction process using mild fixation agreed with the results seen in immunofluorescent experiments, extraction using this method followed by Western blotting was repeated using SVG and human primary glioma cell line, 0906.

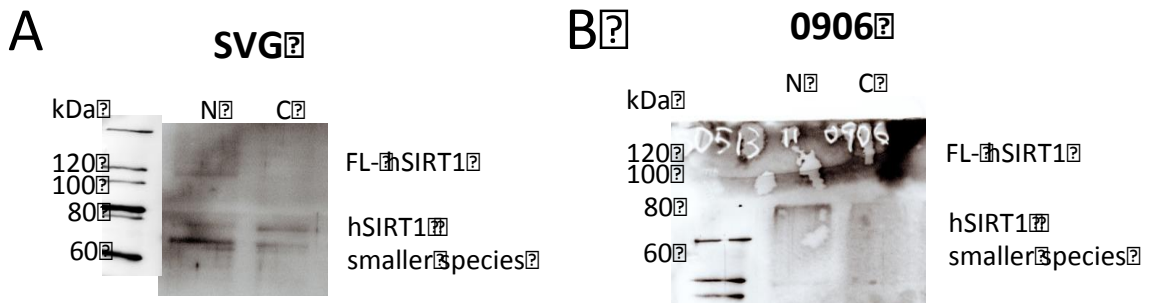

Figure 15. Nuclear/cytoplasmic extraction for SVG and 0906 cells using formaldehyde fixation

Cells were grown for one day to approximately 70% confluency before extraction was performed, using a mild fixative before using the NE-PER extraction kit, and immunoblotting for hSIRT1 for (A) SVG and (B) 0906. Purity and loading controls were not included, n=1.

Results for these cells also agreed with the immunofluorescent staining experiments, with more cytoplasmic hSIRT1 seen with the 0906 primary cells while more nuclear hSIRT1 was seen in SVG cells (Figure 15). As in the preliminary experiment (shown in Figure 14 D), FL-hSIRT1 appeared to be lost. The second protein band, running at about 75 kDa was present, however. This experiment did not have control antibody bands, so the result needs verification using controls.

3.4.4 Changes in hSIRT1 levels before and after primary cell line 0906 immortalisation

Sirt1 protein, but not mRNA levels was found to decrease with increasing serial passage in mouse embryonic fibroblast (MEF) cells undergoing premature senescence, however when these cells spontaneously immortalised, Sirt1 levels were returned to the higher level seen with faster proliferating cells (Pelicano et al 2006). Further investigation by Sasaki *et al* using MEFs and human lung fibroblast cells show Sirt1 levels increased with increased mitotic activity and decreased with replicative senescence.

During culturing, some primary glioma cells entered senescence. One primary cell line, 0906, transformed between passage 8 and passage 16, and emerged from senescence with a smaller and different morphological shape, less spread out on the culture dish and replicating more quickly (Figure 16 A). It was assumed they had become immortalised. To find out if hSIRT1 levels changed after immortalisation of human primary cells, whole cell extraction of 0906 cells before and after transformation, followed by immunoblotting for hSIRT1 was performed.

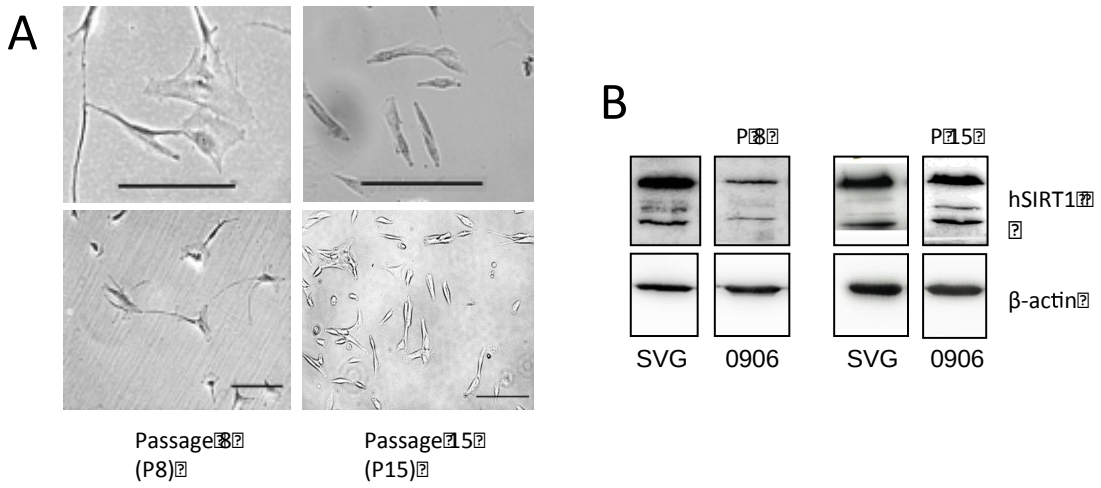

Figure 16. Human primary 0906 cells spontaneously immortalised in culture

(A) Photograph from a light microscope showing 0906 human primary glioma cells before (P8) and after (p15) immortalisation, scale bar 200 μM; (B) Western blot images for hSIRT1 in SVG and 0906 in cells before and after immortalisation. Images representative of three independent extractions.

Results showed that hSIRT1 and 75 kDa SIRT1 were increased after human primary 0906 cells became immortalised in culture to be similar to levels seen in the SVG imortalised cell line (Figure 16 B).

Part 4: Results – Cell Proliferation

Exploring the potential role of SIRT1 in glioma cells in cell proliferation

Minimal research has been done to investigate the role of SIRT1 in the proliferation of glioma cells. A recent study showed SIRT1 knockdown significantly delayed mitotic entry in a panel of glioma cell lines, inhibited growth and proliferation, and promoted apoptosis (Annabi et al 2012). No reports into the role of SIRT1 with respect to proliferation in primary glioma cells could be found in the literature at the time of writing this thesis. As SIRT1 is a key regulator of longevity in yeast, worms and flies (Kaeberlein et al 1999) (Tissenbaum & Guarente 2001) (Rogina & Helfand 2004), and deacetylates key proteins involved in metabolic function and energy homeostasis in many cell types (Brooks & Gu 2009), it is likely to be involved in proliferation and viability of cells in glioblastoma.

4.1 Proliferation measures for murine and human glioma and normal cells using MTT reduction assay

As previously described (Section 2.7), MTT reduction measures metabolic activity but is used widely as a viability assay, and as an indication of proliferation of cells. MTT reduction is a measurement of metabolic activity, and for this study, differences between one and three days were used as a reflection of cell proliferation. Proliferation rates were measured for murine and human glioma cells and compared to the normal astrocyte cell lines, and also compared to SIRT1 levels.

4.1.1 Cell proliferation for murine and human normal and glioma cells compared to full-length SIRT1 levels

C8D1A and GL261 cells (either with 10% or 20% added FBS), SVG and two primary glioma cell lines were grown in 96-well plates, as described in the methods (Section 2.7). MTT reduction was measured at day one and day three and the differences between measurements were analysed (“proliferation”). Additionally, proliferation was measured for a panel of human primary glioma cells, and this was analysed against FL-hSIRT1 levels measured by Western blot (taken from an earlier experiment) to find out if there was a relationship between the two.

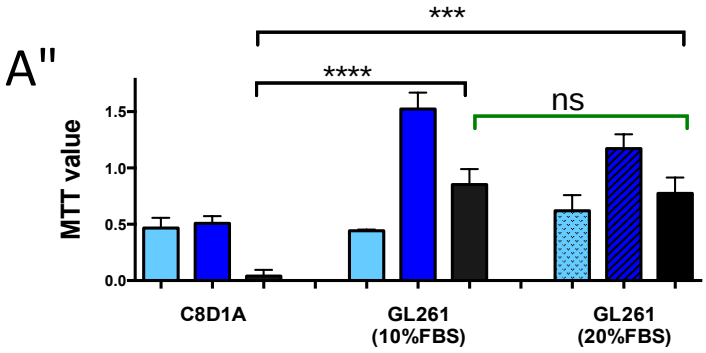
A"
***
****
ns
MTT value
1.5
1.0
0.5
0.0
C8D1A
GL261 (10%FBS)
GL261 (20%FBS)

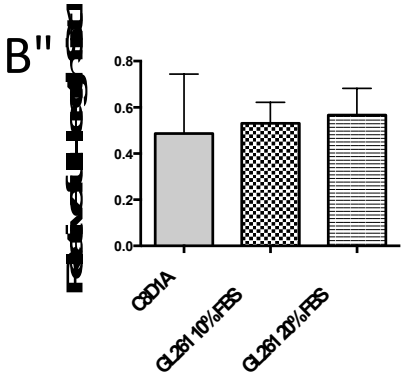
B"
0.8
0.6
0.4
0.2
0.0
C8D1A
GL261 10%FBS
GL261 20%FBS

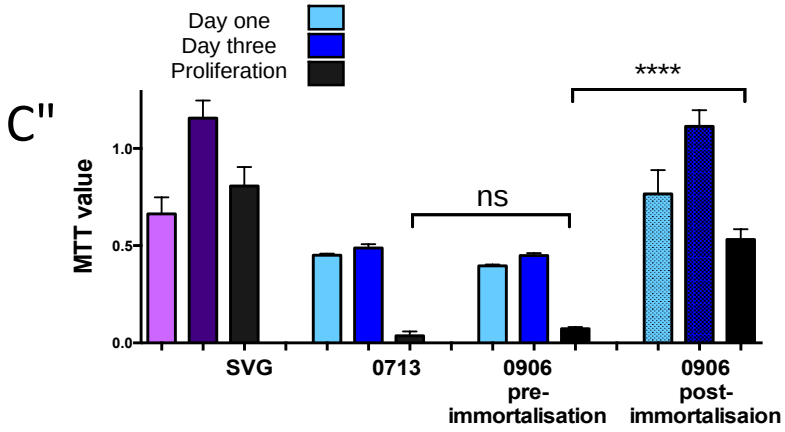
C"
Day one
Day three
Proliferation
****
ns
MTT value
1.0
0.5
0.0
SVG
0713
0906 pre-immortalisation
0906 post-immortalisaion

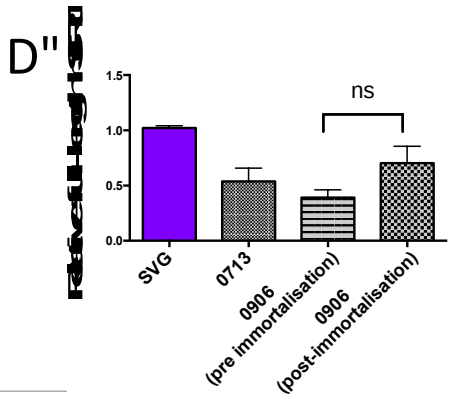
D"
ns
1.5
1.0
0.5
0.0
SVG
0713
0906 (pre immortalisation)
0906 (post-immortalisation)

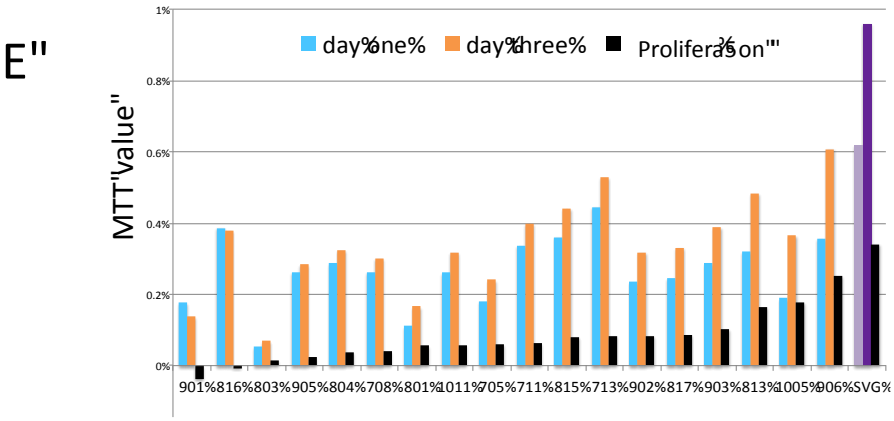
E"
day one%
day three%
Proliferation%
MTT value"
1%
0.8%
0.6%
0.4%
0.2%
0%
901%
816%
803%
905%
804%
708%
801%
1011%
705%
711%
815%
713%
902%
817%
903%
813%
1005%
906%
SVG%

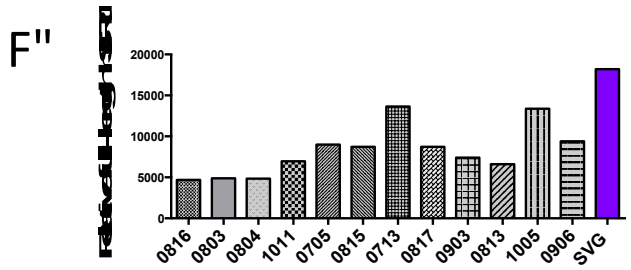
F"
20000
15000
10000
5000
0
0816
0803
0804
1011
0705
0815
0713
0817
0903
0813
1005
0906
SVG

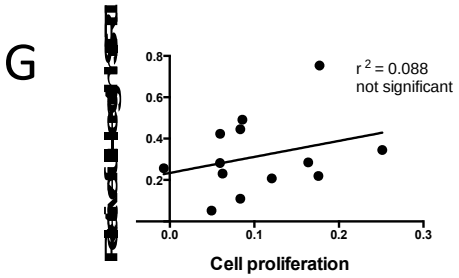
G
r 2 = 0.088
not significant
0.8
0.6
0.4
0.2
0.0
0.1
0.2
0.3
Cell proliferation

Figure 17. Cell proliferation in murine and human glioma and normal astrocytes compared to FL-SIRT1

(Facing page)
*Cells were grown in triplicate in 96 well plates with MTT reduction measured at one and three days. MTT values are amounts of MTT reduced in a 2 hr assay. Proliferation was the average MTT value day three minus average MTT value at day one. Relative FL-SIRT1 was a measure of protein quantity in relation to β-actin after adjustment for loading. (A) MTT values for murine cell lines – with GL261 grown in two levels of FBS, n=3 (B) Bar graph showing triplicate measurements of FL-Sirt1 in murine cell lines from Western blot measurements from previous extractions (Section 3.4), n=3. (C) MTT values for human cell line SVG, and human primary cell lines 0713 and 0906. The 0906 cells were measured before and after immortalisation as described in Section 3.14, n=3.(D) Bar graph of hSIRT1 levels in Western blot experiments done previously, n=2; (E) MTT values from 18 primary gliomas and SVG normal astrocyte cell line. (F) Graphic representation of FL-hSIRT1 levels taken from single Western blot extractions done previously for each primary cell line (Section 3.9). The 0906 cell line is taken from cells after immortalisation. (G) Linear regression of proliferation values against FL-hSIRT1 values of 12 primary gliomas. Student's t-test: ns = not significant; *** p < 0.001; **** p < 0.0001*

The murine glioma cell line GL261, grown in either 10% or 20% FBS, had a significantly higher proliferation rate compared to normal C8D1A astrocytes (black bars, Figure 17 A). There was no significant difference in proliferation between GL261 cells grown in 10% or 20% FBS. FL-Sirt1 levels did not change significantly between untreated C8D1A and GL261 (Figure 17 B), suggesting FL-Sirt1 expression was not linked to the differences in proliferation seen in the murine MTT results.

Results for the human SVG cells and primary glioma cells showed there was a significant difference in the proliferation rate between 0906 primary glioma cells pre- and post-immortalisation ($p < 0.005$) (Figures 17 C and D). SVG has proliferation higher than the glioma cells. This result could be a reflection of a comparison between primary cells and an immortalised cell line, but needs confirming. A panel of 12 glioma primary cell lines were analysed for hSIRT1 levels against proliferation, and while there was a positive trend for more hSIRT1 with higher proliferation it did not reach significance (Figure 17 G). It is understood that linear regression analyses usually require at least 25 sample data to give meaningful relevance, and the correlation here and the ones in other sections are understood to be trends that need investigating with more patient data. The immortalised 0906 cells had significantly increased proliferation compared to pre-immortalised 0906 cells and there was also an increase in hSIRT1 seen on the Western blot but it did not reach significance. As described in the previous section, it is likely that cells in GBM tumours have transformed to become proliferative and invasive – different to the normal astrocyte cells. There is also evidence in the

literature for immortalisation of glioma cells in tumours (Hiraga et al 1998, Kheirollahi et al 2013, Nakatani et al 1997). In these studies, increased telomerase is found in cells from GBM tumours – and there is recent research to suggest SIRT1 directly regulates telomerase expression (Zhang et al 2014).

4.1.2 MTT reduction in human primary glioma cells in relation to survival statistics

To gain a preliminary indication of any relationship between MTT measurements and patient survival, linear regression analyses were made.

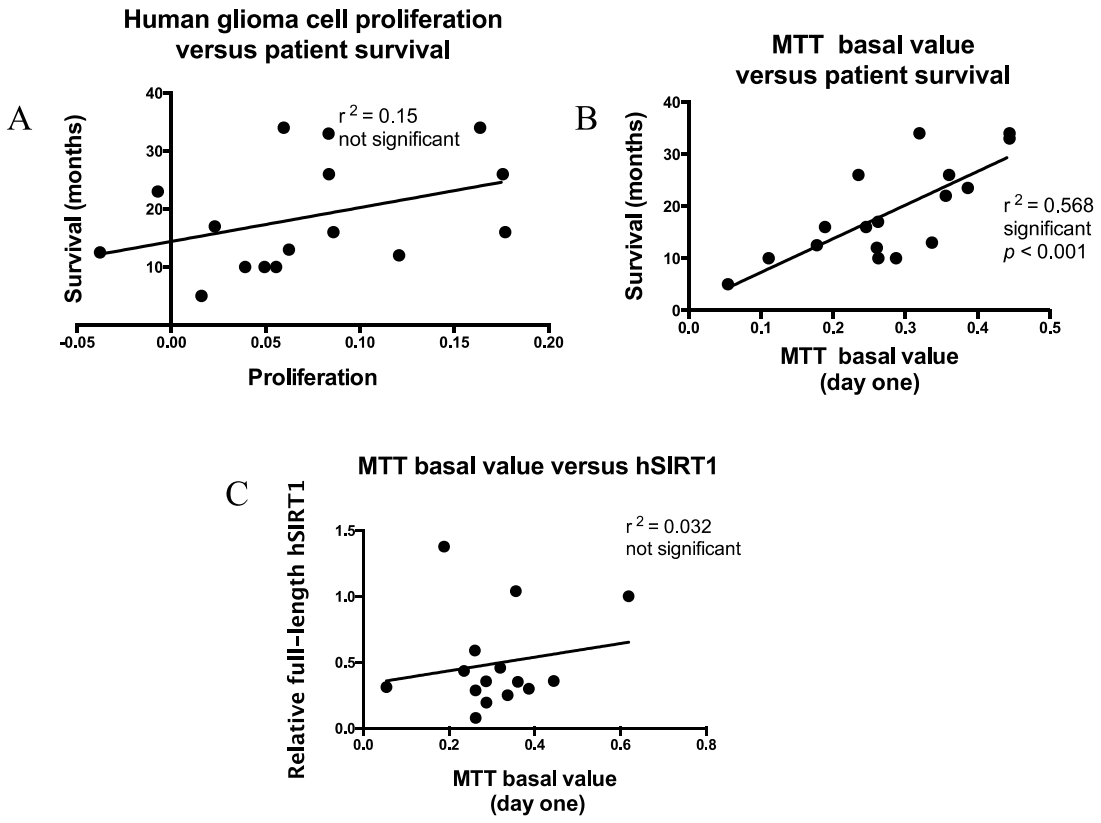

Figure 18. Relationship between MTT reduction, hSIRT1 and patient survival

Linear regression plots for (A) Cell proliferation (measured from the difference of MTT value between day one and day three) and patient survival taken from a panel of 16 primary glioma cells; (B) MTT reduction measurement taken from day one and patient survival for 16 primary glioma cells; (C) MTT taken from day one and levels of FL-hSIRT1 for 15 primary glioma cells measured from a single extraction and compared to SVG from the same blot (set at 1).

Linear regression analysis revealed that while cell proliferation did not correlate with patient survival, there was a positive trend (Figure 18 A). Unexpectedly, there was a statistically significant correlation ($p < 0.001$) between MTT values taken at day one and survival (Figure 18 B) and yet no significant correlation with FL-hSIRT1 and MTT reduction at day one (Figure 18 C). MTT reduction reflects cell metabolic

activity in the cell, and because cancer treatment targets cells with high metabolic rate, this result may be because those cells with higher metabolic rate are more susceptible to radiation and chemotherapy, and the patients who donated these cells had been undergoing treatment, and treatment probably prolonged survival.

4.1.3 **Acetylation of H4K16 in relation to MTT reduction**

To assess if hSIRT1 activity, rather than FL-hSIRT1 expression, may be linked to metabolic rates or proliferation rate in human glioma cells, levels of H4K16-ac were analysed.

Histone extraction from 11 primary glioblastoma cell lines was performed followed by Western blot for H4K16-ac. The level of histone acetylation was compared with MTT measured after 1 d, and with cell proliferation rate calculated as the differences of MTT reduction between day one to day three.

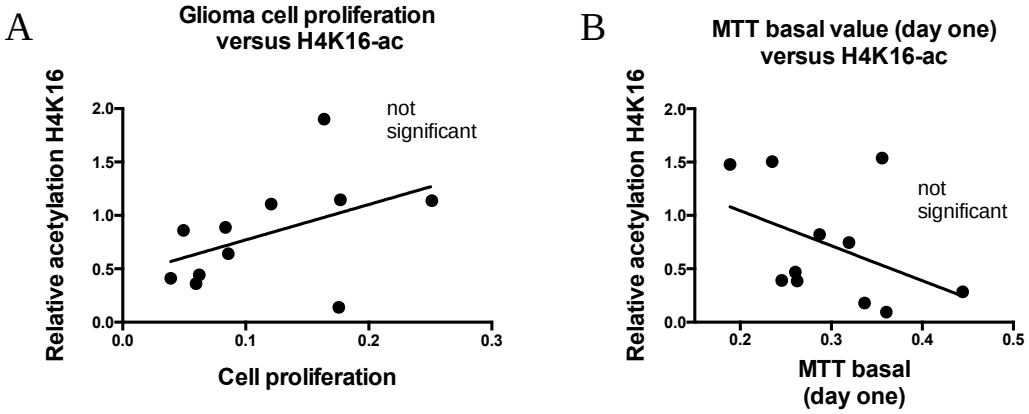

Figure 19. Relative H4K16 acetylation across a panel of human primary glioma cells in relation to MTT reduction

Histone extraction after growing cells for one day, followed by Western blotting, and probing for H4K16-acetylation was performed on 11 human primary glioma cell lines as described in Section 3.5. (A) Linear regression for H4K16-ac plotted against cell proliferation rate for human primary glioma cells; (B) linear regression for H4K16-ac plotted against MTT values at day one. n=1 H4K16-ac extraction, n=3 MTT reduction.

There was no significant correlation between cell proliferation and H4K16-ac, or MTT reduction at day one (Figure 19 A and B) although there was a positive trend between acetylation and proliferation.

4.2 SIRT1 activation and inhibition effects on cell proliferation rates in glioma and normal cells

To examine the potential role of SIRT1 activity in cell proliferation of glioma compared to normal cells, a SIRT1 inhibitor, nicotinamide (NAM) or a SIRT1 activator, resveratrol (RES), was added to cultures after one day of plating out and MTT reduction was measured on day three and the proliferation measurements were compared to untreated cells. NAM is known to be an effective inhibitor of SIRT1 (Bitterman et al 2002), and RES is a known activator of SIRT1 (Howitz et al 2003). The GL261 cells were grown in either 10% or 20% FBS supplemented media to assess the effect of the growth factor, to continue the assessment made in previous experiments.

4.2.1 Assessing the role of Sirt1 activity on proliferation rate for murine normal astrocyte cell line C8D1A and glioma cell line GL261

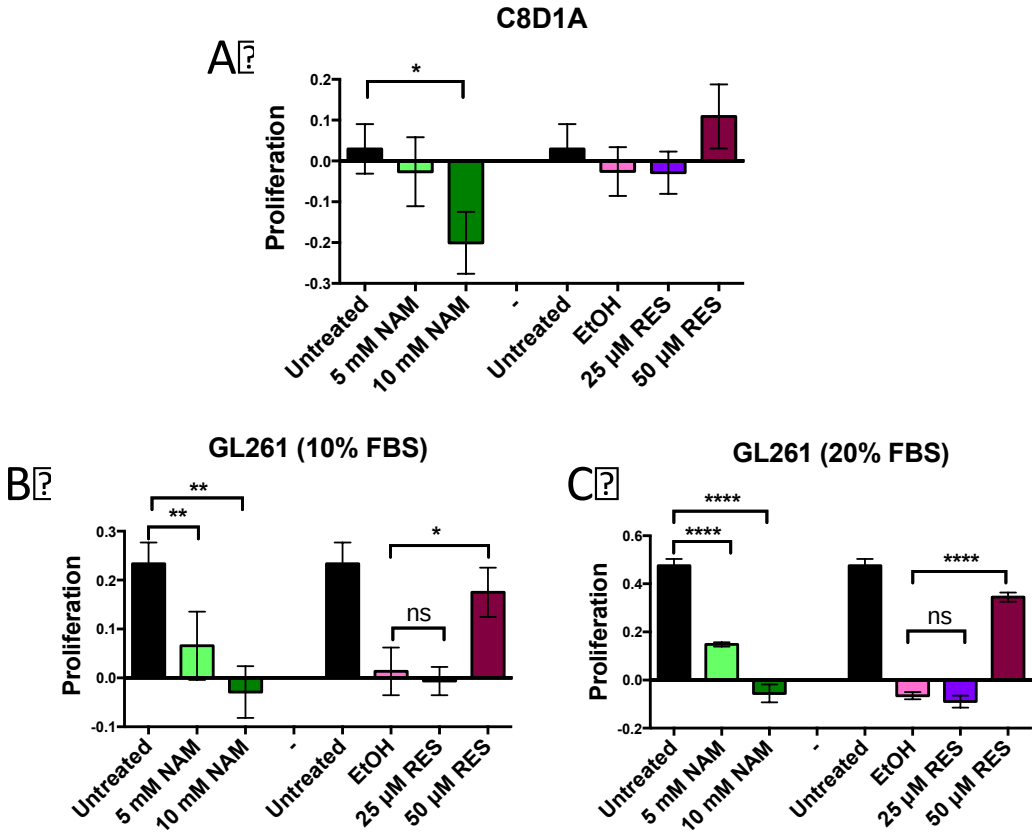

Figure 20. Proliferation in murine astrocyte normal and glioma cell lines with Sirt1 inhibition and activation

*(Facing page) Cells were grown in 96 well plates for one day before treatment with or without inhibitor of Sirt1, nicotinamide (NAM) dissolved in water, or resveratrol (RES) dissolved in diluted ethanol. MTT reduction was measured on day one and three after treatment in (A) normal murine astrocyte cell line, C8D1A. (B) murine glioma cell line, GL261, grown in 20% FBS; (C) murine glioma cell line, GL261, grown in 10% FBS. The difference of MTT reduction between day one and day three was used as a measure of proliferation. * p < 0.05 , ** p <0.01 ***p < 0.001, **** p <0.0001, ns = not significant, by one way ANOVA and Tukey multiple comparison post-test, n=3 for each cell line. Vehicle EtOH was used at 0.1% concentration. Note the y-axis have different scales to make visual comparison easier.*

Treatment with the Sirt1 inhibitor NAM decreased proliferation in all cell lines (Figure 20), and the Sirt1 activator RES increased proliferation at the highest concentration 50 μM, which suggested that Sirt1 was involved in the proliferation rates for these cells. There was a significant negative effect of 10 mM NAM on proliferation of C8D1A cells ($p < 0.05$) (Figure 20). The significance between the GL261 untreated and NAM treated cells was greater than for C8D1A cells, indicating that the faster proliferating cells are more influenced by NAM. Increased FBS supported this as the untreated GL261 cells grown in 20% FBS were more proliferative than the 10% FBS-grown cells, and had significantly greater inhibition from NAM ($p < 0.01$ 10% FBS cultures, $p < 0.00001$ 20% FBS cultures) (Figure 20 A, B and C, green bars).

RES increased proliferation significantly only in GL261 cell lines, at either 10% or 20% FBS (Figure 20 A, B & C pink, purple and red bars). Interestingly, the vehicle control ethanol negatively affected proliferation for all cell lines. Ethanol was used at 0.1% final concentration in the culture media which was the amount used with 50 μM RES treatment, yet the effects of the higher concentration of RES appeared to overcome the toxic effect, making interpretation difficult.

4.2.2 Assessing the role of hSIRT1 on proliferation of human normal astrocyte cell line SVG compared to two primary glioma cell lines

MTT reduction was also used to measure proliferation rate in human normal astrocyte and primary glioma cells with and without NAM or RES treatment, as described in the previous section.

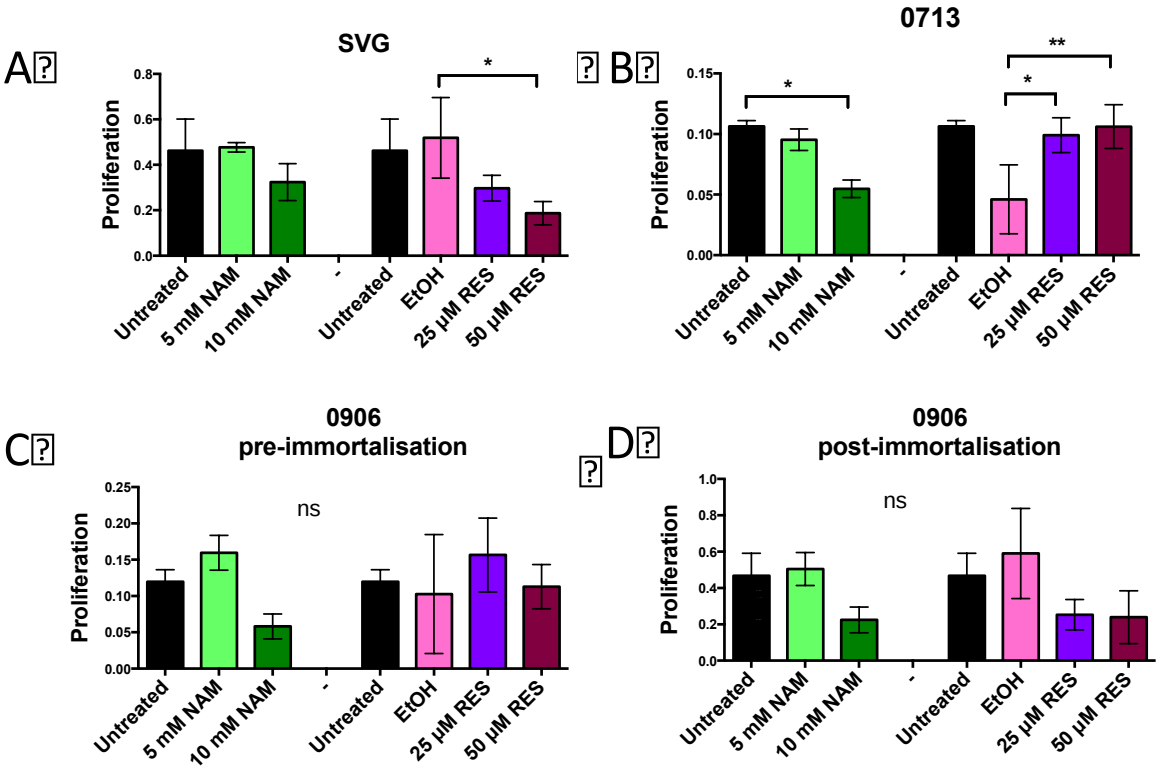

Figure 21. Proliferation for human astrocyte SVG and primary glioma cell lines with hSIRT1 inhibition and activation

*Cells were grown in 96 well plates for one day before treatment with or without, nicotinamide (NAM) or resveratrol (RES). MTT reduction was measured on day one and day three after treatment in (A) normal human astrocyte cell line, SVG; (B) human primary glioma cell line 0713; (C) human primary glioma cell line 0906, before immortalisation as explained in Section 3.14; (D) human primary glioma cell line 0906 after immortalisation. Results are expressed as. * $p < 0.05$, ** $p < 0.01$ ***$p < 0.001$, **** $p < 0.0001$, ns = not significant, by one way ANOVA and Tukey multiple comparison post-test, n=3 for each cell line. Vehicle EtOH was used at 0.1% concentration.*

As in the murine cell lines, NAM treatment decreased proliferation in all cells tested, but RES had different effects. This suggested RES may have been acting on non-hSIRT1 effects in at least some of these cells. NAM had a greater effect decreasing proliferation in the primary glioma cell lines compared to the normal cell line SVG, with a significant difference obtained using 10 mM NAM on the 0713 primary glioma cell line (Figure 21, green bars). RES increased proliferation for 0713 cells, and 0906 cells pre-immortalisation, but appeared to decrease proliferation for SVG cells and post-immortalised 0906 cells, reaching significance in SVG cells for 25 or 50 µM RES (Figure 21, pink, purple and red bars). However, ethanol had varying effects as the 0713 cell line showed decreased proliferation

with ethanol, similar to the murine cell lines, while the other three cell lines apparently did not show these effects.

Taken together with the murine cell lines, these results showed that NAM and RES treatment generally had opposing affects on proliferation, which could indicate a role of SIRT1 in cancer and normal astrocyte cells. NAM apparently had greater effect on the primary glioma cells than on the normal cell line. As NAM and RES both have effects on cell signalling that are not directly related to SIRT1, more specific ways to investigate SIRT1 involvement are needed to examine these results.

4.2.3 **Nicotinamide significantly affected proliferation of human primary glioma cells**

To investigate whether NAM was generally effective in decreasing proliferation of primary glioma cells, a panel of 18 primary glioma cells was used.

The greatest effects of NAM on proliferation were observed in cells with the greatest untreated proliferation rates (Figure 22 A). When averages of the triplicates were measured in a cohort, NAM significantly reduced proliferation across the panel of primary glioma cells (Figure 22 B) ($p < 0.01$).

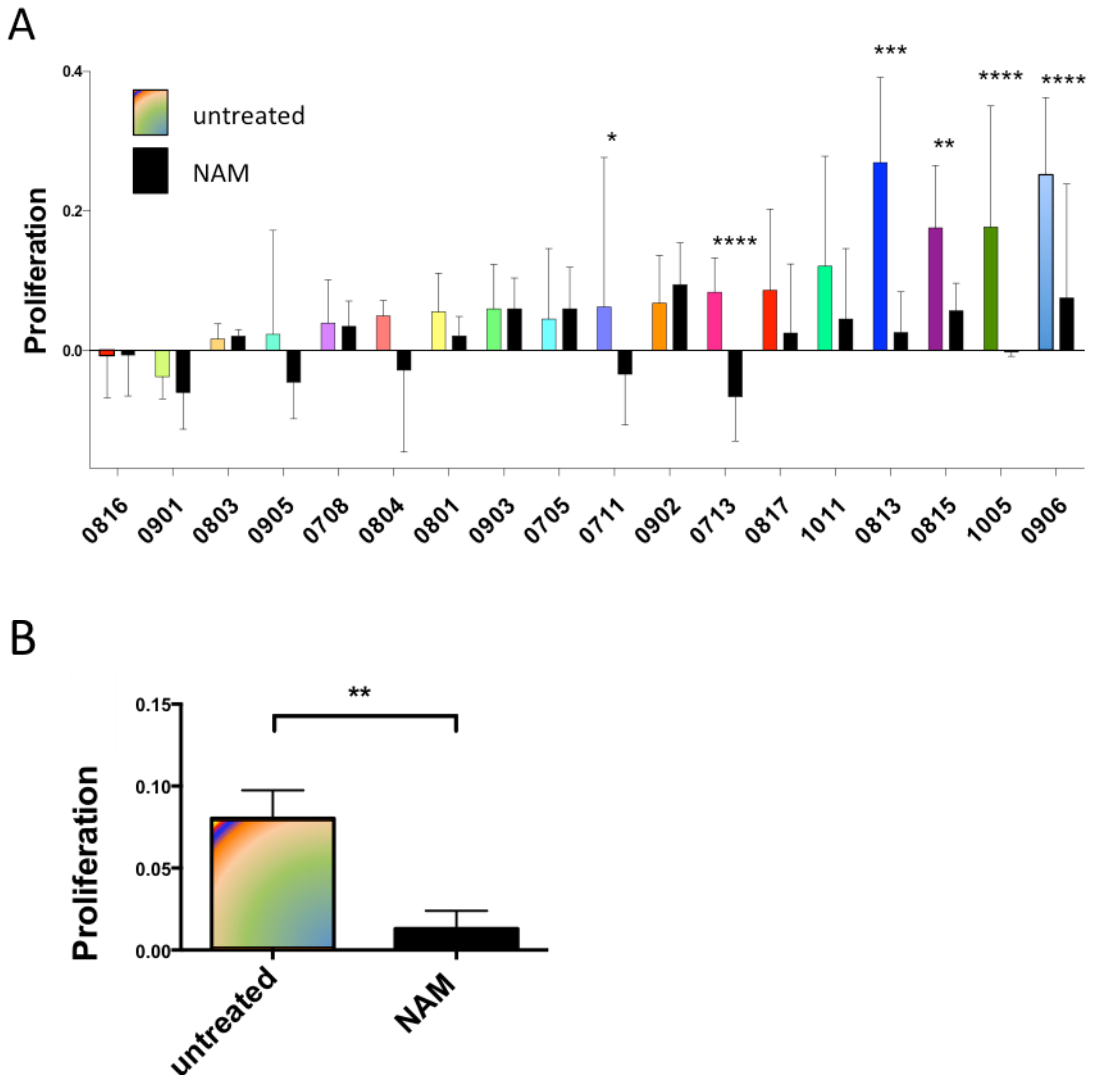

Figure 22. Effect of hSIRT1 inhibition on proliferation in a panel of primary glioma cells

*(A) Bar graph showing proliferation for a panel of primary glioma cells grown in triplicate in 96 well plates, with and without 10 mM NAM. Proliferation is taken as the difference between day one and day three MTT reduction, and where cells MTT values were less on day three compared to day two, the proliferation is shown as negative. 2-way Anova with Sidak's multiple comparison post-test, * p < 0.05, ** p< 0.01, *** p < 0.005. **** p < 0.001; (B) Bar graph showing the average proliferation of untreated primary glioma cells compared to NAM treated cells from the same MTT experiment shown in A. Student's t-test ** p < 0.01.*

4.3 Effects of nicotinamide and resveratrol treatments on SIRT1 protein

At the highest concentration used in this study (50 μM), RES unexpectedly decreased proliferation in the normal SVG cell line. To investigate if changes to levels or quality of SIRT1 may be related to this result, Western blotting for SIRT1 was carried out using cells after 24 hr exposure to RES at different concentrations. As a representative of the GBM cell lines, the human primary glioma 0906 (pre-immortalisation) was used.

4.3.1 Effect of resveratrol on SIRT1 in normal and cancer murine and human cells

The results showed that in both the murine and human normal cell lines, a distinct second band was observed with 50 μM RES (Figure 23 A and D red arrows), while the cancer cell counterparts showed no second band. Recent literature gives evidence for concentration-dependent differential effects using RES in vitro (Faragher et al 2011, Peltz et al 2012, Price et al 2012), with altered signalling pathways given as a possible explanation. The effect of resveratrol on cleavage or splicing of SIRT1 has not been reported, however cleavage and splice variants of SIRT1 are known (Chen et al 2012b, Dvir-Ginzberg et al 2011) (Hong et al 2010, Shah et al 2012). The smaller species of SIRT1 seen here after 24 hr treatment of 50 μM RES could be a splice variant or a product of cleavage.

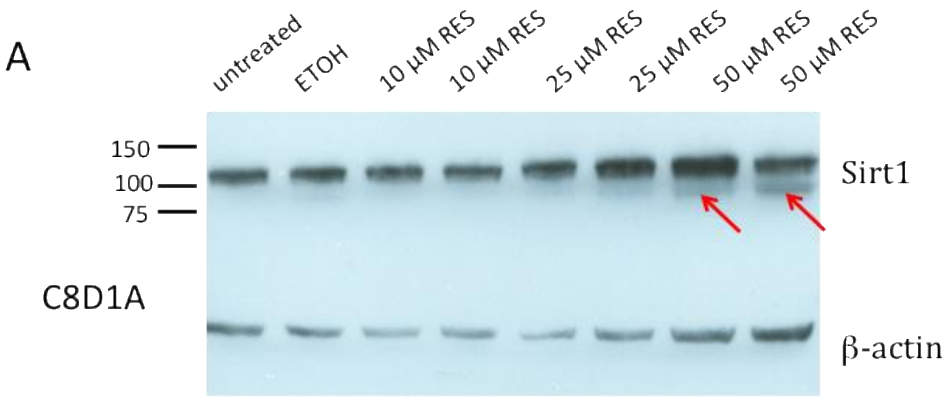
A
untreated
ETOH
10 μM RES
10 μM RES
25 μM RES
25 μM RES
50 μM RES
50 μM RES
150
100
75
Sirt1
C8D1A
β-actin

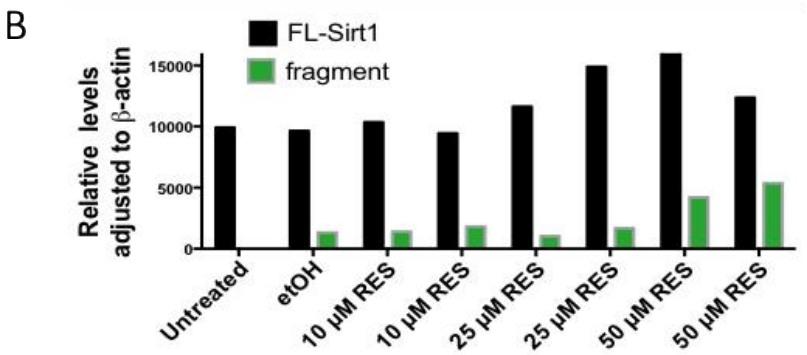
B
FL-Sirt1
fragment
Relative levels adjusted to β-actin
15000
10000
5000
0
Untreated
etOH
10 μM RES
10 μM RES
25 μM RES
25 μM RES
50 μM RES
50 μM RES

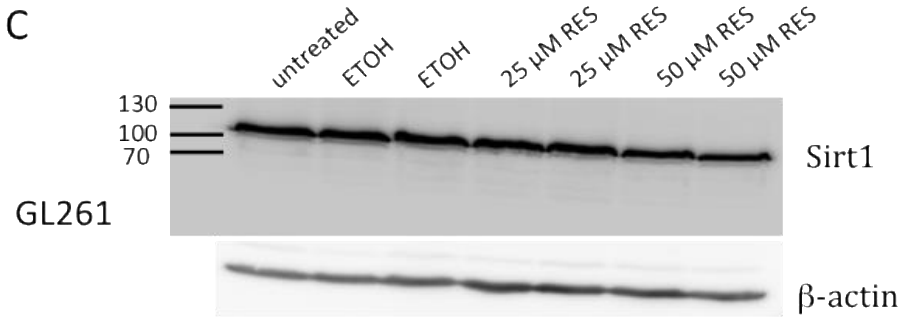
C
untreated
ETOH
ETOH
25 μM RES
25 μM RES
50 μM RES
50 μM RES
130
100
70
Sirt1
GL261
β-actin

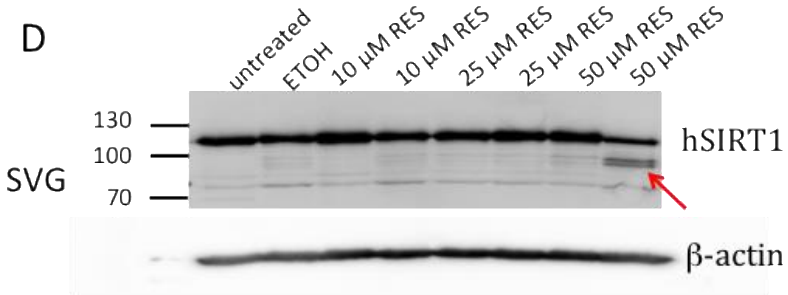
D
untreated
ETOH
10 μM RES
10 μM RES
25 μM RES
25 μM RES
50 μM RES
50 μM RES
130
100
70
hSIRT1
SVG
β-actin

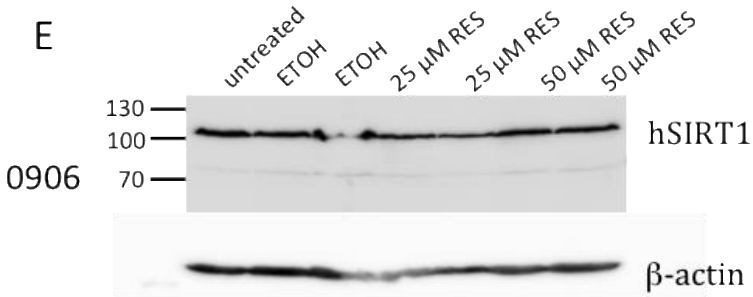
E
untreated
ETOH
ETOH
25 μM RES
25 μM RES
50 μM RES
50 μM RES
130
100
70
hSIRT1
0906
β-actin

Figure 23. Effect of resveratrol on SIRT1

(Facing page) Murine and human glioma and normal cells were grown for 1 d with or without RES at different concentrations, then protein extraction and immuno-blotting for SIRT1 was performed. (A) Image from Western blot for C8D1A normal murine astrocytes and (B) quantification for image shown in A, with adjustment for β-actin loading differences; (C) Image from Western blot for GL261 murine glioma cells; (D) Image from Western blot for normal human astrocytes SVG, and for (E) primary glioma cell line 0906 pre-immortalisation. Ethanol (ETOH) vehicle was used at the same concentration as for 50 μM RES. Red arrows highlight a distinct second band seen on blots.

4.3.2 Effect of nicotinamide on SIRT1 in normal and cancer murine and human astrocytes

To determine if the Western blot profile of SIRT1 is changed by NAM as observed with RES, Western blots were performed on both murine and human normal and cancer astrocyte cells after incubation with or without 10 mM NAM for 20 hr (murine) or 4 hr (human).

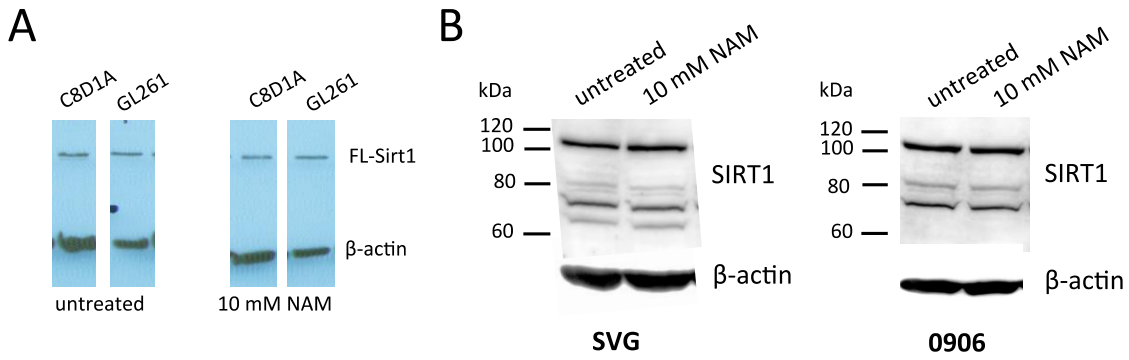

Figure 24. Nicotinamide does not change SIRT1 protein band

(A) Western blots images showing murine normal and cancer astrocytes incubated with or without 10 mM NAM for 1 d. Representative of more than three experiments; (B) Western blots showing normal human SVG astrocytes and cancer primary glioma cells, 0906, with and without 10 mM NAM for 4 hr.

Unlike RES, NAM did not cleave or affect alternate splicing of Sirt1 in either of the murine cell lines at 10 mM after 1 d incubation (Figure 24 A). Also, no evidence of cleavage or alternative splicing is seen after 4 hr incubation with 10 mM NAM in the primary glioma, 0906, nor in the normal human astrocyte, SVG (Figure 24 B). No cleavage was seen at 1 d NAM treatment in normal human SVG cells either (results not shown).

Part 5: Results: Oxidative Stress

Exploring the potential role of SIRT1 in glioma and normal astrocyte cells under oxidative stress

5.1 Introduction to oxidative stress and SIRT1 in GBM

Oxidative stress occurs continuously, as oxygen radicals known commonly as reactive oxygen species (ROS) are formed during normal metabolic activity. Glucose is the basic molecule for normal oxidative cellular metabolism where glucose is broken down to produce ATP. The brain is a particularly active organ for glucose metabolism, consuming over 10% of the body's glucose and oxygen supplies even though it accounts for 1–2% of total body mass (Gjedde 2007), therefore it is exposed to much oxidative stress in the normal setting. Low levels of ROS and antioxidants have important signalling effects, for example, to stimulate growth (Gough & Cotter 2011) and in normal development processes (Dennery 2007). However, too much ROS will activate defence mechanisms and if these are overwhelmed, irreversible cell damage will lead to necrosis or apoptosis. The most common ROS are superoxide anion (O_2-), hydrogen peroxide (H_2O_2), and hydroxyl radicals (OH-)(Salminen et al 2013).

An oxidative environment is postulated as one of the reasons cancer cells become treatment resistant – with altered signalling pathways that support proliferation, metastasis, and genomic instability which also help to propagate disease (Toyokuni et al 1995). Glioblastoma is among the hardest of all cancers to treat where tumours are resistant to radiation and chemotoxic therapies (Furnari et al 2007), and an elevated oxidative environment is observed (Silber et al 2002) (Iida et al 2001). Reasons for oxidative stress conditions in GBM include inflammatory responses, increased nitric oxide from angiongenesis, and hypoxia/reperfusion in the necrotic core (Kalaria et al 1996) (Ziche & Morbidelli 2000) (Brown & Bicknell 2001). Antioxidant treatment can decrease glioma cell proliferation (Martin et al 2007).

SIRT1 can be found to decrease oxidative stress effects in some situations and increase them in others. (Alcendor et al 2007, Salminen et al 2013). SIRT1 activities depend on the context of the situation.

There is limited research into the role of SIRT1 in astrocytes in oxidative stress in relation to glioblastoma. One study found neural progenitor cells (NPCs) will preferentially develop into astrocytes under oxidative conditions in a SIRT1 dependent manner (Prozorovski et al 2008) (Libert et al 2008). In that study, activation of SIRT1 suppressed proliferation and supported differentiation of NPCs to astrocytes.

In this thesis, oxidative stress was induced in conjunction with SIRT1 inhibition and activation to find a preliminary understanding for role of SIRT1 in oxidative stress in glioma compared to normal astrocyte cell lines as described in the previous sections.

Exogenously administered H_2O_2 is commonly used in vitro to induce oxidative stress conditions (Allen & Tresini 2000) (Keyse & Emslie 1992, Park et al 2012) *as* it can cross the plasma membrane and contribute to intracellular oxidative stress (Klaunig & Kamendulis 2004).

5.2 SIRT1 inhibition and activation in glioma and normal cells

5.2.1 Malignant glioma cells are more resistant to H_2O_2 than normal astrocytes

To determine susceptibility to H_2O_2 –induced cell death, cells were treated with increasing concentrations of H_2O_2 for 1 d. Viability was measured with PI exclusion using flow cytometry.

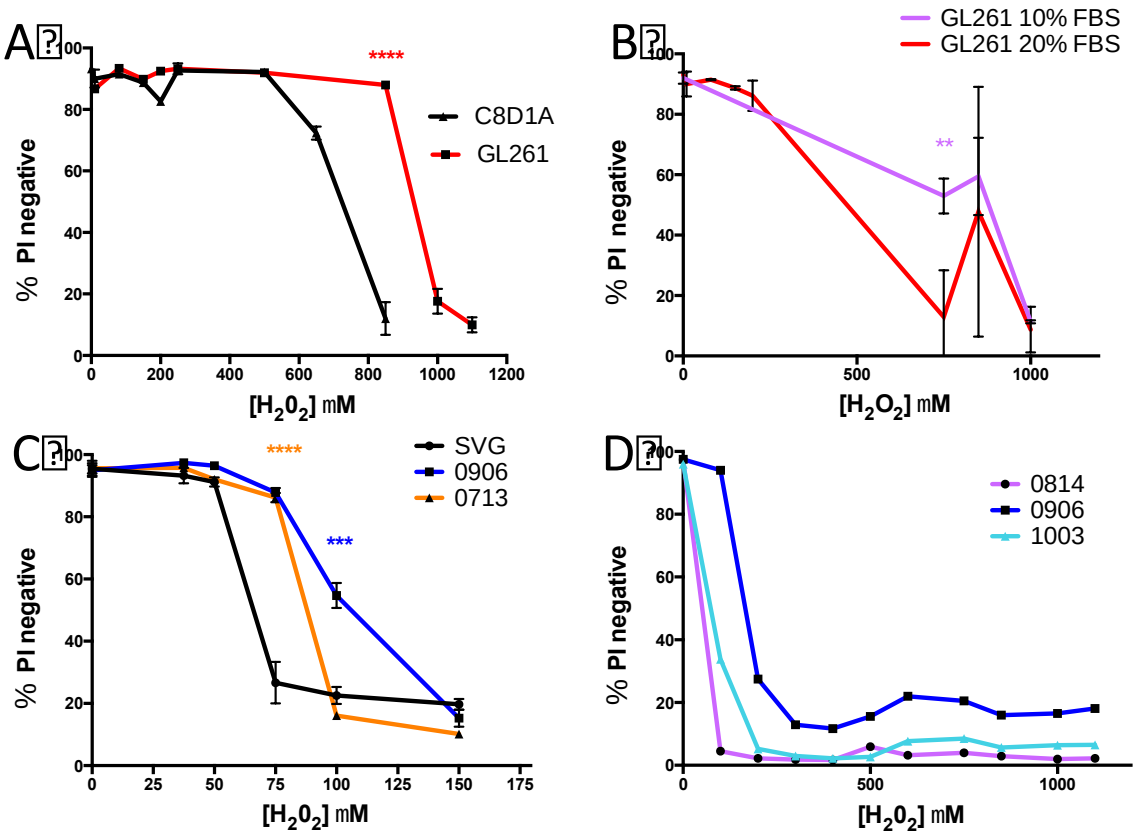

Figure 25. Malignant glioma cells were more resistant to H_2O_2 compared to normal astrocyte cells.

*Viability for a titration of H_2O_2 after 20 hr incubation was measured using PI exclusion and flow cytometry for (A) murine normal astrocytes C8D1A and murine glioma cell line GL261 (B) GL261 cells grown in media with 10% or 20% FBS (C) human normal astrocyte cell line SVG, and two primary cells lines 0906 and 0713. (D) Three primary glioma cell lines exposed to high concentrations of H_2O_2. PI negative values expressed as a percentage. Experiments from A to C values from three experiments are shown; in experiment D, PI percentages shown are the average of measurements from three experiments. ** p<0.01 *** p<0.005, **** p<0.001 Student's t-test, two-tailed, unpaired. Statistics compared glioma to normal astrocytes.*

The effects of H_2O_2 on both human and murine paired normal to glioma cell lines were analysed. While the murine GL261 and C8D1A cells were ten times more resistant than the human cells to H_2O_2 -induced oxidative stress, both the murine and human cancer cells were more H_2O_2 -resistant compared to the normal cell equivalent (Figure 25 A and C).

The GL261 cells were routinely grown in media with 20% FBS- supplement, whereas C8D1A were routinely grown with 10% FBS –supplemented media. To find out if the change in FBS affected stress response pathways, the effect of H_2O_2 treatment was compared between 20% and 10% FBS-supplemented media in

GL261. The FBS levels appeared not to have an influence on the resistance to H_2O_2 in these cells (Figure 25 B).

Glioblastoma tumours are heterogeneous, that is, no two patients have the same tumour cell phenotypes, therefore three human primary GBM cells were analysed for response to H_2O_2 treatment. There were differences in resistance to H_2O_2 between primary cell lines (Figure 25 D), and interestingly, the 0906 cell line appeared to have a large subset of cells that stayed alive despite strong concentrations of H_2O_2 -- around 20% compared to 4-5% in the other primary glioma cells. These 0906 had become immortalised in culture, shown in Figure 16.

5.2.2 **Nicotinamide (NAM), a SIRT1 inhibitor rescued normal but not malignant cells from lethal oxidative stress**

To determine the contribution of SIRT1 to the peroxide stress response, murine normal and malignant astrocyte cells were grown in culture for 1 d, then subjected to a lethal concentration of H_2O_2 for 20 hr, with or without SIRT1 inhibitor NAM, at two different concentrations. Viability was measured using the PI exclusion assay and flow cytometry.

Both concentrations of nicotinamide rescued C8D1A cells from a lethal concentration of peroxide, whereas neither concentration of NAM rescued the malignant GL261 cells from the lethal peroxide levels (Figure 26).

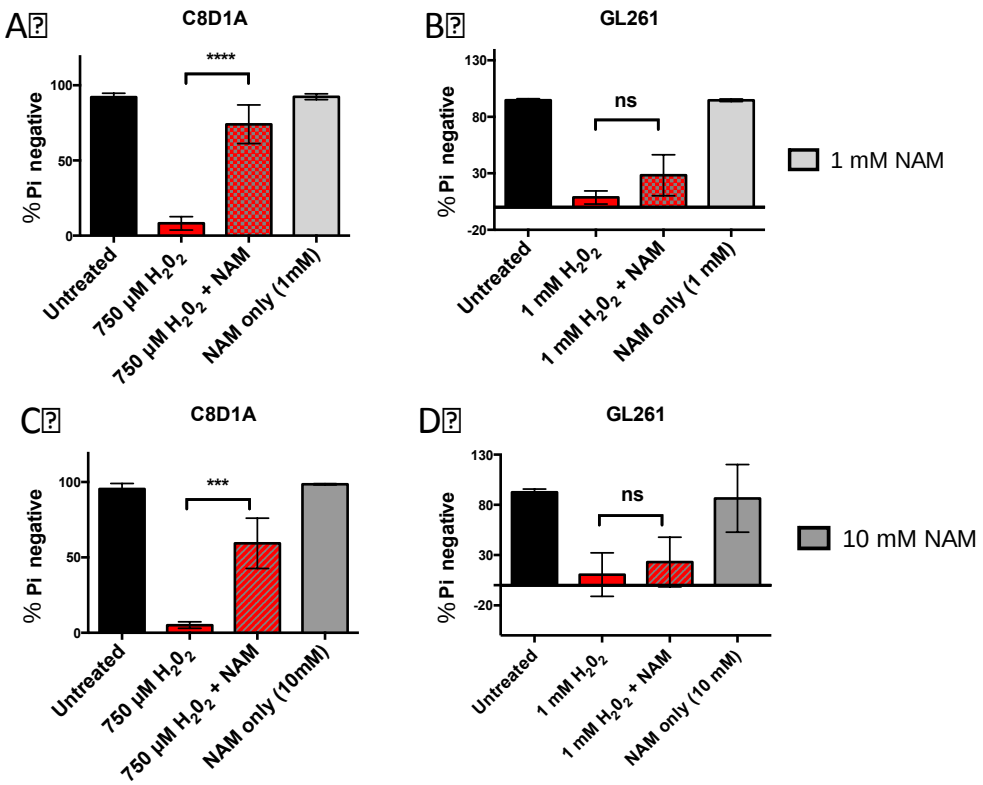

Figure 26. Nicotinamide rescued normal but not malignant murine astrocyte cells from lethal oxidative stress

*(A and B) Bar graph representations of PI exclusion assay of murine normal cells, C8D1A, and malignant glioma cells GL261 after lethal concentrations of H_2O_2 with 1 mM NAM grown for 20 hr. 10,000 cells were measured by flow cytometry. Pooled data from three experiments in triplicate for both of these were performed (C and D) As in A and B, using 10 mM NAM. Graphs show one experiment performed in triplicate for each of these. Student's t-test, two-tailed, unpaired *** $p < 0.005$, **** $p<0.001$; ns = not significant.*

5.2.3 Low concentration nicotinamide rescued malignant murine astrocyte cells grown in reduced FBS

C8D1A and GL261 cells were grown in media using 10% or 20% FBS-supplement for at least two passages, followed by treatment with a lethal concentration of peroxide to ascertain whether the rescue effect by NAM was influenced by change in FBS levels.

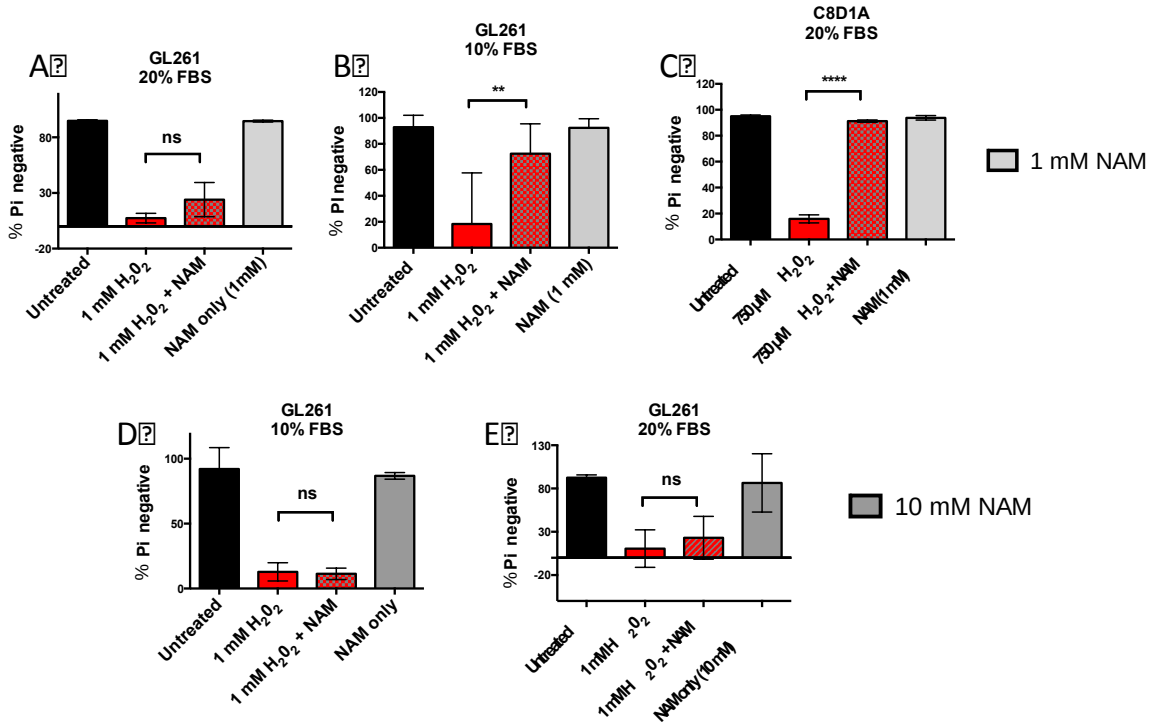

Figure 27. Low concentration nicotinamide rescued malignant murine astrocyte cells with reduced FBS

*C8D1A and GL261 cells were grown for more than two passages in media with either 10% or 20% FBS, then subjected to a lethal concentration of H_2O_2 for 20 hr with or without 1 mM or 10 mM NAM. Cell viability was assessed by PI exclusion assay and flow cytometry. (A) Graphic representation of viability of GL261 cells grown in 20% FBS, with or without H_2O_2 and 1mM NAM; (B and C) As in (A), but with GL261 and C8D1A grown in media with different FBS concentrations (D and E) GL261 cells grown in different levels of FBS with and without H_2O_2 or 10 mM NAM. Graphs show: (A and B) three sets of experiments in triplicate (C, D and E) one set in triplicate. ** p < 0.01, **** p < 0.001 Student's t-test, two-tailed, unpaired, ns = not significant.*

Surprisingly, when murine glioma GL261 cells were grown in the lower percentage of FBS, a rescue was observed with the low concentration of NAM but not at the higher concentration (Figure 27 B and D). The increase of FBS did not alter the rescue effect for the C8D1A which were rescued with 1 mM NAM even when grown in 20% FBS (Figure 27 C).

5.2.4 Nicotinamide rescued normal but not malignant human astrocyte cells

The rescue effect from a lethal concentration of H_2O_2 seen in murine cells was tested in human cells using SVG and human primary glioma cells. Cells were grown in culture with or without H_2O_2, and with or without NAM, for 20 hr.

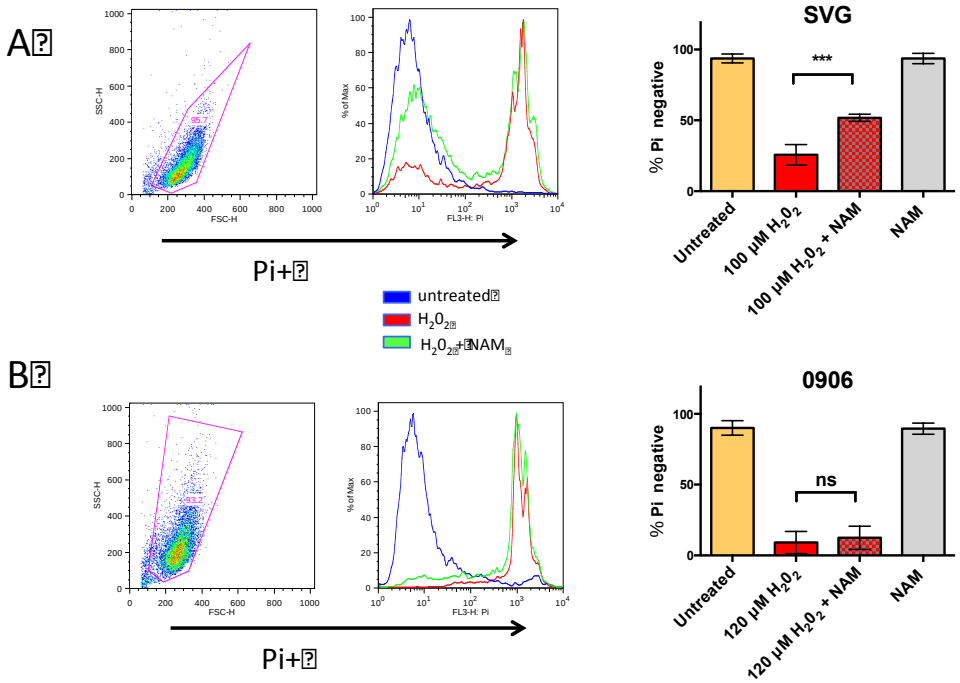

Figure 28. Nicotinamide rescued normal but not malignant human astrocyte cells from lethal oxidative stress

*Cells were grown for 20 hr with or without a lethal concentration of H_2O_2, with or without 10 mM NAM. (A) Dot plot showing flow cytometry gating out of dead cells (first box); histogram showing live untreated cells (blue), H_2O_2 treated (red), and H_2O_2 with NAM treated (green) cells, from cells stained with PI and measured by flow cytometry (second box); graphic representation showing the four separate treatments for SVG astrocytes showing PI negative on the y-axis (third box). (B) As in A, but for glioma primary cells, 0906. Results from one experiment performed in triplicate. *** $p < 0.005$ Student's t-test, two-tailed, unpaired, ns = not significant.*

The human cells lines exhibited the same pattern as seen with the murine cells. While normal SVG cells were rescued by NAM, glioma primary cells 0906, were not rescued by NAM after a lethal peroxide treatment (Figure 28). Further experiments using multiple primary glioma cell lines would be useful to confirm this result.

5.2.5 Resveratrol had an opposing effect to nicotinamide with astrocytes under oxidative stress

The experiment described in the last section was repeated using SIRT1 activator, RES, instead of SIRT1 inhibitor.

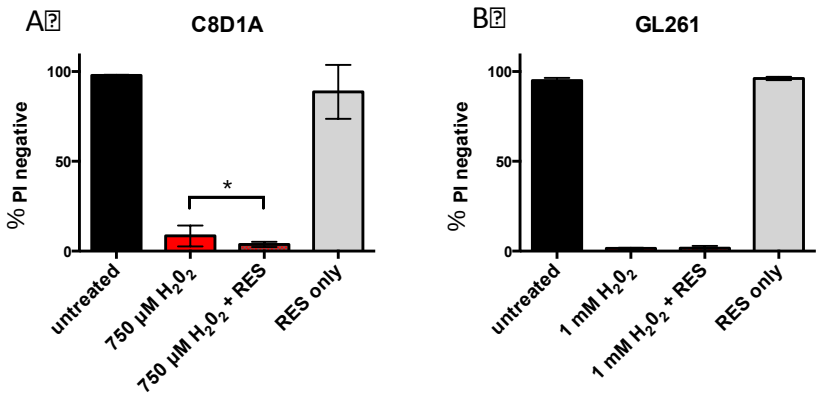

Figure 29. Resveratrol had no rescue effect to lethal H_2O_2 -induced oxidative stress in C8D1A or GL261

*Cells were grown for 20 hr with or without a lethal concentration of H_2O_2 and with or without 50 µM RES. (A) C8D1A cells with H_2O_2 and RES treatment (B) As in A, but for GL261 cells. One experiment performed in triplicate. * $p < 0.05$ Student's t-test, two-tailed, unpaired.*

This experiment showed neither C8D1A nor GL261 were rescued by RES (Figure 29). C8D1A cells showed the opposite effect, where RES with H_2O_2 has a significant additive effect on cell death outcome ($p < 0.05$) (Figure 29 A), which is consistent with NAM having a rescue effect, indicating that this could reflect Sirt1 activity – and a differential Sirt1 role of glioma versus normal cells.

5.2.6 Length of treatment time influenced the rescue effect of NAM, and the additive effect of RES treatment

To investigate a potential Sirt1 mechanism for the rescue effect of NAM, the same experiment was performed as described earlier using C8D1A and GL261 cells, with a shorter treatment time of 6.5 hr – and using two lower concentrations of H_2O_2.

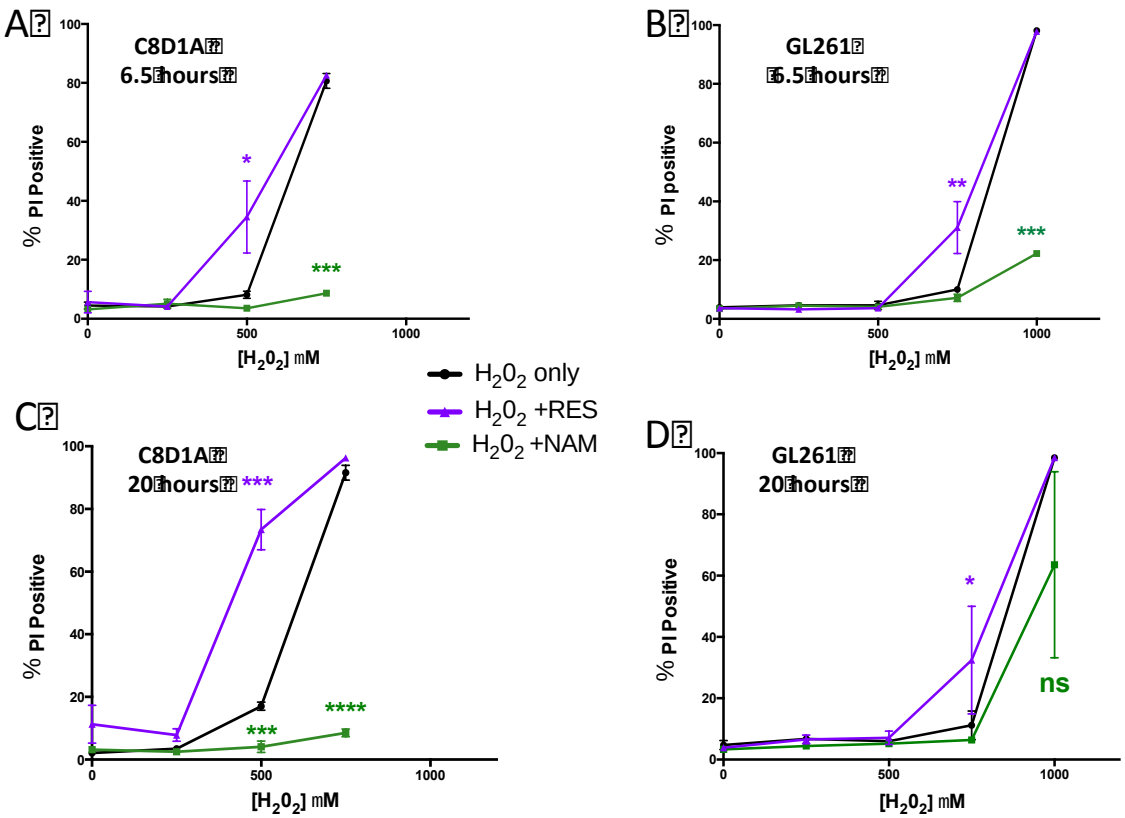

Figure 30. Nicotinamide rescued murine glioma cells from lethal oxidative stress at an early time point, but not at a later time point. Resveratrol had opposing effects

*Cells were grown for 6.5 or 20 hr with three different concentrations of H_2O_2, with or without 10 mM NAM or 50 μM RES. (A) C8D1A grown for 6.5 hr with or without NAM or RES at varying H_2O_2 concentrations (B) As in A, but for GL261. One experiment performed in triplicate for each treatment. * p <0.05, ** p < 0.01 *** p < 0.005, **** p < 0.001 Student's t-test, two-tailed, unpaired, ns = not significant.*

In all cell lines, RES had opposing effects to NAM with increased cell death when RES was added at the same time as H_2O_2 (Figure 30). The effect of the Sirt1 inhibitor or activator was greater for the normal C8D1A cell line than for glioma cells after 20 hr (Figure 30 C and D). Interestingly, there was a rescue effect for GL261 with NAM at the earlier time point, but not at the later time point indicating that the differential effect of NAM in GL261 compared to C8D1A takes some time for response.

5.3 Immunoblotting to investigate changes in SIRT1 protein levels and H4K16-ac after oxidative stress

To investigate if SIRT1 levels change under peroxide stress or nicotinamide, cells were grown for 20 hr with or without sub-lethal or lethal concentrations of H_2O_2, and with or without NAM. The cells were extracted with whole cell lysis, and analysed using Western blotting.

5.3.1 **A prominent second protein band appeared on Western blots for SIRT1 in normal but not malignant cells after H_2O_2 -induced oxidative stress**

Elevated levels of Sirt1 with sub-lethal concentrations of H_2O_2 was seen for both C8D1A and GL261 cell lines after 20 hr treatment (Figure 31 B and D). A lethal concentration of H_2O_2 had no effect on Sirt1 levels in the normal cell line, while in the glioma cell line Sirt1 was reduced after a lethal H_2O_2 concentration. Sirt1 was seen to have a second band, at about 80-85 kDa after H_2O_2 treatment for the normal cell line in both concentrations of H_2O_2, but was not seen in the glioma cell line (Figure 31 A red arrows). While the experiment shown here was performed only once, this second Sirt1 band was seen in further experiments in the normal cells after oxidative stress treatment. NAM treatment had no effect on Sirt1 quantity with or without H_2O_2 (Figure 31 B and D).

The second band was faintly observable at 6.5 hr in the normal cells but not on the glioma cells, suggesting that it takes some time to establish quantity of the putative smaller species of Sirt1 under these conditions (Figure 31 E).

To verify this observation, human SVG normal astrocyte cell line and the primary glioma cell line 0713 were treated with a lethal concentration of H_2O_2, followed by whole cell lysis, protein extraction and Western blotting.

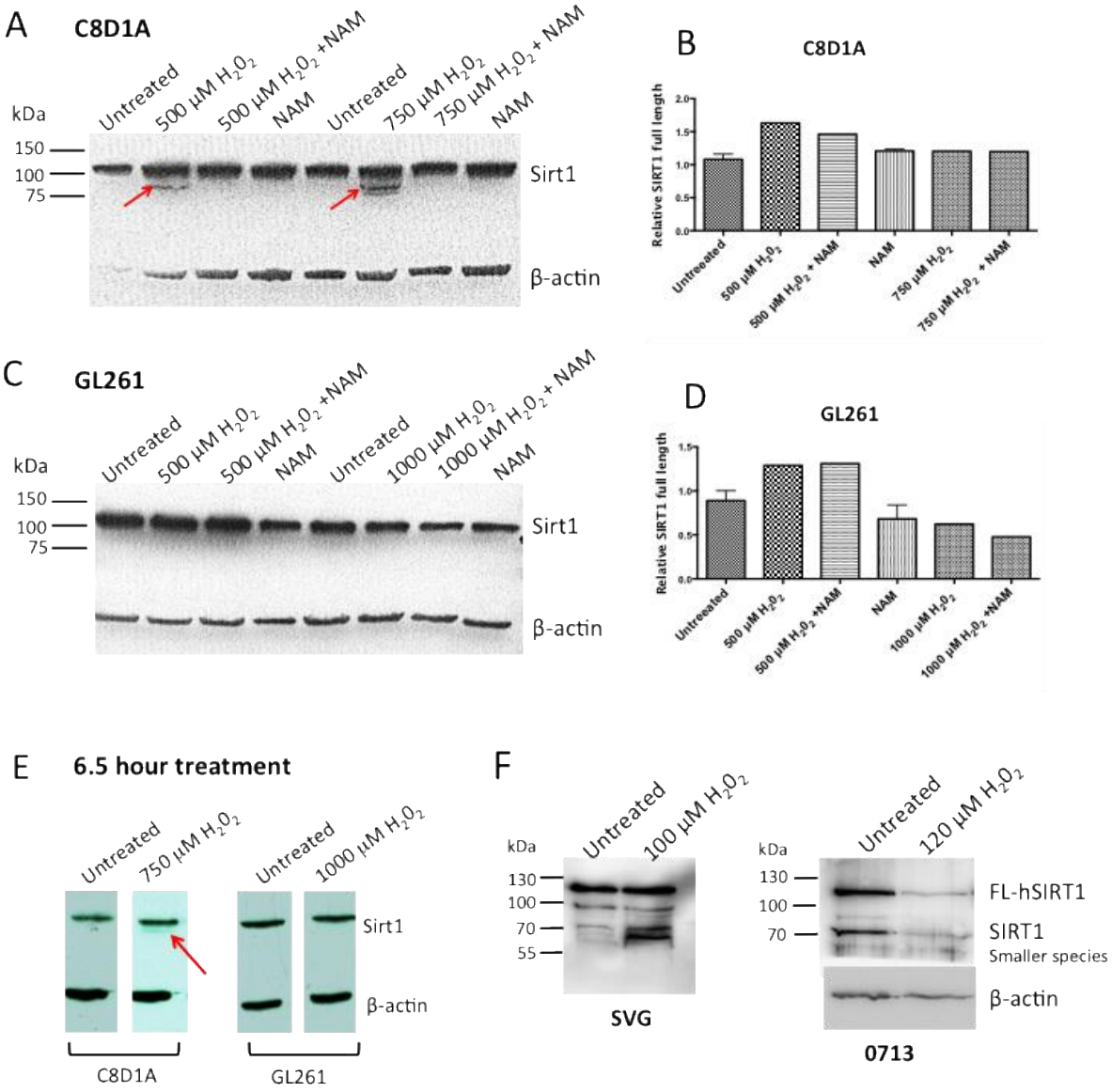

Figure 31. SIRT1 was cleaved under H_2O_2 -induced oxidative stress in murine and human normal astrocyte cells, but not in malignant cells

Cells were seeded for 1 d before treatment of H_2O_2, NAM or combination of both. (A and B) Western blot image and histogram quantification of Sirt1 in C8D1A cells after 20 hr treatment of 500 μM or 750 μM H_2O_2, or 10 mM NAM, or a combination of both. Red arrows indicate extra bands for Sirt1; (C and D) As in A and B, but for GL261 cells, where the higher lethal H_2O_2 concentration used was 1000 μM; (E) Western blot image of Sirt1 in C8D1A cells after 6.5 hr incubation with or without a lethal concentration of H_2O_2. Red arrow indicates extra band for Sirt1; (F) Western blot images of SVG or 0713 cells with or without a lethal concentration of H_2O_2 for 20 hr. Note loading control was absent for SVG. Levels of Sirt1 in histograms were adjusted to β-actin loading controls.

Results confirmed an increase in a second band of hSIRT1 in normal SVG cell line but not glioma cells after H_2O_2 treatment (Figure 31 F). Levels of hSIRT1 had decreased for the human primary glioma cells after a lethal concentration of H_2O_2, reflecting the similar result seen in the murine GL261 cells, indicating that this result was also typical for SIRT1 in glioma.

5.3.2 H4K16 acetylation status changed in murine cell lines after 20 hr treatment with H_2O_2 and nicotinamide

After H_2O_2 treatment, a smaller fragment of Sirt1 was observed in C8D1A cells, but not in GL261 cells. The fragment was lost when NAM was added at the same time as H_2O_2 (Figure 31 A). While this may have something to do with the rescue effect seen in the normal cells after H_2O_2 treatment, it did not explain why the glioma cells -re not rescued. To further investigate these responses, H4K16-ac was measured after these treatments. Histone extraction followed by immunoblotting was performed with and without a lethal concentration of H_2O_2 and with or without NAM treatment for 20 hr in both the normal and glioma cell lines.

As expected, NAM treatment showed an increase of histone 4 acetylation in both the normal and glioma cells (Figure 32 A and B) indicating NAM inhibition of Sirt1 deacetylation for this residue. Treatment with H_2O_2 showed an increase in deacetylation for both cell lines indicating that Sirt1 activity is increased in oxidative stress at the lethal concentration after 20 hr. NAM treatment with H_2O_2 increased H4K16-ac by about 3 x in C8D1A cells, while only 1.3 x in GL261 cells (Figure 32 B red arrows), suggesting that increased H4K16-ac relates to stunting the lethal stress incurred by H_2O_2, as seen with the rescue in Figure 26, where C8D1A cells were recued from lethal H_2O_2-induced stress with NAM treatment, but GL261 were not rescued.

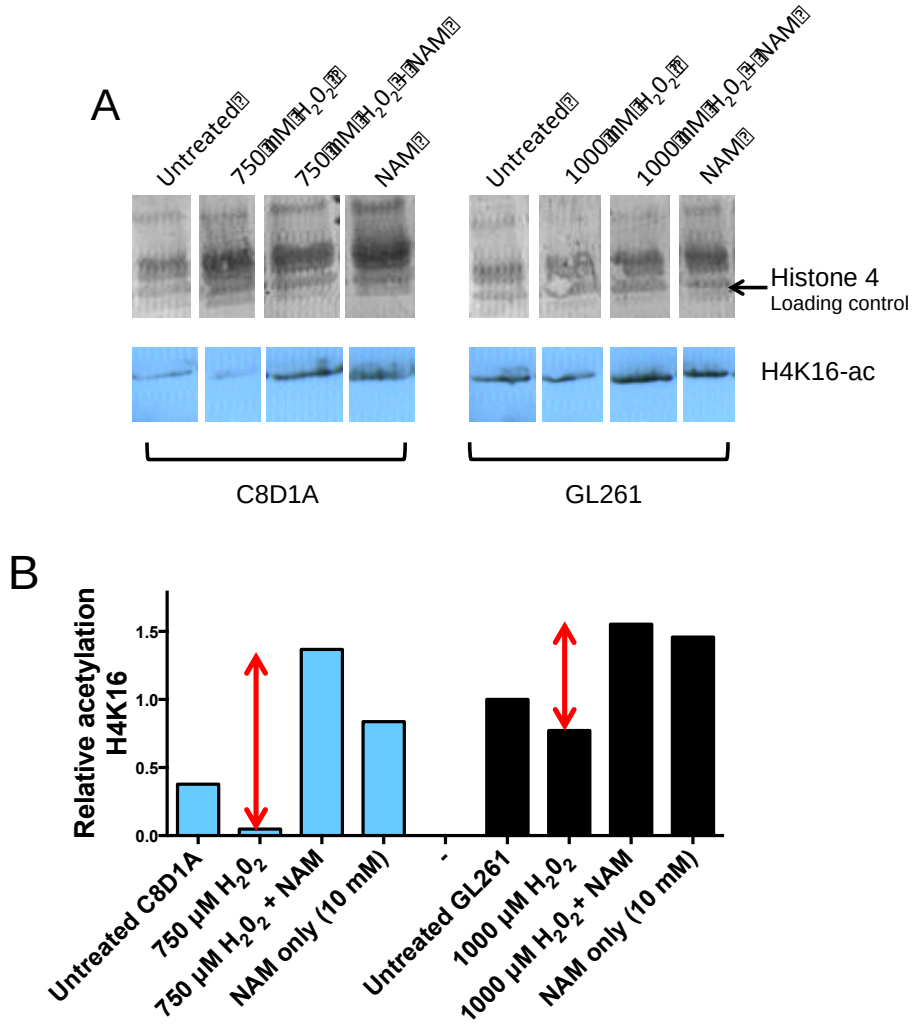

Figure 32. H4K14 acetylation in murine cells after H_2O_2 or nicotinamide treatment for one day

Murine C8D1A and GL261 cells were grown for 1 d in culture then treated with a lethal concentration of H_2O_2 or 10 mM NAM, or a combination of both. Histone extraction and western blotting followed by immunoblotting for H4K16 acetylation. (A) Western blot images for loading control using amido black staining for histone 4 (top panels), and the same membrane probed for H4K16-acetyaltion (bottom panels) for C8D1A and GL261 cells. (B) Histogram showing quantitatively the Western blot images, relative to each other and adjusted for loading levels. Red arrows indicate differences in acetylation of H4K16 after H_2O_2 treatment and H_2O_2 plus NAM treatment for each cell line.

5.3.3 H4K16 acetylation changes in murine cell lines after two-hour treatment with H_2O_2 and nicotinamide

To find out if changes to H4K16-ac after H_2O_2 and NAM treatment had the same result at an earlier time point, histone extraction was performed after 2 hr, followed by immunoblotting.

Figure 33. H4K16 acetylation in murine cells after H_2O_2 or nicotinamide treatment for two hours

Cells were seeded for one day before treatment of a lethal concentration of H_2O_2 or 10 mM NAM for 2 hr, followed by histone extraction and immunoblotting for H4K16-ac. (A) Western blot image showing C8D1A (left panel) and GL261 (right panel) H4K16-ac with or without treatment. Loading control was measured using amido black staining for total protein (top panels); (B) histogram showing quantification for Western blot images, with H4K16-ac adjusted to loading control. GL261 cells grown in 20% FBS.

Untreated GL261 cells had increased H4K16-ac compared to untreated C8D1A cells consistent with previous results (Figure 33 B black bars). H_2O_2 – induced stress and NAM treatment showed opposite effects for H4K16-ac in the different cell lines. For C8D1A cells, H_2O_2 or NAM treatment increased acetylation, whereas the same treatment decreased H4K16-ac in GL261 cells (Figure 33 B yellow and red bars). This indicated different responses to these treatments between the cells. It also differs from H4K16-ac measurements made at 20 hr, where GL261 cells had increased acetylation as did the C8D1A cells, indicating different actions for Sirt1 under oxidative stress at different time points as well as between cancer and normal cell lines.

5.3.4 Localisation changes for Sirt1 in murine normal and cancer astrocytes after two-hour H_20_2 or nicotinamide treatment

In previous results, untreated GL261 cells had higher H4K16-ac levels compared to the normal astrocyte cell line, C8D1A. Correspondingly, Sirt1 was aberrantly found in the cytoplasm GL261 cells, where it was found predominantly in the nucleus in C8D1A cells. It was postulated that changes in localisation of Sirt1 could explain the results seen in histone acetylation after 2 hr H_2O_2 or NAM treatment in these cell lines. To find this out, nuclear/cytoplasmic extraction was performed at the same time as the histone extraction in Section 5.3.3.

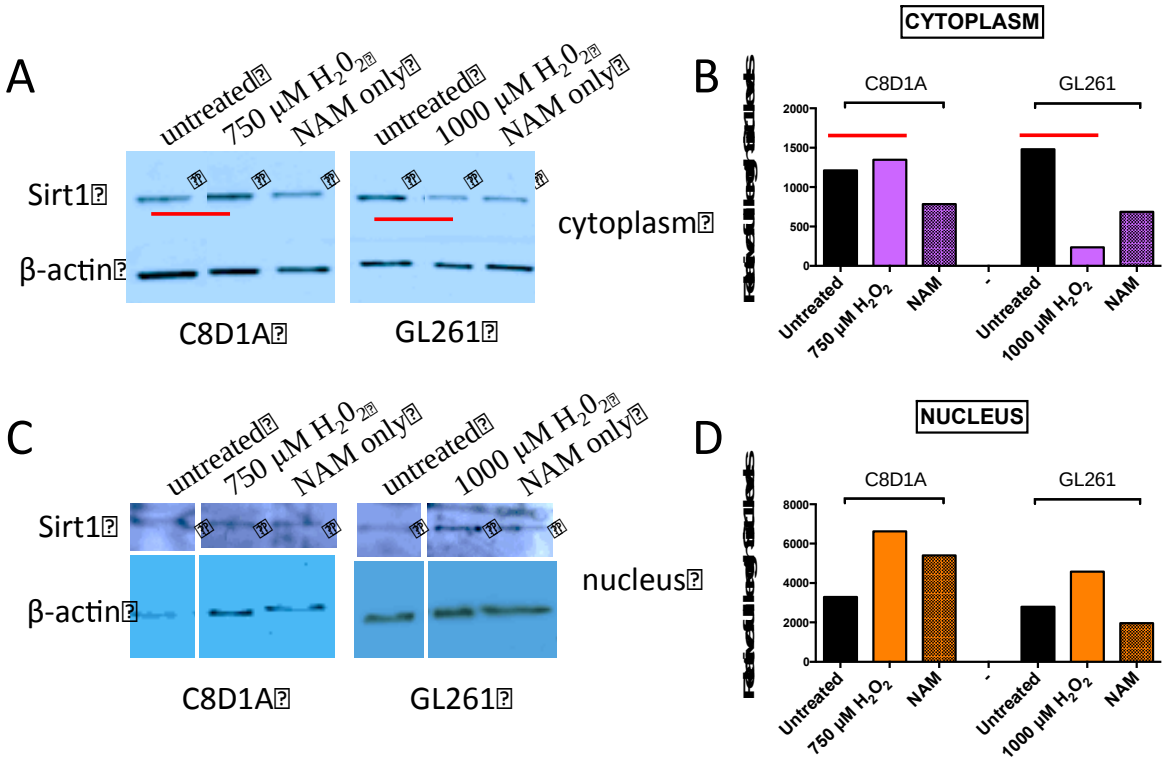

Figure 34. Localisation changes for Sirt1 in murine normal and glioma astrocytes after two-hour H_2O_2 or nicotinamide treatment

Nuclear /cytoplasmic extraction was undertaken for C8D1A and GL261 cells after 2 hr treatment of H_2O_2 at a lethal concentration, or 10 mM NAM using the two buffers made up in the lab, as described in Andrews et al (Andrews & Faller 1991). Western blotting followed by probing for Sirt1 was performed for (A) cytoplasmic compartment and (C) nucleic compartments separately. β-actin was used as the loading control for both compartments, purity of extraction was not tested, and results were analysed by image J and graphically represented (B and D), red lines explained in the text.

Results indicated increased Sirt1 in the cytoplasm in untreated GL261 cells compared to increased levels of nucleic-localised Sirt1 in untreated C8D1A cells, consistent with all previous results (black bars Figure 34 B and D). Treatment with

H_2O_2 increased Sirt1 in the cytoplasm of the C8D1A cells and decreased Sirt1 in the cytoplasm for the GL261 cells, consistent with H4K16 acetylation results seen in earlier (Figure 33). NAM treatment appeared to decrease the level of Sirt1 in the cytoplasm for both cells (Figure 34 B purple thatched bars). The results from the blot for the nuclear compartment were not always consistent, with the cytoplasmic results. This could be explained by a poor extraction either in quantity or purity, therefore this experiment needs repeating. However, results for the cytoplasmic compartment showed a clearer immunoblot and were more consistent with results seen with histone extraction in Section 5.3.3, which was done using a portion of the cells from the same experiment. Taken together with immunofluorescent experimental results shown in Section 3.3, the combined evidence suggests that Sirt1 in untreated glioma cells is localised differently to normal cells, and this localisation is affected differently under oxidative stress and NAM treatment. Additionally, these changes alter between 2 hr and 1 d.

5.3.5 Nuclear/cytoplasmic changes for hSIRT in human SVG astrocytes and primary glioma cells after four-hour H_2O_2 treatment

To verify the results in the response to H_2O_2 treatment where Sirt1 in the mouse model suggested altered localisation after treatment, human astrocyte cell line, SVG, and primary glioma cell line 0906 were exposed to 100 μM and 120 μM (lethal dose) for four-hour and extracted using formaldehyde crosslinking before nuclear/cytoplasmic extraction.

FL-hSIRT1 was not seen clearly in these results. While hSIRT1 was seen clearly in the Western blots for whole cell lysis extraction seen earlier, a similar result showing reduced or absent FL-hSIRT1 this was seen in the other nuclear/cytoplasmic extraction using SVG cells after crosslinking (Figure 15).

FL-hSIRT1 could have been lost during extraction, or perhaps it was in the form of a trimer – kept intact after crosslinking, and was too large for detection in this experiment. There is evidence in the literature to support this (Guo et al 2012).

However, a number of other bands running further in the gel were present, as in other extractions, and a different pattern of these bands was seen after treatment. While it is possible these smaller bands are non-specific antibody binding, as mentioned before, smaller hSIRT1 species have been reported, in particular a band at 68 kDa, 75 kDa and 80 kDa.

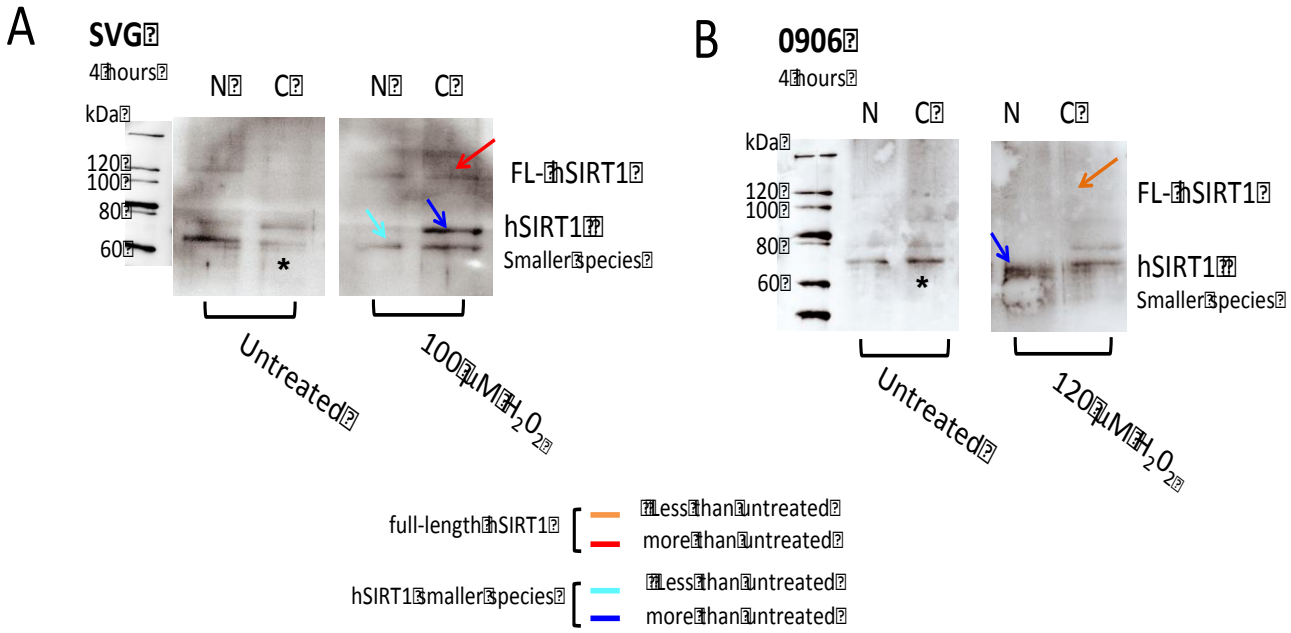

Figure 35. hSIRT1 localisation changes in SVG and primary glioma cells 0906 after four-hour H_2O_2 treatment

SVG and 0906 primary glioma cells were seeded for one day, then treated for four-hour with a lethal concentration of H_2O_2 (100 µM for SVG, 100 µM for 0906), 10 mM NAM or 50 µM RES followed by nuclear/cytoplasmic extraction using the NE-PER kit with prior formaldehyde fixing (as described in methods section) and immunoblotting with hSIRT1 antibody. (A) FL-hSIRT1 and smaller species of hSIRT1 in treated and untreated SVG cells and for (B) treated and untreated 0906 (post-immortalisation) cells. C= cytoplasmic compartment, N= nuclear compartment. Loading controls were attempted but were unsuccessful.

Untreated 0906 cells had more cytoplasmic smaller species than SVG cells (Figure 35 black asterisks). This was consistent with previous experiments that consistently showed more cytoplasmic SIRT1 in glioma cells compared to normal astrocytes. After H_2O_2 treatment, the smaller hSIRT1 species was decreased in the nuclear compartment for SVG cells, but increased in the nuclear compartment for 0906 cells, and consistent with this was an increase and decrease in the cytoplasmic compartments respectively (Figure 35, coloured arrows).

These results, while preliminary, provide an indication that the response of hSIRT1 may involve smaller species of hSIRT1 and changes in localisation under oxidative stress. Importantly, these responses are different between normal and glioma cells.

5.4 Sub-cellular localisation changes for SIRT1 after NAM or RES treatment

SIRT1 has different localisation profiles in untreated glioblastoma and normal cells. It was therefore investigated whether the effect of NAM and RES might be related to differences in localisation of SIRT1.

Extractions of nucleus and cytoplasm were conducted with and without NAM for murine GL261 and C8D1A cells after 20 hr incubation, and for human glioma and SVG normal astrocytes after four-hour incubation with NAM or RES. Formaldehyde fixation prior to extraction was used.

5.4.1 Nuclear/cytoplasmic fractionation and Western blotting for SIRT1 after RES or NAM treatment in human normal astrocytes and primary glioma cells

After 1 d incubation with NAM, there appeared to be decreased cytoplasmic and increased nuclear FL-Sirt1 in murine GL261 cells, but no effect on Sirt1 localisation in C8D1A cells (Figure 36 A and B, orange and red arrows). NAM treatment for four hours showed increased smaller species of hSIRT1 in the cytoplasm of SVG, with a possible decrease of these in the nucleus (Figure 36 C light blue and dark blue arrows – third and fourth lanes), however NAM treatment results were unclear for the human primary glioma 0906 cells. Treatment with RES increased nuclear FL-hSIRT1 after 4-hr treatment in 0906 (Figure 36 D, red arrow). Levels of both smaller species of hSIRT1 changed after RES and NAM treatment in the cytoplasm of SVG cells (Figure 36 C, light blue arrows), while a possible increase in the faster running molecule (possibly the 75 kDa fragment) for 0906 increased in the nucleic but particularly in the cytoplasmic compartment of 0906 cells after RES treatment (Figure 36 C, dark blue arrows last two lanes). No loading or purity controls were successfully used in this Western blot. The antibodies did not work for unknown reasons. These results are preliminary, and need verification.

These results suggest a change in SIRT1 localisation after NAM or RES treatment, and possible cleaving or stabilisation patterns for SIRT1 smaller species under these conditions.

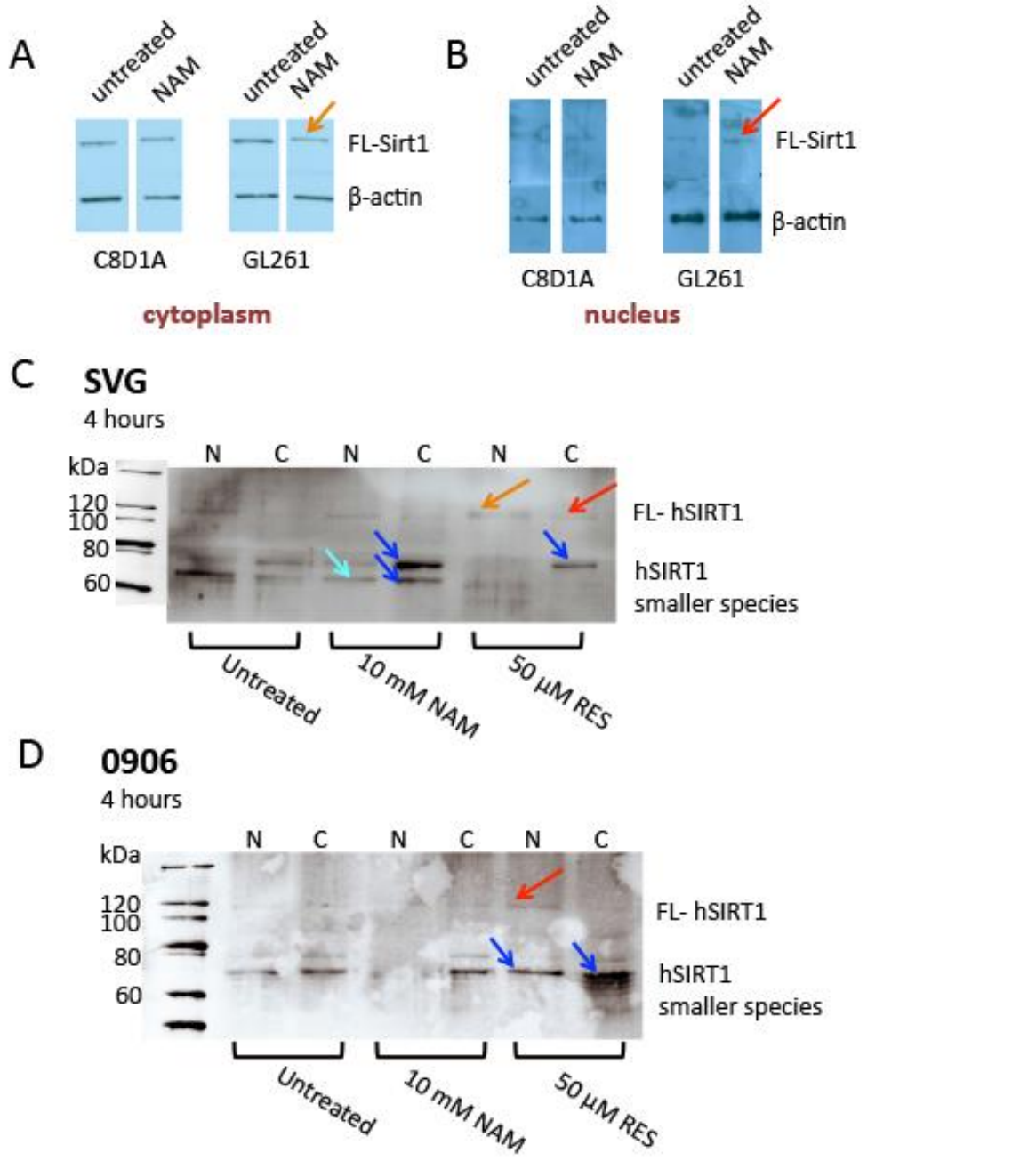

Figure 36. Altered localisation of SIRT1 with NAM or RES treatment

Western blot images for SIRT1 after nuclear-cytoplasmic extractions. (A) Extraction using buffers A and B as described Section 2.2.3 for murine cell lines C8D1A and GL261. Incubation with NAM for 20 h. β-actin was used as a loading control, and more β-actin was observed in the nucleus of GL261. This was seen in other experiments indicating that was the nuclear fraction. (B and C) Extraction using NE-Per kit after formaldehyde fixation, as described in methods section, for SVG and 0906 cells. NAM and RES incubation 4 h. Red arrows show increased FL-SIRT1 compared to untreated cells, light blue arrows indicate decreased smaller SIRT1 species, dark blue arrow indicates increased common smaller SIRT1 species. Abbreviations: N= nuclear compartment; C = cytoplasmic compartment.

5.4.2 Immunofluorescent staining for hSIRT1 in primary glioma cells after NAM treatment

To find out if changes in localisation were valid for NAM treatment of human primary glioma cells, another method was attempted. Immunofluorescent staining was performed with and without 2 hr treatment of 10 mM NAM in three primary glioma cell lines. hSIRT1 was stained green, and using image J, 100 or more non-dividing cells were characterised for localisation in untreated cells or NAM-treated cells.

In each of the three primary gliomas assessed for hSIRT1 localisation, the effect of NAM treatment showed a more nuclear or a predominantly nuclear hSIRT1 profile compared to untreated cells (Table 6 and Figure 37). While this method does not discern between different species of hSIRT1, it does indicate a change in abundance of overall nuclear hSIRT1 after NAM treatment for these cells.

Table 6. Cell counts for sub-cellular localisation of hSIRT1 in primary glioma cells with and without NAM treatment

	nuclear	predominantly nuclear	cytoplasmic	predominantly cytoplasmic	50/50	total
1005						
Untreated	49	86	0	0	8	143
NAM	85	85	1	1	6	178
1003						
Untreated	36	163	16	13	23	251
NAM	41	262	0	0	3	306
0814						
Untreated	2	49	0	10	31	92
NAM	9	88	0	0	12	109

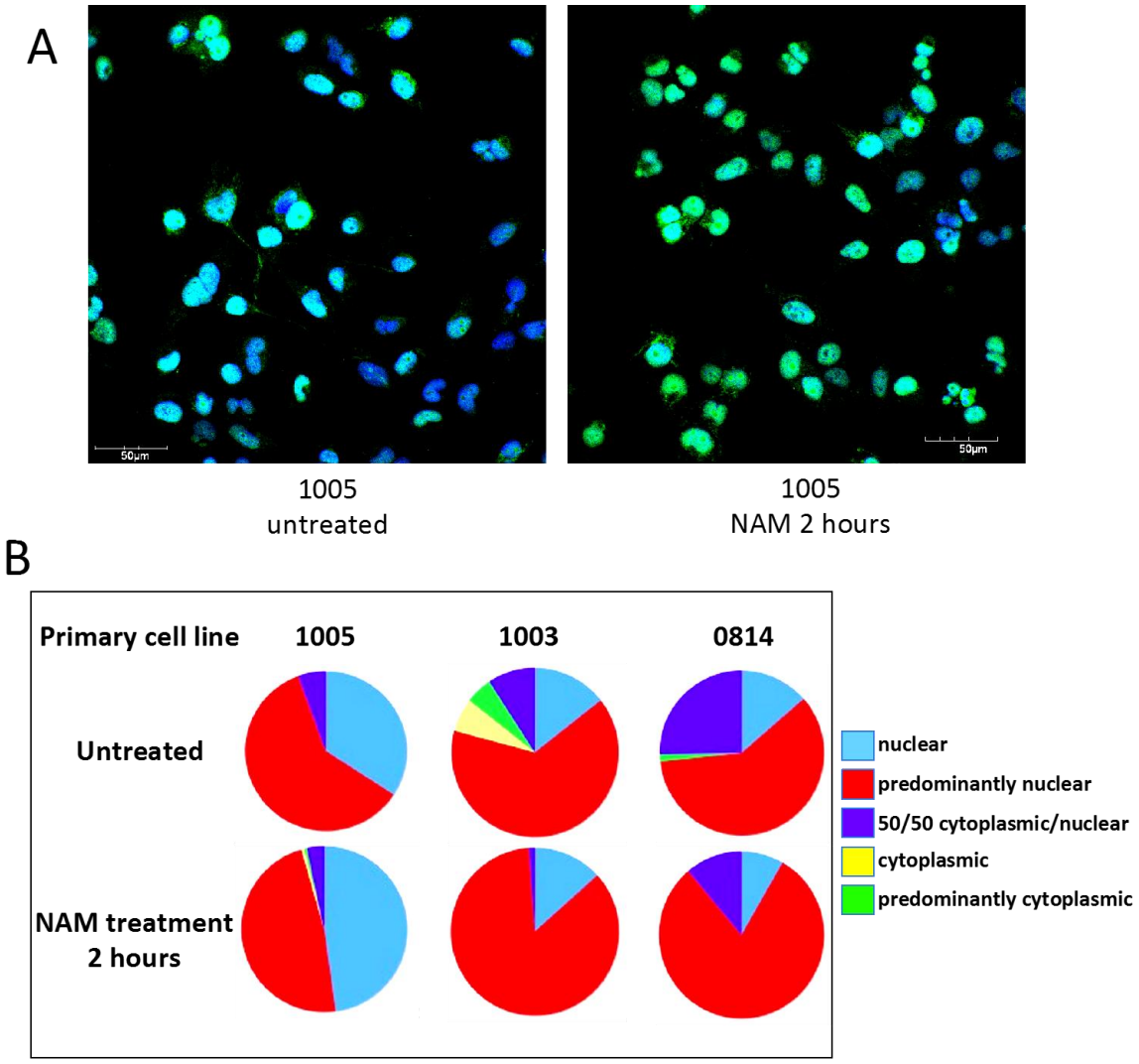

Figure 37. Immunofluorescence of hSIRT1 in primary glioma cells after NAM treatment

Human glioma cells were grown for two days on 8-well chamber slides before treatment of 10 mM NAM. After two hours, the cells were fixed using paraformaldehyde and incubated with hSIRT1 antibody, and secondary antibody, which fluoresced green. DAPI was used to stain for nuclei. At least 100 non-dividing cells were assessed by eye for hSIRT1 localisation for each of three primary cell lines with or without treatment (A) An example of one field of view for one primary glioma cell line, 1005, for untreated and NAM-treated cells (B) Pie charts representing results from treated and untreated for three primary cell lines. Raw data taken from cells counted and assessed for sub-cellular localisation, presented in Table 6 (previous page).

5.5 SIRT1 in the cytoplasm co-localised with mitochondria

5.5.1 hSIRT1 associates and alters mitochondria in normal astrocyte response to oxidative stress

It has been reported that some sirtuins associate with mitochondria, in particular SIRT3 (Webster et al 2012). SIRT1 has also been identified with mitochondrial associated molecules, for example PGC1-α (Sugden et al 2010) but more recent research has identified the 75 kDa SIRT1 fragment and mitochondria associating directly to inhibit cytochrome c release and apoptosis in chondrocytes (Oppenheimer et al 2012). Several different experiments in this thesis indicated that under oxidative stress, SIRT1 in normal astrocytes had an increased presence the cytoplasm. To find out if SIRT1 affected mitochondria under oxidative stress in normal astrocytes, C8D1A cells were treated for 2 hr with H_2O_2 with or without NAM. Median fluorescent intensties (MFI) for Mitotracker green (MTG) and Mitotracker red (MTR) were used to assess changes in mitochondrial membrane potential (MTR) and mitochondrial mass (MTG), in C8D1A normal murine astrocytes.

Additionally, MTG and hSIRT1 antibody immunofluorescent staining were used to assess co-localisation of hSIRT1 with mitochondria visually using human SVG astrocytes. Immunofluorescent experiments using C8D1A were similarly undertaken, but results were unclear.

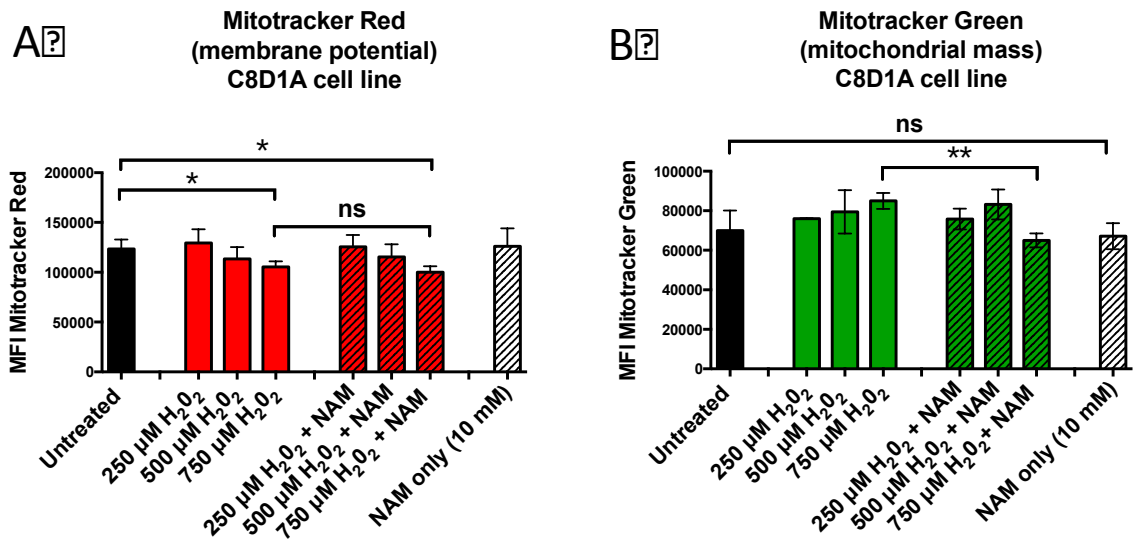

Figure 38. Inhibition of Sirt1 affects mitochondrial mass in normal murine astrocytes under mild oxidative stress

(A and B) C8D1A cells were grown for 1 d, then treated with different concentrations of H_2O_2 or NAM for 2 hr, then harvested and incubated with MTR (A) or MTG (B) and measured by flow cytometry for changes in mean fluorescent intensity (MFI) for MTG/MTR, n=3.

Results showed that for C8D1A cells, after H_2O_2 -induced stress MTR the median fluorescent intensity (MFI) was reduced in a concentration-dependent manner, however NAM treatment did not change the outcome, suggesting Sirt1 is not involved in membrane potential changes after oxidative stress (Figure 38 A). MTG results showed that MFI increased with H_2O_2 -induced stress, but was significantly reduced with NAM treatment in combination with a lethal concentration of H_2O_2 only (Figure 38 B), suggesting that Sirt1 may have some role in changes of mitochondrial mass under H_2O_2 –induced stress. Analysis of immunofluorescent staining indicated that hSIRT1 was more cytoplasmic after H_2O_2 treatment for 2 hr in normal SVG astrocytes (Figure 39 A arrows), and co-localisation of hSIRT1 with mitochondria was occurring (Figure 39 A and B merge panels -orange colour). Different morphology of mitochondria was observed before and after treatment in normal SVG cells, where long filamentous mitochondria became more punctate after treatment (Figure 39 C), which could be related to hSIRT1 activity at mitochondria, given MTG measurements changed under oxidative stress and NAM treatment. Similar experiments for glioma cells were unsuccessful.

A

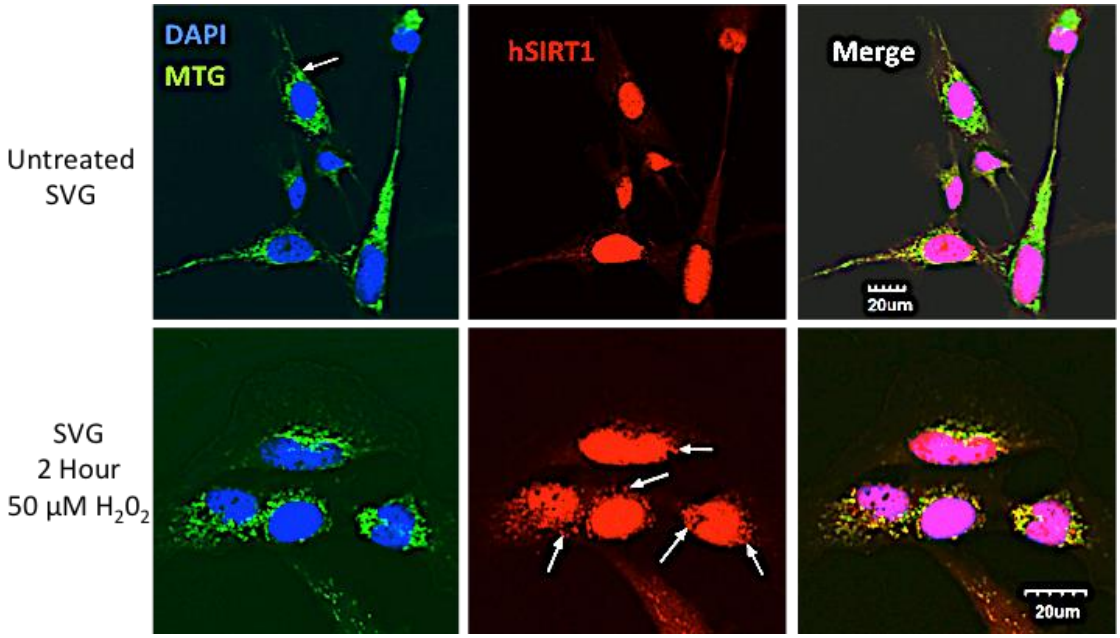
Untreated
SVG
DAPI
MTG
hSIRT1
Merge
20um
SVG
2 Hour
50 µM H_2O_2
20um

B

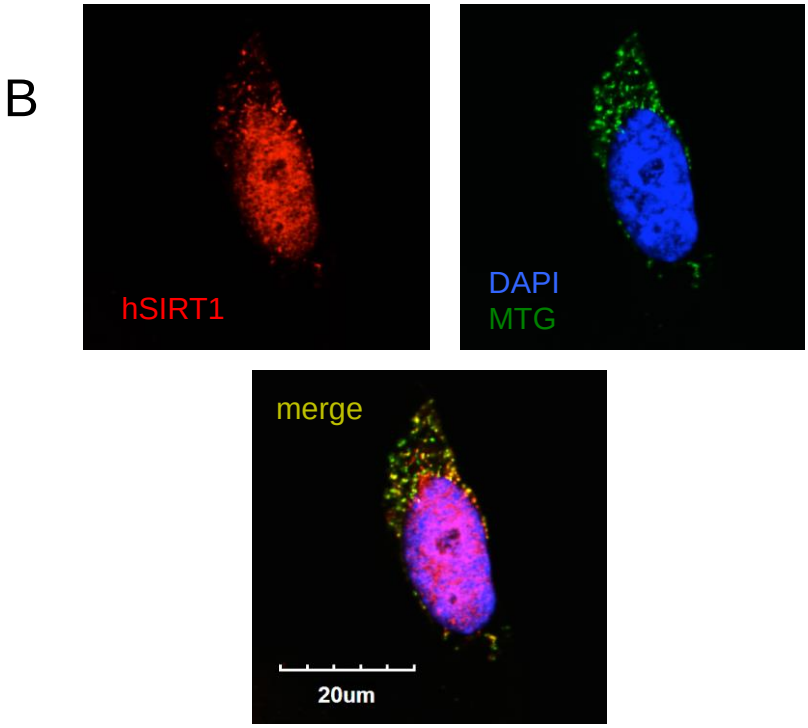
hSIRT1
DAPI
MTG
merge
20um

C

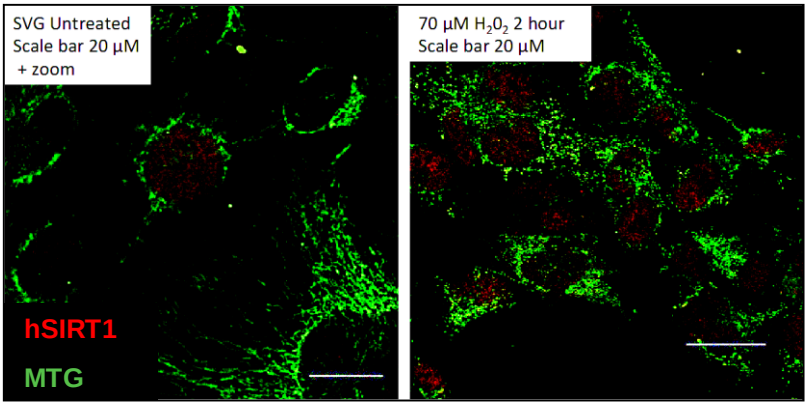
SVG Untreated
Scale bar 20 µM
+ zoom
70 µM H_2O_2 2 hour
Scale bar 20 µM
hSIRT1
MTG

Figure 39. hSIRT1 is increased in the cytoplasm and associates with mitochondria under sub-lethal oxidative stress

(Facing page)
(A) SVG cells were grown in 8-well chamber slides for two days before treatment for 2 hr with 50 μM H_2O_2, fixed and stained for hSIRT1 (red), nuclei (blue) using DAPI, and mitochondria (green) using MTG, arrows point to some examples of fluorescent hSIRT1 that has become visible after treatment; (B) one SVG cell on higher magnification showing hSIRT1 with mitochondria after 50 μM H_2O_2 treatment for 2 hr; (C) morphological changes in mitochondria of SVG cells untreated or treated for 2 hr with H_2O_2, fixed and stained with hSIRT1 (red) or MTG (green).

Part 6: Discussion

Glioblastoma is a disease with a dire outlook for the patient. Treatment for this cancer has remained largely unchanged over the last ten years, and the need to find new ways to tackle this disease is important. The objective of this thesis was to investigate the potential role of SIRT1 in glioblastoma in the context of cell proliferation and under oxidative stress.

SIRT1 is well known to have considerable involvement in maintaining homeostasis in many different cell types in relation to metabolic changes and under oxidative stress conditions. Oxidative stress, cell proliferation and altered metabolic function are conditions highly relevant to the progression of glioblastoma (Bartkova et al 2010). However, to date there is little research into the role of SIRT1 in GBM.

6.1 SIRT1 in untreated normal astrocytes and glioma cells

6.1.1 SIRT1 protein levels in glioma and normal astrocytes

Research into the levels of protein or RNA expression levels for SIRT1 in many different cancers has become of more interest in recent years, but there is scant research into SIRT1 levels in GBM.

A recent study measuring hSIRT1 levels in 43 clinical samples taken from patients with brain tumours from WHO Grade I-IV, show RNA expression of hSIRT1 is increased in grades I-III, but is decreased in grade IV tumours compared to normal tissue (Annabi et al 2012). Notably there was only one sample for GBM grade IV in that study. Reduced levels of SIRT1 are seen in GBM grade IV samples (n=77) compared to normal brain tissue (n=23) in an earlier study (Wang et al 2008), however Dixit et al found elevated SIRT1 protein in human GBM tumour tissue compared to surrounding normal tissue (Dixit et al 2012), and another study found mice with Sirt1 knocked down had increased survival rates after radiotherapy (Chang et al 2009).

Results in this study showed that in the murine glioma cell line, GL261, levels of Sirt1 were increased compared to the normal murine astrocyte, C8D1A however this did not reach significance. Human primary glioma cells taken from patients with glioblastoma tended to show less hSIRT1 compared to the human astrocyte

cell line, SVG, in both Western blotting and intracellular staining. This conflict in SIRT1 level results between glioma and normal cells between species could be because of the general differences between the cell signaling patterns within each cell line, and particularly because the normal cell comparison in the human model is an immortalised cell line. In support of this, one primary glioma cell line, 0906, went into a quiescent phase while in culture, after which it changed to become smaller, faster proliferating cells (personal observation), indicating it had spontaneously immortalised (Gillio-Meina et al 2000). When hSIRT1 levels were analysed in post-immortalised cells, there was an increase compared to pre-immortalised cells, suggesting that immortalised cells have increased SIRT1. This could be important in the context of GBM, for example one study using post-mortem brain tissue taken from fifty patients with GBM uncovered that it was predominantly the small anaplastic cells that were responsible for the proliferative and invasive nature of the disease (Giangaspero & Burger 1983). Additionally, normal astrocytes are capable of dedifferentiating to become mobile, faster proliferating cells (Leavitt et al 1999) and this is thought to be one way glioma is initiated or reestablished after treatment (Maher et al 2001).

However, it is possible that SIRT1 is expressed less in normal brain cells compared to cells from glioblastoma. In support of this, one study which analysed tumours from the World Health Organisation (WHO) Grade I-III reported increased SIRT1 compared to normal brain tissue, however WHO Grade IV (glioblastoma) had comparatively decreased hSIRT1 (Annabi et al 2012), suggesting different roles for hSIRT1 at different stages of the disease. Another study of lung cancer found hSIRT1 activity increased in airway epithelium of smokers but not in non-smokers, yet hSIRT1 activity was significantly decreased in lung adenocarcinoma indicating a protective function for hSIRT1 in an oxidative environment, which was lost after cells were transformed (Beane et al 2012). This may also explain some conflicting research, for example in research for prostate cancer where in one study SIRT1 expression is elevated (Huffman et al 2007) and in another it is reduced (Lapointe et al 2004).

6.1.2 **Unidentified protein bands on Western blots – potential significance**

Several protein bands were seen after immunoblotting for SIRT1. A band at around 75 kDa was seen on human and mouse cells. The faster migrating molecule at

about 75 kDa on the Western blots for primary glioma cells was greater in proportion to FL-SIRT1 than for normal SVG astrocytes. While usually secondary proteins bands on Western blots would be ignored as non-specific protein binding, a truncated SIRT1 species has been listed on the NCBI BioSystems database and is an accepted isoform of hSIRT named SirT1 75 kDa fragment, and so this potential fragment of SIRT1 seen on immunoblots was not ignored in this study.

The roles of these putative SIRT1 forms may be important. For example, TNFα stimulation generates a 75 kDa SIRT1 fragment which moves to the cytoplasm and associates with mitochondria to mitigate apoptosis in osteoarthritic chondrocytes (Oppenheimer et al 2012); caspases cleave SIRT1 and alter location from the nucleus to the cytoplasm in apoptotic HeLa cells (Ohsawa & Miura 2006). A smaller caspase-1 cleaved SIRT1 fragment of around 80 kDa was found in adipose tissue in an inflammatory microenvironment (Chalkiadaki & Guarente 2012a). Additionally, a smaller splice variant of SIRT1, called SIRT1-Δ2/9, at 17 kDa and 34 kDa (suggested to be a dimer of the smaller one) is seen in a range of human normal tissue and human colorectal cancer cell lines, which binds and maintains p53 and opposes the action of FL-SIRT1 (Shah et al 2012). Cathepsin SIRT1 cleavage in endothelial progenitor cells induced premature senescence (Chen et al 2012b). Interestingly, cathepsin B is found elevated in glioblastoma cell lines (Konduri et al 2001) and elevated cathepsin S expression in astrocytomas is linked to tumour progression and poor prognosis for patients with glioblastoma (Flannery et al 2006).

A stress inducible splice variant of SIRT1, SIRT1-Δ8, migrating at 95 kDa is found in human epithelial cells, and in normal mouse tissue including brain (Lynch et al 2010). Yet another SIRT1 isoform formed from NLRP3 inflammasome-activated caspase-1 has been identified in adipocytes at 80 (Chalkiadaki & Guarente 2012a). This variant species, only identified using a carboxy-terminal SIRT1 antibody, was found to be much less stable than FL-Sirt1 and conferred an altered metabolic cell function (Chalkiadaki & Guarente 2012a). It is possible that this is the isoform of SIRT1 seen on the blots here, although with the murine cells, no secondary bands were seen using a carboxy-terminal Sirt1 antibody.

Other possible reasons to see different sizes of SIRT1 proteins on the blot include proteosomal cleavage and degradation of SIRT1, which is reported for SIRT1 (Gao

et al 2011), or SIRT1 mutants arising from DNA mutations in the cancer cells. *SIRT1* is mapped on chromosome 10 (10q21.3) (Mahlknecht & Voelter-Mahlknecht 2009) and 10q is identified as one of the areas in glioblastoma with the most frequent mutations (Inda et al 2003). Polymorphisms have been found in the *SIRT1* gene for several diseases (Figarska et al 2013) (Zheng et al 2012) (Mohtavinejad et al 2015). Polymorphisms in the promoter region could account for different transcripts of SIRT1. For example, the single nucleotide polymorphism rs3758391 T/C, contains a P53 binding site, and the SNP results in nutrient sensitive SIRT1 expression alteration (Naqvi et al 2010).

Verification is needed for the identification of these potential hSIRT1 species, by mass spectrometry.

6.1.3 **SIRT1 activity in untreated glioma and normal astrocytes**

Results from whole cell protein extraction and Western blot experiments did not show clearly if SIRT1 expression levels were increased or reduced for glioma cells compared to normal astrocytes. To investigate further, the focus was turned toward SIRT1 activity rather than expression, which is not necessarily related to levels of protein. SIRT1 is a stress response molecule, and activity of SIRT1 changes according to the local microenvironment.

Histone 4 is a major substrate for SIRT1 in the nucleus, where deacetylation of lysine 16 (H4K16) on this histone residue is common and quite specific for SIRT1 (Imai et al 2000). Deacetylation of this residue has linked life span extension, metabolism and genomic silencing to the activity of SIRT1 (Imai et al 2000). Furthermore hypoacetylation of H4K16 has been observed in a number of human cancers (Fraga et al 2005), and HDAC inhibitors have been investigated in the treatment of a number of cancers, including glioblastoma (Egler et al 2008).

Investigating H4K16-ac was performed using histone extraction and Western blotting. As SIRT1 deacetylates this substrate, *decreased* acetylation indicates more SIRT1 activity. Our results showed that in murine cells, GL261 cells had consistently higher H4K16-ac compared to the normal astrocyte C8D1A cell line, however this did not reach significance. On examining the H4K16-ac status in a panel of human primary glioma cell lines and SVG, a variable acetylation status was found for primary cells, some of which showed increased H4K16-ac and

others decreased H4K16-ac compared to SVG cells. H4K16-ac neither correlated to survival nor to hSIRT1 protein levels. However, unexpectedly, H4K16-ac tended to be increased in primary cells with more hSIRT1 protein.

Hypoacetylation of H4K16 has been found in many cancers, including neuroblastoma, and hypoacetylation on this residue accumulates in the tumourigenic process (Fraga et al 2005), yet this was not found in analysis of these cells. Again, it could be because the comparison normal astrocyte, SVG is an immortalised cell line and may not have H4K16 acetylation patterns in the same way as the primary astrocytes in normal brain tissue.

Additionally, other members of Class III HDACs including SIRT2 and SIRT3 are also known to deacetylate H4K16 (Vaquero et al 2007), and so it cannot be concluded that the changes in histone acetylation were solely due to SIRT1 activity.

6.1.4 **SIRT1 localisation is aberrant in glioma cells**

Analysis of immunofluorescent microscopy and imaging revealed SIRT1 was located predominantly in the nucleus for both murine and human normal astrocyte cell lines, but for the murine glioma cell line and every human primary glioma cell tested, SIRT1 was found both in the cytoplasm as well as in the nucleus. This result was compelling, due to the fact that both species had the same result and also because both C8D1A and GL261 in the murine model are immortalised cell lines, while only SVG in the human model is an immortalised cell line, suggesting aberrant localisation is more likely to be a facet of glioma cell phenotype rather than because cells are immortalised.

Results for nuclear/cytoplasmic extractions and immunoblotting for SIRT1 were less convincing with immunoblots showing SIRT1 predominantly in the cytoplasmic compartment for all cells, even with reasonably pure compartmental fractionation. A novel technique was tried, using a mild cross-linking process before fractionation and Western blotting. Using this technique, SIRT1 was found in a localisation pattern for glioma and normal astrocytes in both mouse and human that agreed with the IF images. However, using controls for loading and purity of compartmental separation presented difficulties.

Other research shows SIRT1 can change localisation in a dynamic process.

SIRT1 has both nuclear localisation and export signals, and there are both nuclear and cytoplasmic localisation patterns for SIRT1 in normal cells and tissue (Tanno et al 2007). Whether SIRT moved location during the extraction process, or there was a differential SIRT1 stabilisation between nuclear and cytoplasmic compartments, with differences between the glioma and normal cells could be assessed in future studies.

During the course of this research aberrant cytoplasmic SIRT1 was reported for several other cancers (Byles et al 2010), but this is the first time, to my knowledge that it is reported for glioblastoma.

SIRT1 is found in the nucleus in most cells of the nervous system that have been studied so far (Zakhary et al 2010), but can be found predominantly in the cytoplasm in some subsets of neurons, in relation to differentiation signals or affecting neurite outgrowth (Sugino et al 2010). Given that dedifferentiation and invasion are central elements of GBM, cytoplasmic SIRT1 in glioma cells needs further exploration.

6.2 SIRT1 in relation to proliferation of glioma cells compared to normal astrocytes

6.2.1 SIRT1 levels and activity in normal and glioma cells in relation to cell proliferation

Knockdown of SIRT1 delayed mitotic entry, enhanced apoptosis and decreased proliferation in glioma cell lines (Qu et al 2012), however the role SIRT1 takes in primary glioma cells could be different to the role it takes in established cell lines. No study showing the involvement of SIRT1 in the proliferation of primary glioma cells could be found.

In this study, the MTT reduction assay was used to assess cell proliferation. MTT reduction measures the metabolic state of the cells over a two-hour period. For cells in a culture dish this measures the additive metabolic activity for all the cells in the dish. So when measured at one time point and then another time point, and the difference between the two is calculated, the result reflects the change in number

of cells in the dish. I tested cells for this difference at different seeding levels to find out if confluency of cells altered the calculation for proliferation, and it did not (results not shown).

The murine glioma and normal astrocyte were used along with human SVG compared to the primary glioma cells.

6.2.2 Comparing FL-SIRT1 levels and H4K16-ac in relation to proliferation rates in glioma and astrocyte cell lines

Analysis of MTT results for C8D1A and GL261 showed that the glioma cells had a significantly increased proliferation rate compared to the normal cell line, and an increase in Sirt1 levels which did not reach significance, however. When the analysis was made for human primary cells, there was also a trend for increased hSIRT1 levels in relation to increased proliferation which also did not reach significance. The SVG and four primary cells tested for hSIRT1 levels against proliferation showed that hSIRT1 levels did reflect the different proliferation rates of the cells. Taken together, these results suggested that FL-SIRT is linked to increased proliferation in these cells. In support of this, immortalised 0906 cells showed a significantly higher proliferation rate compared to pre-immortalised cells, with a corresponding increase in hSIRT1.

On investigation into cell proliferation in relation to H4K16-ac results showed that in murine cells there was a significant increase in proliferation rates between normal and glioma cell lines, that was reflected by increased acetylation of H4K16 between the two cell lines (non-significant however). In the human cells, a panel of glioma cells showed that there was relationship between increased H4K16-ac and greater cell proliferation agreeing with the murine data. Taken together, these results suggested less SIRT1 activity on H4K16 with increased proliferation, but more SIRT1 activity on this residue with increased metabolic rates.

6.2.3 SIRT1 inhibition and activation effects for glioma and normal cells in relation to cell proliferation

Nicotinamide (NAM) and resveratrol (RES) were used for SIRT1 inhibition and activation respectively.

Treatment with NAM decreased proliferation in all cells tested, and importantly, there was a different response to treatment between glioma and normal cells. The effect of NAM on proliferation was more statistically significant for GL261 cells compared to C8D1A cells. However, the effect of NAM showed a difference that had a greater negative value, indicating a stronger inhibitory effect. This highlights difficulties in working with the MTT assay as a measure of proliferation. NAM treatment was more effective to decrease the proliferation of human cancer cells compared to normal cells also, and no results were negative. This suggested again, that there was a role of SIRT1 in cancer cell proliferation in GBM. When 18 primary human gliomas were analysed for cell proliferation with and without NAM, there was a significant effect of NAM to decreased proliferation in all these cells measured together. A study with normal and cancer epithelial cells found siRNA silencing of SIRT1 did not affect normal cells but in cancer cells, proliferation is arrested and apoptosis is enhanced (Ford et al 2005). The Ford *et al* SIRT1 knock-down study also suggests that cancer cells may be more vulnerable to SIRT1 knock-down compared to normal cells. NAM is known to have many other cellular effects besides SIRT1 inhibition. NAM is also anti-inflammatory and has antioxidant effects (Lappas & Permezel 2011) (Godin et al 2011). NAM also inhibits Poly (ADP ribose) polymerase (PARP) involved in DNA repair and affects other sirtuins (Avalos et al 2005, Clark et al 1971).

RES treatment increased cell proliferation for GL261 murine glioma cells, and also for the human primary cells 0713 and 0906 (pre-immortalisation), reinforcing the likelihood of SIRT1 involvement to increase cell proliferation in these cells, with a differential between normal and glioma cells.

In contrast to that result, in SVG and 0906 cells post immortalisation, RES decreased proliferation. These different and unexpected responses indicated that these cells may have different cell signaling pathways for hSIRT1 compared to the primary cells pre-immortalisation. Additionally, RES at low concentration decreased proliferation in murine cells, which may reflect a toxic effect of ethanol, the vehicle for RES seen in other cells, but this is not likely given the result for SVG cells where ethanol showed the least toxic effect, and even at 50 μM RES, SVG cells showed significance in decreased proliferation. Alternatively, it may indicate non-SIRT1 cellular effects, which are concentration dependent. It has been seen before that RES has different cellular effects depending on duration and dosage

(Peltz et al 2012), and it has other cellular effects besides SIRT1 activation. In fact, specific activation of SIRT1 by RES is widely disputed (Pacholec et al 2010). Some believe that activation of SIRT1 by RES is an *in vitro* artifact (Kaeberlein et al 2005, Pacholec et al 2010), others think that RES works by activating non-SIRT1 targets. In particular, RES activates AMP activated Kinase (AMPK) (Dasgupta & Milbrandt 2007) which inhibits phosphodiesterases (PDEs), ATPase or complex III in the electron transport chain, and ultimately activates SIRT1 downstream by elevating levels of SIRT1 co-substrate NAD+ (Canto & Auwerx 2009). However, dose dependent RES treatment has been seen to stimulate AMPK and improve mitochondrial function, which is SIRT1 dependent (Price et al 2012).

However there are some studies to show RES is activating SIRT1 specifically in increased proliferation (Rathbone et al 2009).

Studies using SIRT1 knock-down or over-expression, or using other inhibitors for example sirtinol or EX-527 and activators like SRT1720 (Solomon et al 2006) may help elucidate the role of SIRT1 in glioma and normal cells.

Additionally, using different measures for cell proliferation, for example 5-bromo-2'-deoxyuridine (BrdU) incorporation or trypan blue exclusion assay to verify these results is needed.

6.2.4 **Protein changes for SIRT1 after treatment with resveratrol or nicotinamide**

Normal and glioma cells were treated with NAM or RES to check for changes to SIRT1 protein. Results showed that in C8D1A there was an increase in Sirt1 protein levels after RES treatment at the higher concentrations used (25 and 50 μM), but no increase was seen GL261, SVG nor 0906 primary cells. Other studies have shown increased SIRT1 expression levels (Rathbone et al 2009) (Morita et al 2012). This result needs repeating.

More convincing though was an unexpected second band for SIRT1 in blots for normal cells in both mouse and human cells after 50 μM RES. This was not seen for the cancer cells. It is possible that change in SIRT1 protein under RES treatment is responsible for different cellular responses. This also highlights a possible difference in stabilisation of SIRT1 between cancer and normal cells.

SIRT1 phosphorylation is shown to alter stability of this protein and the functional changes on SIRT1 due to phosphorylation are unknown in GBM. However, JNK2 phosphorylation of serine 27 on SIRT1 confers protein stability in a panel of cancer cell lines (omitting glioblastoma), where it was almost undetectable in normal cell lines (Ford et al 2008). Previous studies have identified phosphorylation of SIRT1 and not changes to mRNA levels are responsible for changes in SIRT1 levels (Ford et al 2008), to sustain cell proliferation (Sasaki et al 2008), and to alter SIRT1 localisation and activity (Nasrin et al 2009). JNK signaling is over activated in GBM (Bubici & Papa 2014), and it may be an informative next step to identify any SIRT1 phosphorylation differences between normal and glioma cells.

NAM treatment did not show any alteration for SIRT1 levels for any of the cells tested.

6.3 SIRT1 in glioma and normal cells under oxidative stress

Results in this research showed that resistance to H_2O_2 was greater for glioma cells both with murine GL261 and human primary glioma cells compared to the normal astrocyte cell lines. This result was not unexpected, as normal cells are often less resistant to oxidative stress compared to cancer cells as cancer cells have increased anti-oxidant mechanisms (Oberley & Oberley 1997). Other possible signaling pathways that could be different between glioma and normal cells to give cancer cells more resistance could involve P53 mutations which are common in GBM (Reifenberger et al 1996) (Gross et al 2005). In a study using glioma cell lines, knock-down of p53 reduced H_2O_2-induced cell death (Datta et al 2002). SIRT1 regulates the expression of p53 and confers resistance under oxidative stress (Luo et al 2001), so at least in p53+ cells, SIRT1 can keep cells resistant to oxidative stress.

6.3.1 SIRT1 inhibition and activation effects in glioma and normal cells under oxidative stress

To assess what effects SIRT1 activity has in response to H_2O_2 – induced oxidative stress, nicotinamide (NAM) and resveratrol (RES) were used for SIRT1 inhibition and activation in glioma and normal astrocyte cell cultures exposed to H_2O_2 – induced oxidative stress.

6.3.2 SIRT1 protein changes under oxidative stress

Under oxidative stress conditions, SIRT1 levels appeared to increase after exposure to non-lethal concentrations of H_2O_2 in murine normal and glioma cells, but this was decreased after exposure to a lethal concentration of H_2O_2. Glioma cells had a greater decrease in hSIRT1 after the lethal H_2O_2 treatment in both murine and human cell lines compared to the normal cells. This was unexpected as human and mouse normal cells were less resistant to oxidative stress compared to the glioma cells. This suggests SIRT1 may not be responsible for the resistance to oxidative stress in glioma cells. However, if further studies verify SIRT1 does confer resistance it would lead to questions about protein stability of SIRT1 between glioma and normal cells.

A clear second protein band was observed on a Western blot for normal cells in both the murine and human cells after oxidative stress, but was absent in the glioma cells. This qualitative difference in the normal astrocytes under oxidative stress is reported here for the first time and offers another difference between the cancer and non-cancer cells that may be worth exploring further. The band sizes show that in SVG cells this potential hSIRT1 fragment was around 68-75 kDa, while it appeared around 80-90 kDa for the C8D1A cells. This faster migrating protein seen after oxidative stress may have been a product of proteosomal cleavage or it could be a product of cleavage to create another form of SIRT1 with specific functions under these conditions as discussed earlier.

6.3.3 SIRT1 inhibition and activation in relation to glioma and normal cells under oxidative stress

To investigate the role of SIRT1 in the oxidative stress response, a SIRT1 inhibitor, nicotinamide (NAM) and SIRT1 activator, resveratrol (RES) were used in conjunction with H_2O_2-induced oxidative stress.

On analysis of SIRT1 inhibition and activation under oxidative stress it was found that after 20 hr H_2O_2-induced oxidative stress, NAM rescued normal cells but not glioma cells from lethal concentrations in both murine and human cells, and RES increased cell death at sub-lethal concentrations of H_2O_2. The opposing outcomes for these treatments suggest SIRT1 involvement in the response to oxidative stress in these cells, and also show a difference in this response between glioma and

normal cells, where NAM rescues normal cells but not glioma cells from prolonged lethal oxidative stress.

Explaining a potential mechanism for the rescue for SIRT1 inhibition, involves SIRT1 activating a cell death pathway at this level of stress. Cell death could occur via the nuclear factor kappa-light-chain-enhancer of B cells (NFκB) pathway. Aberrant NFκB activation is thought to play an important part in gliomagenesis (Korkolopoulou et al 2008) (Bhat et al 2013) through aberrant signaling rather than inflammatory responses (Vineshkumar et al 2014). In particular, increased p65/RelA subunit of NFκB correlates with higher grade glioma, and primary cultures derived from GBMs show constitutively activated NFκB with increased nuclear localisation of p65/RelA compared to normal astrocytes (Robe et al 2004). Typically, the p65/RelA subunit functions to promote the anti-apoptotic response, however it is found to activate pro-apoptotic genes also (Kucharczak et al 2003). In addition to this, under some cytotoxic conditions, this subunit can repress another set of genes that are anti-apoptotic, like Bcl-xL resulting in a p65/RelA association with histone deacetylase HDAC1 and resulting in cell death (Campbell et al 2004). SIRT1 has been shown to regulate NFκB through deacetylation of p65/RelA and can augment the apoptotic response (Yeung et al 2004). There is also other ways that p65/RelA can actively promote cell death, where the tumour suppressor, alternative reading frame (ARF) initiates phosphorylation of p65/RelA, creating an HDAC1 docking site and sensitising cells to TNFα induced cell death (Rocha et al 2005). Moreover, this atypical p65/RelA response, when activated, was found to be dominant over the more normal anti-apoptotic NFκB response. Next steps to find this out could be assessing the way the cells are dying (by apoptosis or necrosis), levels under different conditions, and assessing using inhibition and activation of SIRT1 on acetylation of p65/RelA.

It remains possible, that the effects for both NAM and RES are not specific to SIRT1 activity in this rescue effect. This needs to be tested.

6.3.4 **Localisation changes for SIRT1 under oxidative stress**

Immunoblotting for H4K16-ac revealed that NAM treatment increased H4K16-ac in normal cells after two-hour H_2O_2 treatment but reduced H4K16-ac for glioma cells.

This suggested a different action for SIRT1 in glioma cell response to oxidative stress at an early time point compared to normal astrocytes.

Results in this thesis also showed murine glioma cells were rescued from a lethal dose of H_2O_2 at an earlier time point (6.5 hours), and these same cells, if grown in less serum were rescued even at the later time point, after a lower concentration of NAM treatment. Nuclear /cytoplasmic extraction and immunoblot experiments indicate that at an earlier time point, H_2O_2 treatment increased nuclear sirt1 in murine glioma cells, but increased cytoplasmic Sirt1 in normal astrocytes, agreeing with the H4K16-ac changes. Follow up nuclear/cytoplasmic experiments agreed with murine results where after oxidative stress for a short duration, potentially truncated isoforms of hSIRT1 had increased in the cytoplasm of a human primary cell line, and conversely, increased in the nucleus of human normal astrocyte cells.

Nuclear/cytoplasmic extractions suggested decreased Sirt1 in the cytoplasm after NAM treatment in murine cells, but data were unclear from blots for nuclear compartments. After immunofluorescent imaging analysis of human primary glioma cells, after NAM treatment at the earlier time point hSIRT1 was confirmed to be increased in the nuclear compartment.

Taken together, SIRT1 has different responses to oxidative environments and NAM treatment after different durations of exposure. These different responses could involve changes in localisation and different isoforms of SIRT1. Changes in localisation of SIRT1 after NAM treatment could explain the results seen where there was a rescue from a lethal concentration of H_2O_2 in GL261 cells at an early time point, and when a low concentration of NAM was used. One postulation is that aberrant cytoplasmic SIRT1 moves to the nucleus after NAM treatment, and prevents the action of NAM inhibiting cytoplasmic SIRT1 from promoting a cell death pathway as in the normal cell response. However, this treatment takes some time to affect the localisation changes, and a low concentration of NAM was not sufficient to induce SIRT1 to change localisation.

6.3.5 **SIRT1 associates with mitochondria in normal astrocyte cells**

Results in this study showed SIRT1 increased in the cytoplasm in the normal astrocyte cell response to a short exposure to oxidative stress, and that after oxidative stress in normal but not glioma cells, a new protein band was seen on blots for both human and mouse cells. In a recent study, cathepsin cleavage of SIRT1 due to increased tumour necrosis factor alpha (TNFα) in chondrocytes results in a stable but enzymatically inactive 75 kDa SIRT1 fragment incapable of binding chromatin that is exported to the cytoplasm where it associates with mitochondria to mitigate apoptosis (Dvir-Ginzberg et al 2011) (Oppenheimer et al 2012). From this it was postulated that normal astrocytes have a similar response under oxidative stress, where relocalisation of this smaller fragment of SIRT1 moves to mitochondria.

Mitochondrial membrane potential and mitochondrial content were measured in normal murine astrocytes, using MitoTracker® red and green FM respectively (MTR and MTG). NAM treatment made no difference to membrane potential changes after peroxide-induced stress, however at the lethal dose, NAM treatment reduced mitochondrial mass significantly. Additionally, after fixation and staining SVG normal human astrocytes for hSIRT1 analysis of IF photographs showed that after a short duration of oxidative stress, an increased level of cytoplasmic hSIRT1 was observed, which was co-localised with mitochondria. In addition, we observed that after H_2O_2 treatment, mitochondria morphology appeared to change from long filaments to more punctate structures.

In an ishemic/reperfusion study inducing oxidative stress in rat cardiomyocytes, treatment with antioxidant curcumin attenuated the oxidative damage to mitichondria and stabilised mitochondral membrane potential through activation of SIRT1 (Yang et al 2013). There are numerous other studies showing SIRT1 effects on mitochondria, although none were found at the time of writing this thesis that associated morphological changes of mitochondria associating with SIRT1 action. However, it has been shown that morphological changes to mitochondria affect cell apoptosis (Lee et al 2004). The function for SIRT1 at mitochondria in astroocytes under oxidative stress warrants further investigation, and could be important to understanding disease other than glioblastoma, for example neurodegenerative diseases which have chronic increased oxidative environments.

6.4 Potential therapeutic value of nicotinamide

NAM treatment in conjunction with lethal oxidative stress rescued normal cells, but glioma cells died. Perhaps this could be of therapeutic interest, in particular for potentially protecting normal cells when patients undergo chemo- and radiation treatments, which create oxidative environments.

In addition, NAM treatment may inhibit proliferation in fast proliferating cells that are responsible for migration and tumour recurrence.

RES treatment has been widely observed to have an increased toxic effect on cancer compared to normal cells, including for glioma cells (Figueiro et al 2013) (Jiang et al 2009). However, there are unresolved problems associated with treating patients with RES that include bioavailability (it gets broken down in the liver) and toxicity (Tome-Carneiro et al 2013). NAM, like RES is a natural product (the water soluble form of vitamin B3), but has good bioavailability and is well tolerated until very high doses are used (Sibtain et al 2002), and there have been some promising results using NAM in the treatment for bladder cancer (Hoskin et al 1997) and head and neck cancer (Saunders et al 1997).

6.5 Conclusions and future directions

Glioblastoma is a complex disease, and SIRT1 is a ubiquitous molecule involved in many different cell-signaling responses responding differently under changing conditions, changing response according to length of exposure to conditions, and this will not be the same for different cell types. Unraveling the details of SIRT1 in glioblastoma will take time. This research represents a preliminary investigation into the potential role of SIRT1 in this disease.

Many results were obtained by one or few experimental repeats, or with too few samples, and need verifying. This was often because the experimental repeats failed. In particular extractions for nuclear and cytoplasmic compartments and Western blotting for SIRT1 were difficult, and single experiments only were performed with some controls lost. Also, repeating human or mouse model verification experiments were often omitted. This was sometimes because the importance of the result was not discovered until later, for example SIRT1 responses of between two and six hours are different to the responses at one day.

However, there were some significant results in this research which give good directions for research in the future which are listed here:

1. Aberrant cytoplasmic SIRT1 in glioma cells. Investigating the activity of SIRT1 in the cytoplasm, and whether it confers an altered response to cell proliferation, or a change in oxidative stress resistance or response is important to the understanding of the role of SIRT1 in this disease.
2. NAM treatment inhibits proliferation in glioma cells more effectively than for normal cells, even for immortalised normal astrocytes, indicating a significant difference in cell signalling that could be useful in treatment development. Elucidating the role of SIRT1 in this response using knock-down, other inhibitors or overexpression studies is needed.
3. NAM treatment rescues normal but not glioma cells under lethal oxidative stress. This also could be of use therapeutically, and the function for SIRT1 in this response needs clarification.
4. Modified forms of SIRT1 with altered mass could play a part in the differential responses for glioma and normal astrocytes. Identification and characterisation these potential isoforms by mass spectrometry, and where and under what conditions they occur needs exploration.

Part 7: References

Abdelmohsen K, Pullmann R, Jr., Lal A, Kim HH, Galban S, et al. 2007. Phosphorylation of HuR by Chk2 regulates SIRT1 expression. *Mol Cell* 25: 543-57

Al-Bahrani R, Tuertcher D, Zailaie S, Abuetabh Y, Nagamori S, et al. 2015. Differential SIRT1 expression in hepatocellular carcinomas and cholangiocarcinoma of the liver. *Annals of clinical and laboratory science* 45: 3-9

Alcendor RR, Gao S, Zhai P, Zablocki D, Holle E, et al. 2007. Sirt1 regulates aging and resistance to oxidative stress in the heart. *Circ Res* 100: 1512-21

Allen BK, Stathias V, Maloof ME, Vidovic D, Winterbottom EF, et al. 2015. Epigenetic pathways and glioblastoma treatment: insights from signaling cascades. *J Cell Biochem* 116: 351-63

Allen RG, Tresini M. 2000. Oxidative stress and gene regulation. *Free Radic Biol Med* 28: 463-99

Andrews NC, Faller DV. 1991. A rapid micropreparation technique for extraction of DNA-binding proteins from limiting numbers of mammalian cells. *Nucleic Acids Res* 19: 2499

Annabi B, Lord-Dufour S, Vezina A, Beliveau R. 2012. Resveratrol Targeting of Carcinogen-Induced Brain Endothelial Cell Inflammation Biomarkers MMP-9 and COX-2 is Sirt1-Independent. *Drug Target Insights* 6: 1-11

Avalos JL, Bever KM, Wolberger C. 2005. Mechanism of sirtuin inhibition by nicotinamide: altering the NAD(+) cosubstrate specificity of a Sir2 enzyme. *Mol Cell* 17: 855-68

Bartkova J, Hamerlik P, Stockhausen MT, Ehrmann J, Hlobilkova A, et al. 2010. Replication stress and oxidative damage contribute to aberrant constitutive activation of DNA damage signalling in human gliomas. *Oncogene* 29: 5095-102

Beane J, Cheng L, Soldi R, Zhang X, Liu G, et al. 2012. SIRT1 Pathway Dysregulation in the Smoke-Exposed Airway Epithelium and Lung Tumor Tissue. *Cancer Res* 72: 5702-11

Beckner ME, Chen X, An J, Day BW, Pollack IF. 2005. Proteomic characterization of harvested pseudopodia with differential gel electrophoresis and specific antibodies. *Lab Invest* 85: 316-27

Berenguer M, Martinez L, Giorgetti-Peraldi S, Le Marchand-Brustel Y, Govers R. 2010. A serum factor induces insulin-independent translocation of GLUT4 to the cell surface which is maintained in insulin resistance. *PLoS One* 5: e15560

Berridge MV, Tan AS. 1993. Characterization of the cellular reduction of 3-(4,5-dimethylthiazol-2-yl)-2,5-diphenyltetrazolium bromide (MTT): subcellular localization, substrate dependence, and involvement of mitochondrial electron transport in MTT reduction. *Arch Biochem Biophys* 303: 474-82

Bhat KP, Balasubramaniyan V, Vaillant B, Ezhilarasan R, Hummelink K, et al. 2013. Mesenchymal differentiation mediated by NF-kappaB promotes radiation resistance in glioblastoma. *Cancer cell* 24: 331-46

Bitterman KJ, Anderson RM, Cohen HY, Latorre-Esteves M, Sinclair DA. 2002. Inhibition of silencing and accelerated aging by nicotinamide, a putative negative regulator of yeast sir2 and human SIRT1. *J Biol Chem* 277: 45099-107

Blander G, Guarente L. 2004. The Sir2 family of protein deacetylases. *Annual review of biochemistry* 73: 417-35

Borra MT, Langer MR, Slama JT, Denu JM. 2004. Substrate specificity and kinetic mechanism of the Sir2 family of NAD+-dependent histone/protein deacetylases. *Biochemistry* 43: 9877-87

Bradbury C, Khanim F, Hayden R, Bunce CM, White DA, et al. 2005. Histone deacetylases in acute myeloid leukaemia show a distinctive pattern of expression that changes selectively in response to deacetylase inhibitors. *Leukemia* 19: 1751-59

Bresgen N, Jaksch H, Bauer HC, Eckl P, Krizbai I, Tempfer H. 2006. Astrocytes are more resistant than cerebral endothelial cells toward geno- and cytotoxicity mediated by short-term oxidative stress. *J Neurosci Res* 84: 1821-8
Broadley K, Larsen L, Herst PM, Smith RA, Berridge MV, McConnell MJ. 2011a. The novel phloroglucinol PMT7 kills glycolytic cancer cells by blocking autophagy and sensitizing to nutrient stress. *J Cell Biochem* 112: 1869-79
Broadley KW, Hunn MK, Farrand KJ, Price KM, Grasso C, et al. 2011b. Side population is not necessary or sufficient for a cancer stem cell phenotype in glioblastoma multiforme. *Stem cells* 29: 452-61
Brooks CL, Gu W. 2009. How does SIRT1 affect metabolism, senescence and cancer? *Nat Rev Cancer* 9: 123-8
Brown NS, Bicknell R. 2001. Hypoxia and oxidative stress in breast cancer. Oxidative stress: its effects on the growth, metastatic potential and response to therapy of breast cancer. *Breast Cancer Res* 3: 323-7
Brunet A, Sweeney LB, Sturgill JF, Chua KF, Greer PL, et al. 2004. Stress-dependent regulation of FOXO transcription factors by the SIRT1 deacetylase. *Science* 303: 2011-5
Bubici C, Papa S. 2014. JNK signalling in cancer: in need of new, smarter therapeutic targets. *Br J Pharmacol* 171: 24-37
Byles V, Chmilewski LK, Wang J, Zhu L, Forman LW, et al. 2010. Aberrant cytoplasm localization and protein stability of SIRT1 is regulated by PI3K/IGF-1R signaling in human cancer cells. *International journal of biological sciences* 6: 599-612
Caito S, Rajendrasozhan S, Cook S, Chung S, Yao H, et al. 2010. SIRT1 is a redox-sensitive deacetylase that is post-translationally modified by oxidants and carbonyl stress. *FASEB J* 24: 3145-59
Campbell KJ, Rocha S, Perkins ND. 2004. Active repression of antiapoptotic gene expression by RelA(p65) NF-kappa B. *Mol Cell* 13: 853-65
Canto C, Auwerx J. 2009. PGC-1alpha, SIRT1 and AMPK, an energy sensing network that controls energy expenditure. *Curr Opin Lipidol* 20: 98-105
Cao YW, Li YC, Wan GX, Du XM, Li F. 2015. Clinicopathological and prognostic role of SIRT1 in breast cancer patients: a meta-analysis. *International journal of clinical and experimental medicine* 8: 616-24
Carafa V, Nebbioso A, Altucci L. 2012. Sirtuins and disease: the road ahead. *Frontiers in pharmacology* 3: 4
Chalkiadaki A, Guarente L. 2012a. High-Fat Diet Triggers Inflammation-Induced Cleavage of SIRT1 in Adipose Tissue To Promote Metabolic Dysfunction. *Cell Metab* 16: 180-8
Chalkiadaki A, Guarente L. 2012b. Sirtuins mediate mammalian metabolic responses to nutrient availability. *Nat Rev Endocrinol* 8: 287-96
Chang CJ, Hsu CC, Yung MC, Chen KY, Tzao C, et al. 2009. Enhanced radiosensitivity and radiation-induced apoptosis in glioma CD133-positive cells by knockdown of SirT1 expression. *Biochem Biophys Res Commun* 380: 236-42
Chen J, Li Y, Yu TS, McKay RM, Burns DK, et al. 2012a. A restricted cell population propagates glioblastoma growth after chemotherapy. *Nature* 488: 522-6
Chen J, Xavier S, Moskowitz-Kassai E, Chen R, Lu CY, et al. 2012b. Cathepsin cleavage of sirtuin 1 in endothelial progenitor cells mediates stress-induced premature senescence. *Am J Pathol* 180: 973-83
Cheng Y, Takeuchi H, Sonobe Y, Jin S, Wang Y, et al. 2014. Sirtuin 1 attenuates oxidative stress via upregulation of superoxide dismutase 2 and catalase in astrocytes. *Journal of neuroimmunology* 269: 38-43
Clark JB, Ferris GM, Pinder S. 1971. Inhibition of nuclear NAD nucleosidase and poly ADP-ribose polymerase activity from rat liver by nicotinamide and 5'-methyl nicotinamide. *Biochim Biophys Acta* 238: 82-5
Clarke J, Penas C, Pastori C, Komotar RJ, Bregy A, et al. 2013. Epigenetic pathways and glioblastoma treatment. *Epigenetics* 8: 785-95

Cohen HY, Miller C, Bitterman KJ, Wall NR, Hekking B, et al. 2004. Calorie restriction promotes mammalian cell survival by inducing the SIRT1 deacetylase. *Science* 305: 390-2
Dasgupta B, Milbrandt J. 2007. Resveratrol stimulates AMP kinase activity in neurons. *Proc Natl Acad Sci U S A* 104: 7217-22
Datta K, Babbar P, Srivastava T, Sinha S, Chattopadhyay P. 2002. p53 dependent apoptosis in glioma cell lines in response to hydrogen peroxide induced oxidative stress. *The international journal of biochemistry & cell biology* 34: 148-57
Dennery PA. 2007. Effects of oxidative stress on embryonic development. *Birth Defects Res C Embryo Today* 81: 155-62
Dion MF, Altschuler SJ, Wu LF, Rando OJ. 2005. Genomic characterization reveals a simple histone H4 acetylation code. *Proceedings of the National Academy of Sciences of the United States of America* 102: 5501-06
Dixit D, Sharma V, Ghosh S, Mehta VS, Sen E. 2012. Inhibition of Casein kinase-2 induces p53-dependent cell cycle arrest and sensitizes glioblastoma cells to tumor necrosis factor (TNFalpha)-induced apoptosis through SIRT1 inhibition. *Cell Death Dis* 3: e271
Dreyfuss JM, Johnson MD, Park PJ. 2009. Meta-analysis of glioblastoma multiforme versus anaplastic astrocytoma identifies robust gene markers. *Mol Cancer* 8: 71
Dubrow R, Darefsky AS, Jacobs DI, Park LS, Rose MG, et al. 2013. Time trends in glioblastoma multiforme survival: the role of temozolomide. *Neuro Oncol* 15: 1750-61
Dunn GP, Rinne ML, Wykosky J, Genovese G, Quayle SN, et al. 2012. Emerging insights into the molecular and cellular basis of glioblastoma. *Genes Dev* 26: 756-84
Dvir-Ginzberg M, Gagarina V, Lee EJ, Booth R, Gabay O, Hall DJ. 2011. Tumor necrosis factor alpha-mediated cleavage and inactivation of SirT1 in human osteoarthritic chondrocytes. *Arthritis Rheum* 63: 2363-73
Egler V, Korur S, Failly M, Boulay JL, Imber R, et al. 2008. Histone deacetylase inhibition and blockade of the glycolytic pathway synergistically induce glioblastoma cell death. *Clin Cancer Res* 14: 3132-40
Fadul CE, Fisher JL, Hampton TH, Lallana EC, Li Z, et al. 2011. Immune response in patients with newly diagnosed glioblastoma multiforme treated with intranodal autologous tumor lysate-dendritic cell vaccination after radiation chemotherapy. *Journal of immunotherapy* 34: 382-9
Faragher RG, Burton DG, Majecha P, Fong NS, Davis T, et al. 2011. Resveratrol, but not dihydroresveratrol, induces premature senescence in primary human fibroblasts. *Age (Dordr)* 33: 555-64
Fassl A, Tagscherer KE, Richter J, Berriel Diaz M, Alcantara Llaguno SR, et al. 2012. Notch1 signaling promotes survival of glioblastoma cells via EGFR-mediated induction of anti-apoptotic Mcl-1. *Oncogene* 31: 4698-708
Figarska SM, Vonk JM, Boezen HM. 2013. SIRT1 polymorphism, long-term survival and glucose tolerance in the general population. *PLoS One* 8: e58636
Figueiro F, Bernardi A, Frozza RL, Terroso T, Zanotto-Filho A, et al. 2013. Resveratrol-loaded lipid-core nanocapsules treatment reduces in vitro and in vivo glioma growth. *J Biomed Nanotechnol* 9: 516-26
Flannery T, McQuaid S, McGoohan C, McConnell RS, McGregor G, et al. 2006. Cathepsin S expression: An independent prognostic factor in glioblastoma tumours--A pilot study. *Int J Cancer* 119: 854-60
Ford J, Ahmed S, Allison S, Jiang M, Milner J. 2008. JNK2-dependent regulation of SIRT1 protein stability. *Cell Cycle* 7: 3091-7
Ford J, Jiang M, Milner J. 2005. Cancer-specific functions of SIRT1 enable human epithelial cancer cell growth and survival. *Cancer Res* 65: 10457-63
Fraga MF, Ballestar E, Villar-Garea A, Boix-Chornet M, Espada J, et al. 2005. Loss of acetylation at Lys16 and trimethylation at Lys20 of histone H4 is a common hallmark of human cancer. *Nat Genet* 37: 391-400

Furnari FB, Fenton T, Bachoo RM, Mukasa A, Stommel JM, et al. 2007. Malignant astrocytic glioma: genetics, biology, and paths to treatment. *Genes Dev* 21: 2683-710
Gao Z, Zhang J, Kheterpal I, Kennedy N, Davis RJ, Ye J. 2011. Sirtuin 1 (SIRT1) protein degradation in response to persistent c-Jun N-terminal kinase 1 (JNK1) activation contributes to hepatic steatosis in obesity. *J Biol Chem* 286: 22227-34
Gardner PJ, Yazid S, Chu CJ, Copland DA, Adamson P, et al. 2015. TNFalpha Regulates SIRT1 Cleavage during Ocular Autoimmune Disease. *Am J Pathol*
Ghosh HS, McBurney M, Robbins PD. 2010. SIRT1 negatively regulates the mammalian target of rapamycin. *PLoS One* 5: e9199
Giammona LM, Panuganti S, Kemper JM, Apostolidis PA, Lindsey S, et al. 2009. Mechanistic studies on the effects of nicotinamide on megakaryocytic polyploidization and the roles of NAD+ levels and SIRT inhibition. *Exp Hematol* 37: 1340-52 e3
Giangaspero F, Burger PC. 1983. Correlations between cytologic composition and biologic behavior in the glioblastoma multiforme. A postmortem study of 50 cases. *Cancer* 52: 2320-33
Gillio-Meina C, Swan CL, Crellin NK, Stocco DM, Chedrese PJ. 2000. Generation of stable cell lines by spontaneous immortalization of primary cultures of porcine granulosa cells. *Molecular reproduction and development* 57: 366-74
Gjedde A. 2007. Coupling of brain function to metabolism: evaluation of energy requirements In *Handbook of Neurochemistry and Molecular Neurobiology*, ed. A Lajtha
Godin AM, Ferreira WC, Rocha LT, Seniuk JG, Paiva AL, et al. 2011. Antinociceptive and anti-inflammatory activities of nicotinamide and its isomers in different experimental models. *Pharmacol Biochem Behav* 99: 782-8
Gough DR, Cotter TG. 2011. Hydrogen peroxide: a Jekyll and Hyde signalling molecule. *Cell Death Dis* 2: e213
Gross MW, Kraus A, Nashwan K, Mennel HD, Engenhart-Cabillic R, Schlegel J. 2005. Expression of p53 and p21 in primary glioblastomas. *Strahlentherapie und Onkologie : Organ der Deutschen Rontgengesellschaft ... [et al]* 181: 164-71
Guo X, Kesimer M, Tolun G, Zheng X, Xu Q, et al. 2012. The NAD(+)-dependent protein deacetylase activity of SIRT1 is regulated by its oligomeric status. *Sci Rep* 2: 640
Haigis MC, Guarente LP. 2006. Mammalian sirtuins--emerging roles in physiology, aging, and calorie restriction. *Genes Dev* 20: 2913-21
Haigis MC, Sinclair DA. 2010. Mammalian sirtuins: biological insights and disease relevance. *Annu Rev Pathol* 5: 253-95
Han L, Zhou R, Niu J, McNutt MA, Wang P, Tong T. 2010. SIRT1 is regulated by a PPAR{gamma}-SIRT1 negative feedback loop associated with senescence. *Nucleic Acids Res* 38: 7458-71
Hariharan N, Maejima Y, Nakae J, Paik J, Depinho RA, Sadoshima J. 2010. Deacetylation of FoxO by Sirt1 Plays an Essential Role in Mediating Starvation-Induced Autophagy in Cardiac Myocytes. *Circ Res* 107: 1470-82
Hasegawa K, Wakino S, Yoshioka K, Tatematsu S, Hara Y, et al. 2008. Sirt1 protects against oxidative stress-induced renal tubular cell apoptosis by the bidirectional regulation of catalase expression. *Biochem Biophys Res Commun* 372: 51-6
Hasegawa K, Yoshikawa K. 2008. Necdin regulates p53 acetylation via Sirtuin1 to modulate DNA damage response in cortical neurons. *J Neurosci* 28: 8772-84
Hendrix ND, Wu R, Kuick R, Schwartz DR, Fearon ER, Cho KR. 2006. Fibroblast growth factor 9 has oncogenic activity and is a downstream target of Wnt signaling in ovarian endometrioid adenocarcinomas. *Cancer Res* 66: 1354-62

Herranz D, Maraver A, Canamero M, Gomez-Lopez G, Inglada-Perez L, et al. 2013. SIRT1 promotes thyroid carcinogenesis driven by PTEN deficiency. *Oncogene* 32: 4052-6
Hida Y, Kubo Y, Murao K, Arase S. 2007. Strong expression of a longevity-related protein, SIRT1, in Bowen's disease. *Archives of dermatological research* 299: 103-6
Hiraga S, Ohnishi T, Izumoto S, Miyahara E, Kanemura Y, et al. 1998. Telomerase activity and alterations in telomere length in human brain tumors. *Cancer Res* 58: 2117-25
Hisahara S, Chiba S, Matsumoto H, Tanno M, Yagi H, et al. 2008. Histone deacetylase SIRT1 modulates neuronal differentiation by its nuclear translocation. *Proc Natl Acad Sci U S A* 105: 15599-604
Hong EH, Lee SJ, Kim JS, Lee KH, Um HD, et al. 2010. Ionizing radiation induces cellular senescence of articular chondrocytes via negative regulation of SIRT1 by p38 kinase. *J Biol Chem* 285: 1283-95
Hori YS, Kuno A, Hosoda R, Horio Y. 2013. Regulation of FOXOs and p53 by SIRT1 modulators under oxidative stress. *PLoS One* 8: e73875
Hoskin PJ, Saunders MI, Phillips H, Cladd H, Powell ME, et al. 1997. Carbogen and nicotinamide in the treatment of bladder cancer with radical radiotherapy. *Br J Cancer* 76: 260-3
Hou J, Chong ZZ, Shang YC, Maiese K. 2010. Early apoptotic vascular signaling is determined by Sirt1 through nuclear shuttling, forkhead trafficking, bad, and mitochondrial caspase activation. *Current neurovascular research* 7: 95-112
Howitz KT, Bitterman KJ, Cohen HY, Lamming DW, Lavu S, et al. 2003. Small molecule activators of sirtuins extend Saccharomyces cerevisiae lifespan. *Nature* 425: 191-6
Huang B, Cheng X, Wang D, Peng M, Xue Z, et al. 2014. Adiponectin promotes pancreatic cancer progression by inhibiting apoptosis via the activation of AMPK/Sirt1/PGC-1alpha signaling. *Oncotarget* 5: 4732-45
Huffman DM, Grizzle WE, Bamman MM, Kim J-s, Eltoum IA, et al. 2007. SIRT1 is significantly elevated in mouse and human prostate cancer. *Cancer Research* 67: 6612-18
Hunn MK, Bauer E, Wood CE, Gasser O, Dzhelali M, et al. 2015. Dendritic cell vaccination combined with temozolomide retreatment: results of a phase I trial in patients with recurrent glioblastoma multiforme. *J Neurooncol* 121: 319-29
Iida T, Furuta A, Kawashima M, Nishida J, Nakabeppu Y, Iwaki T. 2001. Accumulation of 8-oxo-2'-deoxyguanosine and increased expression of hMTH1 protein in brain tumors. *Neuro Oncol* 3: 73-81
Ikenoue T, Inoki K, Zhao B, Guan KL. 2008. PTEN acetylation modulates its interaction with PDZ domain. *Cancer Res* 68: 6908-12
Imai S, Armstrong CM, Kaeberlein M, Guarente L. 2000. Transcriptional silencing and longevity protein Sir2 is an NAD-dependent histone deacetylase. *Nature* 403: 795-800
Inda MM, Fan X, Munoz J, Perot C, Fauvet D, et al. 2003. Chromosomal abnormalities in human glioblastomas: gain in chromosome 7p correlating with loss in chromosome 10q. *Mol Carcinog* 36: 6-14
Jiang H, Shang X, Wu H, Gautam SC, Al-Holou S, et al. 2009. Resveratrol downregulates PI3K/Akt/mTOR signaling pathways in human U251 glioma cells. *J Exp Ther Oncol* 8: 25-33
Jiang Y, Sun Y, Yuan Y. 2012. [Mechanism of temozolomide-induced anti-tumor effects on glioblastoma cells in vitro is via ROS-dependent SIRT1 signaling pathway]. *Zhonghua Zhong Liu Za Zhi* 34: 734-8
Jin Q, Yan T, Ge X, Sun C, Shi X, Zhai Q. 2007. Cytoplasm-localized SIRT1 enhances apoptosis. *J Cell Physiol* 213: 88-97
Kaeberlein M, McDonagh T, Heltweg B, Hixon J, Westman EA, et al. 2005. Substrate-specific activation of sirtuins by resveratrol. *J Biol Chem* 280: 17038-45
Kaeberlein M, McVey M, Guarente L. 1999. The SIR2/3/4 complex and SIR2 alone promote longevity in Saccharomyces cerevisiae by two different mechanisms. *Genes Dev* 13: 2570-80

Kalaria RN, Premkumar DR, Pax AB, Cohen DL, Lieberburg I. 1996. Production and increased detection of amyloid beta protein and amyloidogenic fragments in brain microvessels, meningeal vessels and choroid plexus in Alzheimer's disease. *Brain Res Mol Brain Res* 35: 58-68
Kanfi Y, Peshti V, Gozlan YM, Rathaus M, Gil R, Cohen HY. 2008. Regulation of SIRT1 protein levels by nutrient availability. *FEBS Lett* 582: 2417-23
Keyse SM, Emslie EA. 1992. Oxidative stress and heat shock induce a human gene encoding a protein-tyrosine phosphatase. *Nature* 359: 644-7
Kheirollahi M, Mehrazin M, Kamalian N, Mohammadi-asl J, Mehdipour P. 2013. Telomerase activity in human brain tumors: astrocytoma and meningioma. *Cellular and molecular neurobiology* 33: 569-74
Kim EJ, Kho JH, Kang MR, Um SJ. 2007. Active regulator of SIRT1 cooperates with SIRT1 and facilitates suppression of p53 activity. *Mol Cell* 28: 277-90
Kim JE, Chen J, Lou Z. 2008. DBC1 is a negative regulator of SIRT1. *Nature* 451: 583-6
Klaunig JE, Kamendulis LM. 2004. The role of oxidative stress in carcinogenesis. *Annu Rev Pharmacol Toxicol* 44: 239-67
Konduri S, Lakka SS, Tasiou A, Yanamandra N, Gondi CS, et al. 2001. Elevated levels of cathepsin B in human glioblastoma cell lines. *International journal of oncology* 19: 519-24
Korkolopoulou P, Levidou G, Saetta AA, El-Habr E, Eftichiadis C, et al. 2008. Expression of nuclear factor-kappaB in human astrocytomas: relation to pI kappa Ba, vascular endothelial growth factor, Cox-2, microvascular characteristics, and survival. *Hum Pathol* 39: 1143-52
Krakstad C, Chekenya M. 2010. Survival signalling and apoptosis resistance in glioblastomas: opportunities for targeted therapeutics. *Mol Cancer* 9: 135
Kucharczak J, Simmons MJ, Fan Y, Gelinas C. 2003. To be, or not to be: NF-kappaB is the answer--role of Rel/NF-kappaB in the regulation of apoptosis. *Oncogene* 22: 8961-82
Kume S, Haneda M, Kanasaki K, Sugimoto T, Araki S, et al. 2006. Silent information regulator 2 (SIRT1) attenuates oxidative stress-induced mesangial cell apoptosis via p53 deacetylation. *Free Radic Biol Med* 40: 2175-82
Kurdistani SK, Grunstein M. 2003. Histone acetylation and deacetylation in yeast. *Nature Reviews Molecular Cell Biology* 4: 276-84
Lagouge M, Argmann C, Gerhart-Hines Z, Meziane H, Lerin C, et al. 2006. Resveratrol improves mitochondrial function and protects against metabolic disease by activating SIRT1 and PGC-1alpha. *Cell* 127: 1109-22
Landry J, Slama JT, Sternglanz R. 2000. Role of NAD(+) in the deacetylase activity of the SIR2-like proteins. *Biochem Biophys Res Commun* 278: 685-90
Lapointe J, Li C, Higgins JP, van de Rijn M, Bair E, et al. 2004. Gene expression profiling identifies clinically relevant subtypes of prostate cancer. *Proc Natl Acad Sci U S A* 101: 811-6
Lappas M, Permezel M. 2011. The anti-inflammatory and antioxidative effects of nicotinamide, a vitamin B(3) derivative, are elicited by FoxO3 in human gestational tissues: implications for preterm birth. *J Nutr Biochem* 22: 1195-201
Lau AW, Liu P, Inuzuka H, Gao D. 2014. SIRT1 phosphorylation by AMP-activated protein kinase regulates p53 acetylation. *American journal of cancer research* 4: 245-55
Leavitt BR, Hernit-Grant CS, Macklis JD. 1999. Mature astrocytes transform into transitional radial glia within adult mouse neocortex that supports directed migration of transplanted immature neurons. *Exp Neurol* 157: 43-57
Lee IH, Cao L, Mostoslavsky R, Lombard DB, Liu J, et al. 2008. A role for the NAD-dependent deacetylase Sirt1 in the regulation of autophagy. *Proc Natl Acad Sci U S A* 105: 3374-9
Lee SE, Paques F, Sylvan J, Haber JE. 1999. Role of yeast SIR genes and mating type in directing DNA double-strand breaks to homologous and non-homologous repair paths. *Current biology : CB* 9: 767-70

Lee YJ, Jeong SY, Karbowski M, Smith CL, Youle RJ. 2004. Roles of the mammalian mitochondrial fission and fusion mediators Fis1, Drp1, and Opa1 in apoptosis. *Mol Biol Cell* 15: 5001-11
Li L, Sun Q, Li Y, Yang Y, Yang Y, et al. 2015. Overexpression of SIRT1 Induced by Resveratrol and Inhibitor of miR-204 Suppresses Activation and Proliferation of Microglia. *Journal of molecular neuroscience : MN*
Li L, Yuan L, Luo J, Gao J, Guo J, Xie X. 2012. MiR-34a inhibits proliferation and migration of breast cancer through down-regulation of Bcl-2 and SIRT1. *Clin Exp Med*
Li Y, Backesjo CM, Haldosen LA, Lindgren U. 2009. Resveratrol inhibits proliferation and promotes apoptosis of osteosarcoma cells. *Eur J Pharmacol* 609: 13-8
Libert S, Cohen D, Guarente L. 2008. Neurogenesis directed by Sirt1. *Nat Cell Biol* 10: 373-4
Lim SK, Llaguno SR, McKay RM, Parada LF. 2011. Glioblastoma multiforme: a perspective on recent findings in human cancer and mouse models. *BMB reports* 44: 158-64
Lin JN, Lin VC, Rau KM, Shieh PC, Kuo DH, et al. 2010. Resveratrol modulates tumor cell proliferation and protein translation via SIRT1-dependent AMPK activation. *J Agric Food Chem* 58: 1584-92
Lino MM, Merlo A. 2011. PI3Kinase signaling in glioblastoma. *J Neurooncol* 103: 417-27
Lino MM, Merlo A, Boulay JL. 2010. Notch signaling in glioblastoma: a developmental drug target? *BMC medicine* 8: 72
Liu G, Yuan X, Zeng Z, Tunici P, Ng H, et al. 2006. Analysis of gene expression and chemoresistance of CD133+ cancer stem cells in glioblastoma. *Mol Cancer* 5: 67
Liu TF, Yoza BK, El Gazzar M, Vachharajani VT, McCall CE. 2011. NAD+-dependent SIRT1 deacetylase participates in epigenetic reprogramming during endotoxin tolerance. *J Biol Chem* 286: 9856-64
Liu Y, Dentin R, Chen D, Hedrick S, Ravnskjaer K, et al. 2008. A fasting inducible switch modulates gluconeogenesis via activator/coactivator exchange. *Nature* 456: 269-73
Lou G, Liu Y, Wu S, Xue J, Yang F, et al. 2015. The p53/miR-34a/SIRT1 Positive Feedback Loop in Quercetin-Induced Apoptosis. *Cellular physiology and biochemistry : international journal of experimental cellular physiology, biochemistry, and pharmacology* 35: 2192-202
Louis DN, Ohgaki H, Wiestler OD, Cavenee WK, Burger PC, et al. 2007. The 2007 WHO classification of tumours of the central nervous system. *Acta Neuropathol* 114: 97-109
Lu M, Sarruf DA, Li P, Osborn O, Sanchez-Alavez M, et al. 2013. Neuronal Sirt1 deficiency increases insulin sensitivity in both brain and peripheral tissues. *J Biol Chem* 288: 10722-35
Luo J, Nikolaev AY, Imai S, Chen D, Su F, et al. 2001. Negative control of p53 by Sir2alpha promotes cell survival under stress. *Cell* 107: 137-48
Lynch CJ, Shah ZH, Allison SJ, Ahmed SU, Ford J, et al. 2010. SIRT1 undergoes alternative splicing in a novel auto-regulatory loop with p53. *PLoS One* 5: e13502
Maher EA, Furnari FB, Bachoo RM, Rowitch DH, Louis DN, et al. 2001. Malignant glioma: genetics and biology of a grave matter. *Genes Dev* 15: 1311-33
Mahlknecht U, Voelter-Mahlknecht S. 2009. Chromosomal characterization and localization of the NAD+-dependent histone deacetylase gene sirtuin 1 in the mouse. *Int J Mol Med* 23: 245-52
Mantel CR, Wang RH, Deng C, Broxmeyer HE. 2008. Sirt1, notch and stem cell "age asymmetry". *Cell Cycle* 7: 2821-5
Marmorstein R. 2001. Structure of histone deacetylases: insights into substrate recognition and catalysis. *Structure* 9: 1127-33
Martin SG, Laroche T, Suka N, Grunstein M, Gasser SM. 1999. Relocalization of telomeric Ku and SIR proteins in response to DNA strand breaks in yeast. *Cell* 97: 621-33

Martin V, Herrera F, Garcia-Santos G, Antolin I, Rodriguez-Blanco J, Rodriguez C. 2007. Signaling pathways involved in antioxidant control of glioma cell proliferation. *Free Radic Biol Med* 42: 1715-22
Megee PC, Morgan BA, Smith MM. 1995. Histone H4 and the maintenance of genome integrity. *Genes & Development* 9: 1716-27
Merksamer PI, Liu Y, He W, Hirschey MD, Chen D, Verdin E. 2013. The sirtuins, oxidative stress and aging: an emerging link. *Aging (Albany NY)* 5: 144-50
Mohtavinejad N, Nakhaee A, Harati H, Poodineh J, Afzali M. 2015. SIRT1 gene is associated with cardiovascular disease in the Iranian population. *The Egyptian Journal of Medical Human Genetics*
Morita Y, Wada-Hiraike O, Yano T, Shirane A, Hirano M, et al. 2012. Resveratrol promotes expression of SIRT1 and StAR in rat ovarian granulosa cells: an implicative role of SIRT1 in the ovary. *Reproductive biology and endocrinology : RB&E* 10: 14
Nakane K, Fujita Y, Terazawa R, Atsumi Y, Kato T, et al. 2012. Inhibition of cortactin and SIRT1 expression attenuates migration and invasion of prostate cancer DU145 cells. *International Journal of Urology* 19: 71-79
Nakatani K, Yoshimi N, Mori H, Yoshimura S, Sakai H, et al. 1997. The significant role of telomerase activity in human brain tumors. *Cancer* 80: 471-6
Naqvi A, Hoffman TA, DeRicco J, Kumar A, Kim CS, et al. 2010. A single-nucleotide variation in a p53-binding site affects nutrient-sensitive human SIRT1 expression. *Hum Mol Genet* 19: 4123-33
Narayan RS, Fedrigo CA, Stalpers LJ, Baumert BG, Sminia P. 2013. Targeting the Akt-pathway to improve radiosensitivity in glioblastoma. *Current pharmaceutical design* 19: 951-7
Nasrin N, Kaushik VK, Fortier E, Wall D, Pearson KJ, et al. 2009. JNK1 phosphorylates SIRT1 and promotes its enzymatic activity. *PLoS One* 4: e8414
Newcomb EZ, D. 2009. The Murine GL261 Glioma Experimental Model to Assess Novel Brain Tumor Treatments In *CNS Cancer*, ed. M E, pp. pp 227-41: Humana Press
Nie Y, Erion DM, Yuan Z, Dietrich M, Shulman GI, et al. 2009. STAT3 inhibition of gluconeogenesis is downregulated by SirT1. *Nat Cell Biol* 11: 492-500
North BJ, Verdin E. 2004. Sirtuins: Sir2-related NAD-dependent protein deacetylases. *Genome biology* 5: 224
Oberley TD, Oberley LW. 1997. Antioxidant enzyme levels in cancer. *Histol Histopathol* 12: 525-35
Ohsawa S, Miura M. 2006. Caspase-mediated changes in Sir2alpha during apoptosis. *FEBS Lett* 580: 5875-9
Oppenheimer H, Gabay O, Meir H, Haze A, Kandel L, et al. 2012. 75-kd sirtuin 1 blocks tumor necrosis factor alpha-mediated apoptosis in human osteoarthritic chondrocytes. *Arthritis Rheum* 64: 718-28
Ota H, Eto M, Kano MR, Ogawa S, Iijima K, et al. 2008. Cilostazol inhibits oxidative stress-induced premature senescence via upregulation of Sirt1 in human endothelial cells. *Arteriosclerosis, thrombosis, and vascular biology* 28: 1634-9
Oudard S, Arvelo F, Miccoli L, Apiou F, Dutrillaux AM, et al. 1996. High glycolysis in gliomas despite low hexokinase transcription and activity correlated to chromosome 10 loss. *Br J Cancer* 74: 839-45
Pacholec M, Bleasdale JE, Chrunyk B, Cunningham D, Flynn D, et al. 2010. SRT1720, SRT2183, SRT1460, and resveratrol are not direct activators of SIRT1. *J Biol Chem* 285: 8340-51
Pan M, Yuan H, Brent M, Ding EC, Marmorstein R. 2012. SIRT1 contains N- and C-terminal regions that potentiate deacetylase activity. *J Biol Chem* 287: 2468-76
Park SJ, Lee JH, Kim HY, Choi YH, Park JS, et al. 2012. Astrocytes, but not microglia, rapidly sense H(2)O(2)via STAT6 phosphorylation, resulting in cyclooxygenase-2 expression and prostaglandin release. *J Immunol* 188: 5132-41

Pelicano H, Xu RH, Du M, Feng L, Sasaki R, et al. 2006. Mitochondrial respiration defects in cancer cells cause activation of Akt survival pathway through a redox-mediated mechanism. *J Cell Biol* 175: 913-23
Peltz L, Gomez J, Marquez M, Alencastro F, Atashpanjeh N, et al. 2012. Resveratrol exerts dosage and duration dependent effect on human mesenchymal stem cell development. *PLoS One* 7: e37162
Pillai VB, Sundaresan NR, Gupta MP. 2014. Regulation of Akt signaling by sirtuins: its implication in cardiac hypertrophy and aging. *Circ Res* 114: 368-78
Price NL, Gomes AP, Ling AJ, Duarte FV, Martin-Montalvo A, et al. 2012. SIRT1 is required for AMPK activation and the beneficial effects of resveratrol on mitochondrial function. *Cell Metab* 15: 675-90
Prozorovski T, Schulze-Topphoff U, Glumm R, Baumgart J, Schroter F, et al. 2008. Sirt1 contributes critically to the redox-dependent fate of neural progenitors. *Nat Cell Biol* 10: 385-94
Pruitt K, Zinn RL, Ohm JE, McGarvey KM, Kang SH, et al. 2006. Inhibition of SIRT1 reactivates silenced cancer genes without loss of promoter DNA hypermethylation. *PLoS Genet* 2: e40
Qu Y, Zhang J, Wu S, Li B, Liu S, Cheng J. 2012. SIRT1 promotes proliferation and inhibits apoptosis of human malignant glioma cell lines. *Neurosci Lett* 525: 168-72
Rathbone CR, Booth FW, Lees SJ. 2009. Sirt1 increases skeletal muscle precursor cell proliferation. *European journal of cell biology* 88: 35-44
Rauscher FJ, 3rd. 2005. It is time for a Human Epigenome Project. *Cancer Res* 65: 11229
Raver-Shapira N, Marciano E, Meiri E, Spector Y, Rosenfeld N, et al. 2007. Transcriptional activation of miR-34a contributes to p53-mediated apoptosis. *Mol Cell* 26: 731-43
Reifenberger J, Ring GU, Gies U, Cobbers L, Oberstrass J, et al. 1996. Analysis of p53 mutation and epidermal growth factor receptor amplification in recurrent gliomas with malignant progression. *J Neuropathol Exp Neurol* 55: 822-31
Reynes G, Vila V, Martin M, Parada A, Fleitas T, et al. 2011. Circulating markers of angiogenesis, inflammation, and coagulation in patients with glioblastoma. *J Neurooncol* 102: 35-41
Robe PA, Bentires-Alj M, Bonif M, Rogister B, Deprez M, et al. 2004. In vitro and in vivo activity of the nuclear factor-kappaB inhibitor sulfasalazine in human glioblastomas. *Clin Cancer Res* 10: 5595-603
Rocha S, Garrett MD, Campbell KJ, Schumm K, Perkins ND. 2005. Regulation of NF-kappaB and p53 through activation of ATR and Chk1 by the ARF tumour suppressor. *EMBO J* 24: 1157-69
Rodgers JT, Lerin C, Haas W, Gygi SP, Spiegelman BM, Puigserver P. 2005. Nutrient control of glucose homeostasis through a complex of PGC-1alpha and SIRT1. *Nature* 434: 113-8
Rogina B, Helfand SL. 2004. Sir2 mediates longevity in the fly through a pathway related to calorie restriction. *Proc Natl Acad Sci U S A* 101: 15998-6003
Salminen A, Kaarniranta K, Kauppinen A. 2013. Crosstalk between Oxidative Stress and SIRT1: Impact on the Aging Process. *Int J Mol Sci* 14: 3834-59
Salminen A, Kauppinen A, Suuronen T, Kaarniranta K. 2008. SIRT1 longevity factor suppresses NF-kappaB -driven immune responses: regulation of aging via NF-kappaB acetylation? *BioEssays : news and reviews in molecular, cellular and developmental biology* 30: 939-42
Sanchez-Carbayo M, Socci ND, Lozano J, Saint F, Cordon-Cardo C. 2006. Defining molecular profiles of poor outcome in patients with invasive bladder cancer using oligonucleotide microarrays. *J Clin Oncol* 24: 778-89
Sasaki T, Maier B, Koclega KD, Chruszcz M, Gluba W, et al. 2008. Phosphorylation regulates SIRT1 function. *PLoS One* 3: e4020
Saunders LR, Verdin E. 2007. Sirtuins: critical regulators at the crossroads between cancer and aging. *Oncogene* 26: 5489-504
Saunders MI, Hoskin PJ, Pigott K, Powell ME, Goodchild K, et al. 1997. Accelerated radiotherapy, carbogen and nicotinamide (ARCON) in locally advanced head and neck cancer: a feasibility study. *Radiother Oncol* 45: 159-66

Schneider CA, Rasband WS, Eliceiri KW. 2012. NIH Image to ImageJ: 25 years of image analysis. *Nature methods* 9: 671-5
Shah ZH, Ahmed SU, Ford JR, Allison SJ, Knight JR, Milner J. 2012. A deacetylase-deficient SIRT1 variant opposes full-length SIRT1 in regulating tumor suppressor p53 and governs expression of cancer-related genes. *Mol Cell Biol* 32: 704-16
Sibtain A, Hill S, Goodchild K, Shah N, Saunders M, Hoskin PJ. 2002. The modification of human tumour blood flow using pentoxifylline, nicotinamide and carbogen. *Radiother Oncol* 62: 69-76
Silber JR, Bobola MS, Blank A, Schoeler KD, Haroldson PD, et al. 2002. The apurinic/apyrimidinic endonuclease activity of Ape1/Ref-1 contributes to human glioma cell resistance to alkylating agents and is elevated by oxidative stress. *Clin Cancer Res* 8: 3008-18
Sinclair DA, Guarente L. 1997. Extrachromosomal rDNA circles--a cause of aging in yeast. *Cell* 91: 1033-42
Smith CM, Gafken PR, Zhang ZL, Gottschling DE, Smith JB, Smith DL. 2003. Mass spectrometric quantification of acetylation at specific lysines within the amino-terminal tail of histone H4. *Analytical Biochemistry* 316: 23-33
Solomon JM, Pasupuleti R, Xu L, McDonagh T, Curtis R, et al. 2006. Inhibition of SIRT1 catalytic activity increases p53 acetylation but does not alter cell survival following DNA damage. *Mol Cell Biol* 26: 28-38
Stenzinger A, Endris V, Klauschen F, Sinn B, Lorenz K, et al. 2013. High SIRT1 expression is a negative prognosticator in pancreatic ductal adenocarcinoma. *BMC Cancer* 13: 450
Stuenkel W, Peh BK, Tan YC, Nayagam VM, Wang X, et al. 2007. Function of the SIRT1 protein deacetylase in cancer. *Biotechnology Journal* 2: 1360-68
Sugden MC, Caton PW, Holness MJ. 2010. PPAR control: it's SIRTainly as easy as PGC. *J Endocrinol* 204: 93-104
Sugino T, Maruyama M, Tanno M, Kuno A, Houkin K, Horio Y. 2010. Protein deacetylase SIRT1 in the cytoplasm promotes nerve growth factor-induced neurite outgrowth in PC12 cells. *FEBS Lett* 584: 2821-6
Sulaiman M, Matta MJ, Sunderesan NR, Gupta MP, Periasamy M, Gupta M. 2010. Resveratrol, an activator of SIRT1, upregulates sarcoplasmic calcium ATPase and improves cardiac function in diabetic cardiomyopathy. *Am J Physiol Heart Circ Physiol* 298: H833-43
Sun L, Li H, Chen J, Dehennaut V, Zhao Y, et al. 2013. A SUMOylation-dependent pathway regulates SIRT1 transcription and lung cancer metastasis. *Journal of the National Cancer Institute* 105: 887-98
Sundaresan NR, Pillai VB, Wolfgeher D, Samant S, Vasudevan P, et al. 2011. The deacetylase SIRT1 promotes membrane localization and activation of Akt and PDK1 during tumorigenesis and cardiac hypertrophy. *Sci Signal* 4: ra46
Tafani M, Di Vito M, Frati A, Pellegrini L, De Santis E, et al. 2011. Pro-inflammatory gene expression in solid glioblastoma microenvironment and in hypoxic stem cells from human glioblastoma. *J Neuroinflammation* 8: 32
Tanno M, Sakamoto J, Miura T, Shimamoto K, Horio Y. 2007. Nucleocytoplasmic shuttling of the NAD+-dependent histone deacetylase SIRT1. *J Biol Chem* 282: 6823-32
Tiberi L, van den Ameele J, Dimidschstein J, Piccirilli J, Gall D, et al. 2012. BCL6 controls neurogenesis through Sirt1-dependent epigenetic repression of selective Notch targets. *Nature neuroscience* 15: 1627-35
Tissenbaum HA, Guarente L. 2001. Increased dosage of a sir-2 gene extends lifespan in Caenorhabditis elegans. *Nature* 410: 227-30
Tome-Carneiro J, Larrosa M, Gonzalez-Sarrias A, Tomas-Barberan FA, Garcia-Conesa MT, Espin JC. 2013. Resveratrol and clinical trials: the crossroad from in vitro studies to human evidence. *Current pharmaceutical design* 19: 6064-93
Toyokuni S, Okamoto K, Yodoi J, Hiai H. 1995. Persistent oxidative stress in cancer. *FEBS Lett* 358: 1-3
Vaquero A, Scher M, Lee DH, Erdjument-Bromage H, Tempst P, Reinberg D. 2004. Human SirT1 interacts with histone H1 and promotes formation of facultative heterochromatin. *Molecular Cell* 16: 93-105

Vaquero A, Sternglanz R, Reinberg D. 2007. NAD(+)-dependent deacetylation of H4 lysine 16 by class IIIHDACs. *Oncogene* 26: 5505-20
Vineshkumar PT, Kimmo JH, Sharmistha C, Amyn AH. 2014. The role of NF-κB in the pathogenesis of glioma. *Molecular & Cellular Oncology* 1
Vlashi E, Lagadec C, Vergnes L, Matsutani T, Masui K, et al. 2011. Metabolic state of glioma stem cells and nontumorigenic cells. *Proc Natl Acad Sci U S A* 108: 16062-7
Wang B, Hasan MK, Alvarado E, Yuan H, Wu H, Chen WY. 2011. NAMPT overexpression in prostate cancer and its contribution to tumor cell survival and stress response. *Oncogene* 30: 907-21
Wang C, Chen L, Hou X, Li Z, Kabra N, et al. 2006. Interactions between E2F1 and SirT1 regulate apoptotic response to DNA damage. *Nat Cell Biol* 8: 1025-31
Wang R-H, Sengupta K, Li C, Kim H-S, Cao L, et al. 2008. Impaired DNA damage response, genome instability, and tumorigenesis in SIRT1 mutant mice. *Cancer cell* 14: 312-23
Wang YQ, Cao Q, Wang F, Huang LY, Sang TT, et al. 2015. SIRT1 protects against oxidative stress-induced endothelial progenitor cells apoptosis by inhibiting FOXO3a via FOXO3a ubiquitination and degradation. *J Cell Physiol*
Webster BR, Lu Z, Sack MN, Scott I. 2012. The role of sirtuins in modulating redox stressors. *Free Radic Biol Med* 52: 281-90
Wu A, Ying Z, Gomez-Pinilla F. 2006. Oxidative stress modulates Sir2alpha in rat hippocampus and cerebral cortex. *Eur J Neurosci* 23: 2573-80
Wu M, Pastor-Pareja JC, Xu T. 2010. Interaction between Ras(V12) and scribbled clones induces tumour growth and invasion. *Nature* 463: 545-8
Yang H, Zhang W, Pan H, Feldser HG, Lainez E, et al. 2012. SIRT1 activators suppress inflammatory responses through promotion of p65 deacetylation and inhibition of NF-kappaB activity. *PLoS One* 7: e46364
Yang Y, Duan W, Lin Y, Yi W, Liang Z, et al. 2013. SIRT1 activation by curcumin pretreatment attenuates mitochondrial oxidative damage induced by myocardial ischemia reperfusion injury. *Free Radic Biol Med* 65: 667-79
Yang Y, Fu W, Chen J, Olashaw N, Zhang X, et al. 2007. SIRT1 sumoylation regulates its deacetylase activity and cellular response to genotoxic stress. *Nat Cell Biol* 9: 1253-62
Ye F, Zhang Y, Liu Y, Yamada K, Tso JL, et al. 2013. Protective properties of radio-chemoresistant glioblastoma stem cell clones are associated with metabolic adaptation to reduced glucose dependence. *PLoS One* 8: e80397
Yeung F, Hoberg JE, Ramsey CS, Keller MD, Jones DR, et al. 2004. Modulation of NF-kappaB-dependent transcription and cell survival by the SIRT1 deacetylase. *EMBO J* 23: 2369-80
Yoon H, Shin SH, Shin DH, Chun YS, Park JW. 2014. Differential roles of Sirt1 in HIF-1alpha and HIF-2alpha mediated hypoxic responses. *Biochem Biophys Res Commun* 444: 36-43
Yoshizaki T, Milne JC, Imamura T, Schenk S, Sonoda N, et al. 2009. SIRT1 exerts anti-inflammatory effects and improves insulin sensitivity in adipocytes. *Mol Cell Biol* 29: 1363-74
Zakhary SM, Ayubcha D, Dileo JN, Jose R, Leheste JR, et al. 2010. Distribution analysis of deacetylase SIRT1 in rodent and human nervous systems. *Anat Rec (Hoboken)* 293: 1024-32
Zhang B, Chen J, Cheng AS, Ko BC. 2014. Depletion of sirtuin 1 (SIRT1) leads to epigenetic modifications of telomerase (TERT) gene in hepatocellular carcinoma cells. *PLoS One* 9: e84931
Zhang F, Li ZL, Xu XM, Hu Y, Yao JH, et al. 2015. Protective effects of icariin-mediated SIRT1/FOXO3 signaling pathway on intestinal ischemia/reperfusion-induced acute lung injury. *Mol Med Rep* 11: 269-76
Zheng J, Chen LL, Xiao F, Hu X, Deng X, Li H. 2012. Three single nucleotide variants of the SIRT1 gene are associated with overweight in a Chinese population: a case control study. *Endocrine journal* 59: 229-37
Zhou Y, Zhou Y, Shingu T, Feng L, Chen Z, et al. 2011. Metabolic alterations in highly tumorigenic glioblastoma cells: preference for hypoxia and high dependency on glycolysis. *J Biol Chem* 286: 32843-53

Zhu GY, Shi BZ, Li Y. 2014. FoxM1 regulates Sirt1 expression in glioma cells. *European review for medical and pharmacological sciences* 18: 205-11
Ziche M, Morbidelli L. 2000. Nitric oxide and angiogenesis. *J Neurooncol* 50: 139-48
Zu Y, Liu L, Lee MY, Xu C, Liang Y, et al. 2010. SIRT1 promotes proliferation and prevents senescence through targeting LKB1 in primary porcine aortic endothelial cells. *Circ Res* 106: 1384-93